Molecular Mechanisms Underlying the Development of Type 2 Diabetes

Dissertation
zur
Erlangung der naturwissenschaftlichen Doktorwürde
(Dr. sc. nat.)

vorgelegt der
Mathematisch-naturwissenschaftlichen Fakultät
der
Universität Zürich
von

Simone Boller
von
Zürich ZH

Promotionskomitee
Prof. Dr. Alex Hajnal
Dr. Markus Niessen
Dr. Marianne Böni-Schnetzler
Prof. Dr. Marc Donath

Zürich, 2009

TABLE OF CONTENTS

Part A: A new role for insulin receptor substrate (IRS) proteins in signal transduction?

Part B: Do free fatty acids regulate the expression of interleukin-1β and chemokine KC via Toll-like receptors in mouse islets?

LIST OF FIGURES

A. List of Figures

B. List of Figures

LIST OF TABLES

A. List of tables

B. List of tables

Part A:

A new role for insulin receptor substrate (IRS) proteins in signal transduction?

A. Summary (English)

Insulin receptor substrate (IRS) proteins are evolutionarily conserved proteins that are recruited to the activated insulin receptor (IR) and to other activated receptors like the insulin-like growth factor 1 receptor and growth hormone receptor. Mammals express four family members termed IRS1 through IRS4. It is the current view that IRS proteins act as adaptors linking activated membrane receptors to intracellular signalling pathways. Indeed, IRS proteins contain both, domains that are involved in receptor binding and regions that mediate downstream signalling. An N-terminal pleckstrin homology (PH) domain and a phospho Tyr binding (PTB) region confer binding to the activated receptors. The extended C-termini of IRS contain numerous Tyr-based motives which, if phosphorylated, serve as binding sites for downstream signalling components. Among the known IRS-binding proteins are the regulatory subunit of phospatidyl inositol 3 kinase (PI3K/p85), growth factor receptor-bound protein 2 (Grb2) and SH2-containing phosphatase (SHP2). In addition to Tyr, IRS also contain many consensus Ser/Thr phosphorylation motives that usually negatively influence IRS function.

Even though IRS1 and IRS2 are structurally highly homologous, they can not always substitute each others function in insulin signalling. The choice of which IRS is recruited to the IR depends on tissue type, stage and extracellular stimuli (context). Furthermore, depending on the context, each IRS isoform can initiate several different downstream pathways. Beyond that, several receptors beside the IR can recruit IRS proteins. Facing such complexity in IRS-mediated signalling, we propose that the adaptor-model is not fully compatible to explain the generation of context-specificity.

Expanding the adapter-model we hypothesise that IRS proteins act as integrators of signalling information. We suggest that context-specific cellular responses depend on an interplay of *cis-elements* on IRS with specific downstream binding compexes consisting of known and unknown proteins. As IRS proteins contain many Thr, Ser and Tyr residues, we speculate that combinations of phosphorylated and non-phosphorylated sites on IRS constitute a code. Each combination (pattern) encodes context-specific signalling information and it is decoded by binding of specific complexes that mediate context-specific signal transduction.

The first aim of the project was to define the postulated *cis-elements* on IRS. To this end we intended to determine the exact binding regions of glucose regulated protein 78 (GRP78) and cell growth regulator 19 (CGR19), two previously identified binding partners. Furthermore it was planned to identify stimulus-dependent phosphorylation patterns on

IRS. It was intended to stimulate via distinct receptors and ligands as e.g. insulin or IGF-1 and combinations. The second aim was the identification of stimulus-specific binding complexes by mass spectroscopy (MS).

For aim one, a search for new proteins that bind to IRS2 was performed previously using the yeast 2-hybrid system. GRP78 and CGR19 were identified in this screen. The interactions of GRP78 and CGR19 with IRS2 were confirmed in GST-pulldown and Co-immunopreciopitation experiments. Additionally GRP78 and CGR19 were shown to bind to IRS1. GRP78 is a molecular chaperone and regulator of the unfolded protein response during ER-stress and was recently shown to regulate insulin signalling. Very little is known about the function of CGR19. It was identified as a repressor of proliferation downstream of p53.

We found that GRP78 binds to IRS1(270-517) and IRS1(974-1169), whereas CGR19 binds to IRS1(1-271) and IRS1(517-974). Sequence alignment revealed that IRS1(270-517) and IRS1(974-1169) share only 24.5 % identical amino acids, however more than two randomly chosen sequences. IRS1(270-517) and IRS1(974-1169) were also compared to IRS2, revealing two highly homologues regions. These findings indicate that two distinct binding sites for GRP78 exist on IRS1. Functional assays in 3T3-L1 adipocytes and CHO-IR cells confirmed our results showing that both regions, IRS1(270-517) and IRS1(974-1169), are necessary for binding to GRP78 (Linha Xu, manuscript in preparation).

To test for stimulus-dependent phoshorylation patterns on IRS1, IRS1-myc-his was purified and concentrated after stimulation with insulin. Unfortunately appropriate collaborators for the required MS analysis could not be found. 2D gel electrophoresis to separate and visualise the differently phosphorylated IRS1 proteins did not succeed within a reasonable time frame.

For aim two, the identification of stimulus-specific binding partners of IRS, we intended to apply co-immunoprecipitation in combination with MS. Before these experiments were started, we decided to stop the project.

A. Summary (Deutsch)

Insulinrezeptor-Substrat (IRS) Proteine sind evolutionär konservierte Proteine, welche vom aktivierten Insulinrezeptor (IR) sowie von anderen aktivierten Rezeptoren wie beispielsweise dem IGF-1R und dem GH Rezeptor rekrutiert werden. Säuger exprimieren vier Mitglieder der IRS-Famile, welche als IRS1 bis 4 bezeichnet werden. Gegenwärtig besteht die Ansicht, dass IRS Proteine als Adaptoren wirken, welche Membranrezeptoren mit intrazellulären Signalübermittlungswegen verbinden. Tatsächlich bestehen IRS Proteine aus Domänen, welche in die Rezeptorbindung involviert sind und Regionen, welche die intrazelluläre Weiterleitung des Signals ermöglichen. Eine N-terminale PH Domäne und eine PTB Region erlauben Bindung an aktivierte Rezeptoren. Die ausgedehnten C-terminalen Enden enthalten zahlreiche Tyr-basierte Motive, welche in phosphoryliertem Zustand als Bindungsstellen für intrazelluläre Signalübertragungs-Moleküle dienen. Bekannte Bindungspartner von IRS sind die regulatorische Untereinheit (p85) von PI3K, sowie Grb2 und SHP2. Neben den Tyr-Stellen enthalten IRS auch viele Ser/Thr Phosphorylierungs-Motive, welche im Allgemeinen die IRS Funktion hemmen.

Aber obwohl IRS1 und IRS2 strukturell homolog sind, können sie ihre Funktion in der Insulin-Signalübertragung nicht vollständig geegnseitig ersetzen. Die Wahl, welches IRS Protein vom IR rekrutiert wird, hängt vom Gewebe, Stadium der Zelle und extrazellulären Stimuli ab (Kontext). Zudem kann jede IRS Isoform in Kontext-spezifischer Weise verschiedene Signalübertragungswege initiieren. Darüber hinaus können neben dem IR noch verschiedene andere Rezeptoren die IRS Proteine rekrutieren. Angesichts dieser Komplexität denken wir, dass das Adaptor-Modell nicht ausreicht, um die Kontext-Spezifität der Signaltransduktion zu erklären.

Wir bauen das Adapter-Modell aus und stellen die Hypothese auf, dass IRS Proteine auch als Integratoren von Signalinformation wirken. Wir postulieren, dass Kontext-spezifische zelluläre Antworten von einem Zusammenspiel von *cis-Elementen* auf IRS mit spezifischen Bindungs-Komplexen abhängen, welche aus bekannten und unbekannten Proteinen bestehen. Viele mögliche Kombinationen von phosphorylierten und nicht-phosphorylierten Thr, Ser und Tyr Stellen auf IRS könnten einen Code darstellen. Jedes Verschlüsselungsmuster enthält Kontext-spezifische Signalübertraguns-Informationen und wird durch Bindung spezifischer Partner decodiert, wodurch Kontext-spezifische Signalübermittlung ermöglicht wird.

Das erste Ziel in diesem Projekt war, die postulierten c*is-Elemente* auf IRS zu definieren. Dies beinhaltete auch die Bestimmung der exakten Bindungsstellen von GRP78 (glucose-

regulated protein 78) und CGR19 (cell growth regulator 19), zweier zuvor identifizierter Bindungspartner von IRS. Ausserdem war geplant, Stimulus-abhängige Phosphorylierungs-Muster auf IRS zu identifizieren. Wir beabsichtigten, via verschiedene Rezeptoren und Liganden zu stimulieren, beispielsweise mit Insulin oder IGF-1oder Kombinationen. Das zweite Ziel war die Identifizierung Stimulus-spezifischer Bindungspartner mittels Massenspektrometrie (MS).

Für das erste Ziel wurden neue Bindungspartner für IRS2 mit Hefe-2-Hybrid-Experimenten gesucht, wobei GRP78 und CGR19 gefunden wurden. Die Interaktionen von GRP78 und von CGR19 mit IRS2 wurden in GST-pulldown- und Co-Immunopräzipitations-Experimenten bestätigt. Zudem wurde gezeigt, dass GRP78 sowie CGR19 an IRS1 binden. GRP78 ist ein molekulares Chaperon und Regulator der UPR (unfolded protein response) während ER-Stress der Zelle. Kürzlich wurde gezeigt, dass GRP78 die Insulin-Signaltransduktion reguliert. Über CGR19 ist sehr wenig bekannt, es wurde als Proliferations-Repressor downstream von p53 identifiziert.

Wir lokalisierten die Bindungsstellen von GRP78 auf IRS1(270-517) und IRS1(974-1169), sowie diejenigen von CGR19 auf IRS1(1-271) und IRS1(517-974). Ein Test auf Sequenzhomologie zeigte, dass IRS1(270-517) und IRS1(974-1169) nur 24.5 % identische Aminosäuren aufweisen. Dies entspricht allerdings einem höheren Anteil als in zwei zufällig gewählten Sequenzen. IRS1(270-517) und IRS1(974-1169) wurden auch je mit IRS2 verglichen. Der Sequenzvergleich zeigte zwei Sequenzen auf IRS2 mit sehr starker Homologie zu je einer Region auf IRS1. Diese Ergebnisse weisen darauf hin, dass zwei verschiedene Bindungsstellen für GRP78 auf IRS1 existieren. Funktionelle Experimente bekräftigten unsere Resultate: In 3T3-L1 Adipozyten und CHIO-IR Zellen wurde gezeigt, dass beide Bindungsstellen IRS1(270-517) und IRS1(974-1169) für die Bindung mit GRP78 nötig sind (Linhua Xu, Manuskript in Vorbereitung).

Um das Vorkommen der Stimulus-abhängigen Phosphorylierungs-Muster auf IRS1 zu überprüfen, wurde IRS1-myc-his nach Insulin-Stimulation aufgereinigt und konzentriert. Leider konnten keine Kollaboratoren für die benötigten MS Experimente gefunden werden. Die 2D-Gelelektrophorese, mit welcher die verschieden-phosphorylierten IRS1 Proteine separieren und visualisiert werden sollten, konnte im gegebenen Zeitrahmen nicht erfolgreich abgeschlossen werden.

Für das zweite Ziel, die Identifikation Simulus-spezifischer Bindungspartner auf IRS, hatten wir geplant, Co-Immunopräzipitation in Kombination mit MS anzuwenden. Bevor jedoch diese Experimente gestartet werden konnten, mussten wir uns entscheiden, das Projekt zu beenden.

A. Abbreviations

aa	amino acid
ADP	adenosine diphosphate
APS	adapter protein containing a PH and SH2 domain
ATF6	activating transcription factor 6
ATP	adenosine triphosphate
Cbl	casitas B-lineage lymphoma
CGR19	cell growth regulator 19
CHO	chinese hamster ovary
DOK	downstream of kinase
EGFR	epidermal growth factor receptor
ER	endoplasmic reticulum
ERK	extracellular signal-regulated kinase
FCS	fetal calf serum
Gab-1	GRB2-associated binding protein 1
GDP	guanosine diphosphate
GH	growth hormone
GLUT4	glucose transporter 4
GPCR	G-protein-coupled receptor
Grb2	growth factor receptor-bound protein 2
GRP78	glucose regulated protein 78
GS3K	glycogen synthase 3-kinase
GST	glutathione S-transferase
GTP	guanosine triphosphate
HEK	human embryonic kidney
HFD	high fat diet
IGF-1	insulin-like growth factor 1
IGF-1R	insulin-like growth factor 1 receptor
IL	interleukin
IL-4R	interleukin-4 receptor
IP	immunoprecipitation
IR	insulin receptor
IRE1	inositol-requiring enzyme
IRS	insulin receptor substrate
JNK	c-Jun N-terminal kinase

LAR	leukocyte common antigen-related
LRP	leukocyte antigen-related phosphatase
MyD88	myeloid differentiation factor 88
mTOR	mammalian target of rapamycin
PBS	phosphate-buffered saline
PCR	polymerase chain reaction
PDFGR	platelet-derived growth factor receptor
PDK1	PIP3-dependent protein kinase 1
PERK	PKR-like endoplasmic reticulum kinase
PH	pleckstrin homology
PI3K	phosphatidyl inositol 3 kinase
PKB	protein kinase B
PKC	protein kinase C
PMSF	phenylmethylsulphonyl fluoride
PTB	phospho-Tyr binding
PTPB1	protein-Tyr phosphatise 1B
Ras	rat sarcoma
SDS	sodium dodecyl sulfate
SDS-PAGE	SDS-polyacrylamide gel electrophoresis
SH2	Src-homology domain 2
Shc	SH2-containing collagen-related protein
SHP2	SH2-domain-containing phospho-Tyr phosphatase 2
shRNA	short hairpin ribonucleic acid
siRNA	short interfering ribonucleic acid
SOS	Son of Sevenless
TNFα	tumour necrosis factor-α
UPR	unfolded protein response

A.1 Introduction

A.1.1 Insulin and the regulation of glucose homeostasis

Healthy humans show blood glucose concentrations between 4 and 7 mM [1]. Only D-glucose (not L-glucose) is metabolised by cells and it will be referred to as glucose throughout this work. Regulation of blood glucose homeostasis depends on an integrated system. Whereas many hormones enhance blood glucose (e.g. glucagon, adrenaline, growth hormone and epinephrine), the main hormone with glucose-lowering effects is insulin. IGF-1 exhibits glucose-lowering effects as well, primarily via IGF-1 receptor (IGF-1R) [2]. IGF-1 is structurally related to proinsulin, and can bind to the insulin receptor (IR) and also to IR/IGF-1R hybrids. However in vivo, circulating IGF-1 is tightly bound to other proteins and has low affinity for the IR. As a consequence most of the effects of IGF-1 on insulin signalling are mediated via IGF-1R or indirectly e.g. via suppression of growth hormone [3].

Insulin is a polypeptide hormone of the pancreas and produced by the β-cells of the islets of Langerhans. The hormone consists of two peptide chains, an A chain with 21 and a B chain with 30 amino acids. Two disulfide bridges connect the two chains. Mature insulin is processed from preproinsulin in two steps. First, preproinsulin, which contains an N-terminal signal peptide to target the nascent protein into the endoplasmic reticulum (ER), is cleaved by microsomal enzymes to proinsulin. Then proinsulin is transported to the Golgi apparatus and packed into clathrin-coated secretory granules. During maturation of these vesicles, the clathrin-coat is shed and proinsulin is proteolytically cleaved into insulin and C-peptide [4].

Insulin release is biphasic consisting of an initial transient (lasting ca. 10 min) first phase followed by a sustained second phase. The differences in the mechanisms underlying the two phases are not fully understood. The main steps of secretion are common in both first and second phase, while the second phase is additionally influenced by different pathways as e.g. by kinases of the PKA and PKC families [5]. Two distinct pools of insulin granules have also been proposed [6]. In short, insulin secretion occurs as follows: glucose enters the β-cells via glucose transporter 2 (GLUT2) and is metabolised to ATP. The resulting increase in ATP/ADP ratio results in closure of ATP-sensitive K^+ channels, leading to accumulation of K^+ in the cytosol and membrane depolarisation. As a consequence cell-surface voltage-dependent Ca^{2+} channels are opened, facilitating

extracellular Ca^{2+} influx into the β-cells. This rise in free cytosolic Ca^{2+} triggers exocytosis of insulin containing granules.

A.1.2 Type 1 and type 2 diabetes mellitus

Diabetes mellitus is characterized by elevated levels of blood glucose and is caused by insufficient production or release of insulin. With time chronic hyperglycaemia leads to serious damage and dysfunction of many organs, e.g. eyes, kidney, nerves and blood vessels. In the year 2000, there were approximately 171 million people worldwide with diabetes. The disease causes about 5 % of all deaths globally each year [7]. Furthermore the World Health Organisation (WHO, [7]) estimates that the number of people with diabetes is likely to at least double till 2030, to reach a total of 366 million affected people.

The prevalent types of diabetes mellitus are type 1 and 2. In type 1 diabetes, autoimmune reactions selectively destroy the insulin-producing β-cells in the pancreas. As a consequence, no or too low amounts of insulin are produced giving rise to overt hyperglycemia. Type 2 diabetes is usually a combination of insulin resistance in liver, muscle and fat and inadequate insulin secretion by pancreatic β-cells. In a first step, high metabolic demand for insulin due to insulin resistance is compensated by an increase in functional β-cell mass. Later, β-cell compensation fails due to a loss of β-cell function and mass. Hyperglycemia, dislipidemia and changes in cytokine composition contribute to maladaption and apoptosis of the β-cells [8]. The official classification of diabetes mellitus was challenged recently [9], as the pathogenesis of type 1 and type 2 diabetes share certain characteristics. Hence type 1 and type 2 diabetes might be considered as the two extremes of a continuum and not as strictly different types [9].

Insulin resistance and β-cell failure are the two main characteristics of type 2 diabetes. These two attributes relate to the two projects of this thesis:

In project A we investigated the function of IRS proteins whose malfunction is linked to insulin resistance in the periphery. In obesity, a major risk factor for diabetes, stress kinases are activated and phosphorylate IRS1 and IRS2 on Ser and Thr residues. Elevated Ser and Thr phosphorylation abolishes Tyr phosphorylation of IRS impairing insulin signalling, finally leading to insulin resistance [10, 11].

In project B we studied the regulation of the proinflammatory cytokine IL-1β. IL-1β regulates β-cell function and β-cell mass [12]. Prolonged exposure of islets to high IL-1β concentrations is linked to β-cell failure in the pancreas of type 2 diabetic patients.

A.1.3 Summary of insulin signal transduction

The insulin receptor is a heterotetramer composed of two extracellular α-subunits and two transmembrane β-subunits, linked by disulfide bonds. Binding of insulin to the α-subunits induces conformational changes in the receptor thereby activating the intracellular Tyr kinase domains on the β-subunits. Consequently, several Tyr residues of the intracellular β-subunit of the IR are (cis- and trans-) autophosphorylated [13, 14].

Phospho-Tyr on the IR serve as docking sites for several adapter proteins, such as insulin receptor substrates, SH2-containing collagen-related protein (Shc) [15], Grb2-associated binding protein 1 (Gab-1) [16], p60dok [17, 18], casitas B-lineage lymphoma protein (Cbl) [17] and adapter protein containing a PH and SH2 domain (APS) [19]. IRS proteins play a central role in insulin signalling. Binding of IRS to the IR and their subsequent phosphorylation attracts downstream signalling proteins, like the regulatory subunit of inositol 3 kinase (PI3K), growth factor receptor-bound protein 2 (Grb2) or Src-homology-2 (SH2) domain-containing Tyr phosphatase 2 (SHP2) [20]. There is evidence that binding of Grb2 to IRS promotes gene transcription via ras and extracellular signal-regulated kinase (ERK). Recruitment of p85 activates PI3K, resulting in generation of the phospholipids phosphatidylinositol-(3,4)biphosphate and phosphatidylinositol-(3,4,5)triphosphate. These phospholipids recruit protein kinase B (PKB/Akt) to the plasma membrane. PKB promotes glucose transport, protein synthesis, glycogen synthesis, cell proliferation and cell survival. The exact role of SHP2 is not well defined yet. Its binding to IRS1 promotes dephosphorylation of phospho-Tyr, thereby attenuating insulin signalling [20]. Signalling downstream of some IRS binding partners is described in part A.1.5 of this work, a summary of IRS-dependent insulin signalling is given in Figure A.1.

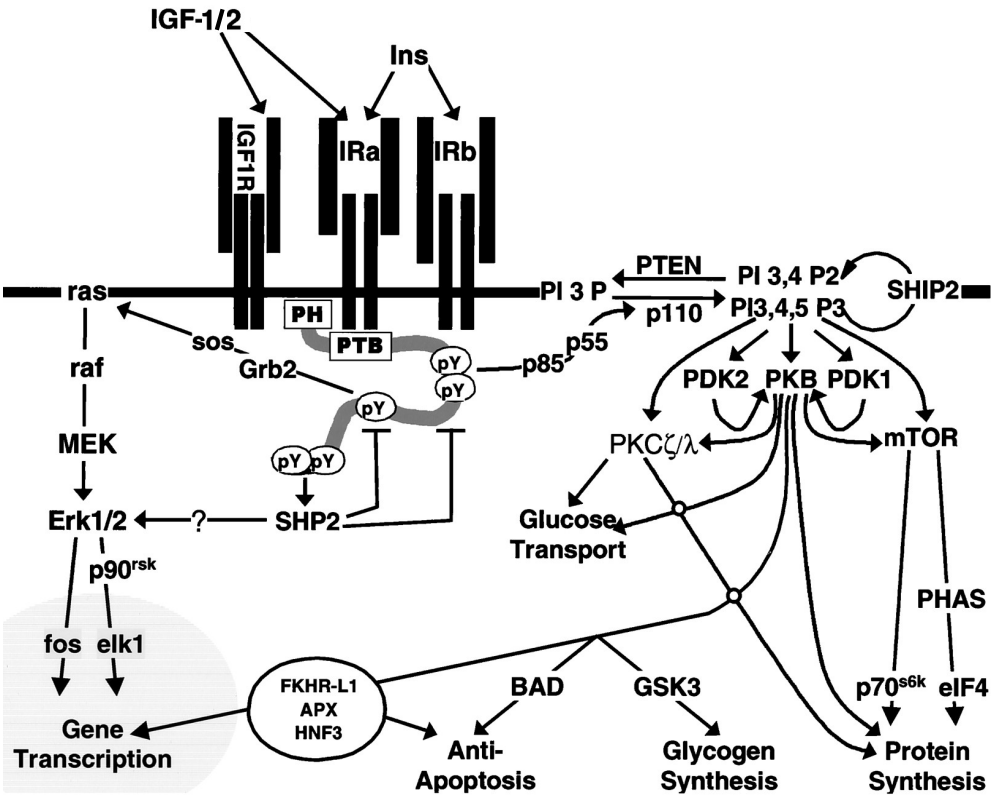

FIGURE A. 1: THE INSULIN SIGNALLING PATHWAY (ADAPTED FROM [20])
Among the members of the insulin/IGF family, insulin is the highest affinity ligand for insulin receptor (IR). Activation of IR mediates signalling via intracellular phosphorylation of insulin receptor substrate (IRS) proteins. IRS play a central role in insulin signalling, as they serve as binding sites for many adapter proteins, like the regulatory subunit p85 of phosphatidyl inositol 3 kinase (PI3K), growth factor receptor-bound protein 2 (Grb2), or Src-homology-2(SH2) domain containing Tyr phosphatase 2 (SHP2). Recruitment of Grb2 to IRS promotes gene transcription via the ras/ ERK-pathway. Binding of p85 activates PI3K, which then activates protein kinase B (PKB). PKB promotes cell proliferation and cell survival, glycogen synthesis, protein synthesis and glucose transport. The exact function of SHP2 is not well defined yet.

A.1.4 IRS proteins

A.1.4.1 Structure of IRS proteins

Insulin receptor substrate proteins are evolutionarily conserved proteins that are recruited to several receptors, including the IR, IGF-1R and growth hormone (GH) receptor. The fruit fly *Drosophila melanogaster* expresses a single IRS homologue called *chico* [21]. Mammals express four family members termed IRS1 through IRS4, however, the human genome does not encode functional IRS3 [22].

IRS proteins contain domains that are involved in receptor binding and regions that bind to downstream signalling components. N-terminal pleckstrin homology (PH) domains and

phospho-Tyr binding (PTB) regions mediate interaction with activated receptors, the interfaces for binding to downstream signalling molecules are mainly located in the C-terminal parts. The PH and PTB domains of all the isoforms are highly conserved, whereas the COOH-parts vary in sequence and length [22].

IRS1 and IRS2 are expressed in many tissues in mammals and are important players in insulin signalling. Furthermore they are also the best studied isoforms. IRS1 and IRS2 are 75 % identical in their N-terminal domains and 35 % in their C-terminal parts, where they contain many similar Tyr phosphorylation motifs.

Two other tandem PH-PTB domain proteins are expressed in humans, IRS4/DOK4 and IRS6/DOK5 [23]. They are both Tyr-phosphorylated by the IR and the IGF-1R just as the other IRS proteins are. The sequences of IRS4/DOK4 and IRS6/DOK5 are more similar to one another than to any other members of the IRS or DOK family, but as they bind to IR and IGF-1R they were defined as IRS proteins [23].

A.1.4.2 Regulation of IRS proteins by phosphorylation of Tyr or Ser/Thr residues, respectively

IRS proteins are phosphorylated downstream of different receptors, for example the IR, IGF-1R or the interleukin-4 receptor (IL-4R) [24] and they can be phosphorylated by different intra-cellular kinases, e.g. PKB or c-Jun N-terminal kinase (JNK). Binding of IRS1/2 to the activated IR results in Tyr phosphorylation of several sites.

Insulin signal transduction depends on phosphorylation of numerous Tyr-based motives on IRS, many of which are located in the extended C-termini. IRS1 and IRS2 have the longest tails of all IRS isoforms, they contain several potential Tyr phosphorylation domains. There is some degree of conservation of these Tyr-motives between IRS1 and IRS2 but some sites are unique [25, 26]. Src-homology (SH2) region-containing downstream signalling components, like the regulatory subunit (p85) of PI3K, GRB2 and SHP2 bind to phosphorylated Tyr–based motifs and mediate downstream signalling. The signalling pathways via PI3K, GRB2 and SHP2 proteins are described in more detail below in part A.1.5.1. Known binding partners and kinases that can phosphorylate IRS *in vivo* are depicted in Figure A.2. A recent study revealed potential phospho-Tyr residues on IRS1 and IRS2 with quantitative interaction proteomics [27]. The detected Tyr residues on IRS1/2 and the found binding partners are shown in Figure A.3. As downstream signalling components bind to phospho-Tyr motifs, Tyr phosphorylation usually has a positive influence on signalling.

In addition to Tyr residues the C-terminal tail of IRS contains many consensus Ser and Thr residues. In IRS1, 242 out of 1'242 amino acids (19.5 %) are Ser or Thr sites. On average 14 % of residues in eukaryotic proteins are Ser or Thr [28]. Phosphorylation of Ser and Thr sites usually negatively influences IRS signal transduction. The exact mechanisms for this phospho-Ser-mediated alteration in IRS signalling are not clear. In some cases Ser/Thr and Tyr phosphorylation seem to be mutually exclusive. As an example, tumour necrosis factor (TNF)-α stimulates phosphorylation of IRS1 at Ser307. This inhibits insulin-induced Tyr phosphorylation of IRS1 and even leads to its ubiquitination and proteolytic breakdown [29, 30]. Generally it is thought that Ser phosphorylation of specific motifs in IRS1 and IRS2 recruits ubiquitin ligases finally leading to degradation of the protein. Like TNF-α also activation of mTOR (mammalian target of rapamycin) can induce IRS degradation [31]. Degradation of IRS1 and IRS2 may contribute to insulin resistance, as IRS protein levels are decreased in diabetic animal models and type 2 diabetics [31]. However the exact mechanisms for regulation of IRS ubiquitinylation and degradation remain unclear.

Another mechanism of Ser phosphorylation-mediated negative regulation of insulin signalling is interference of phospho-Ser with functional domains on IRS. In this way phosphorylation of Ser307 on IRS1, which is located in the PTB domain, negatively regulates insulin signalling by impeding PTB domain to interact with the IR. It was shown *in vitro* that phosphorylation of this Ser residue disrupts the interaction between IR and IRS1 [32].

In short it can be stated that phosphorylation of IRS proteins regulates the amplitude of insulin signalling.

It can be assumed that not all IRS1 molecules in a cell show the same phosphorylation pattern. As a consequence a given phospho-Tyr site is only phosphorylated in a part of the IRS1 population and the number of IRS1 proteins phosphorylated at a certain docking site also determines the amplitude of the signal. Important in this context are phospatases and kinases.

Several kinases have been found to phosphorylate IRS under various conditions. Some Ser kinases are activated by insulin as a part of a negative feedback loop; others are activated upon cellular stress [33]. A number of Ser/Thr kinases downstream of PI3K as glycogen synthase kinase 3 (GSK3), mTOR, PKCξ, PKB negatively regulate IRS1 [25]. Another important kinase in the context of insulin resistance is JNK. JNK mediates phosphorylation at Ser307 (Ser312 in human) on IRS1 [34]. Several studies revealed that

phosphorylation of this site decreased insulin signalling. However, the phosphorylation pattern on IRS is an interplay of many different factors, so one single phosphorylation site can be affected by many kinases (as IKK, JNK and PKCξ can phosphorylate Ser307) [25]. Consistent with the finding that Ser phosphorylation has normally a negative effect on insulin signalling, the basal activity of Ser and Thr kinases is elevated in muscle and adipose sample from type 2 diabetic patients [35]. The activation of IRS by phosphorylation on Tyr residues is mostly mediated downstream of receptors and kinases.

Besides the numerous kinases there are also many phosphatases which alter the phosphorylation state of IRS. Unfortunately they are not well explored so far. Several Tyr phosphatases are discussed to dephosphorylate IRS1, e.g. protein-Tyr phosphatase 1B (PTPB1), SHP2, leukocyte common antigen-related (LAR) and leucocyte antigen-related phosphatase (LRP) [36]. In one study, the specific activity of these phosphatases towards IRS1 was compared *in vitro* using recombinant proteins. PTPB1 was significantly more active than LAR, LRP (2500-5500 times) and SHP2 (12 times) and it showed the highest specific activity (compared to dephosphorylation of a synthetic phospho-Tyr-containing peptide). Co-immunoprecipitation revealed that binding of Tyr-phosphorylated IRS1 and PTP1B was entirely dependent on the presence of Grb2 [36].

Like PTP1B, several other phosphatases are known that act upstream of IRS at the level of the IR. Since these phosphatases reduce the activity of the receptor, it is difficult to distinguish between reduced phosphorylation of IRS1 due to reduced activation of the receptor and de-phosphorylation by phosphatase action [36].

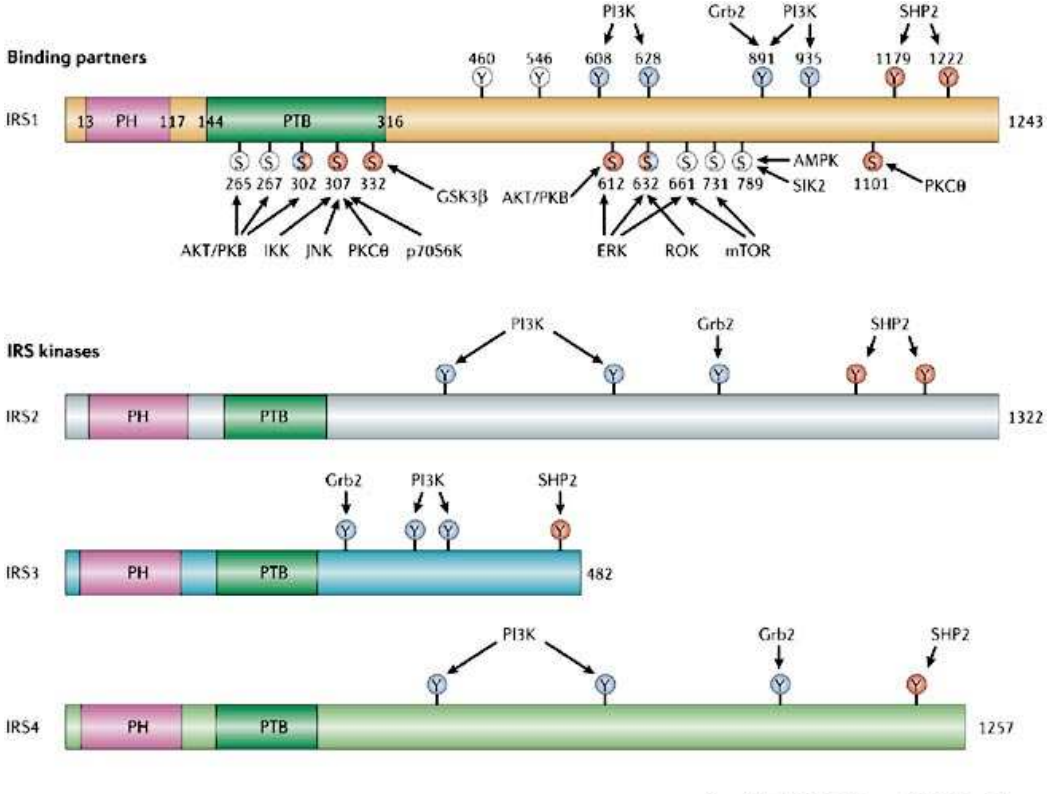

FIGURE A. 2: PHOSPHORYLATION SITES ON IRS ISOFORMS, BINDING PARTNERS AND KINASES (TAKEN FROM [32])

The four mammalian insulin receptor substrate isoforms IRS1, IRS2, IRS3, IRS4 show highly conserved N-terminal pleckstrin homology (PH) and phospho-Tyr-binding (PTB) domains. The C-terminal tail contains many Tyr sites (indicated by Y) that are phosphorylated by the IR and that serve as binding sites for the indicated binding partners (denoted above the proteins). Below Ser kinases are shown, S stands for affected Ser sites. Blue circles represent sites of positive regulation, red circles sites of negative regulation, combination of both colours stands for sites that have been reported to have positive or negative influence dependent on the condition. For sites with white circles the effect of phosphorylation is unknown.

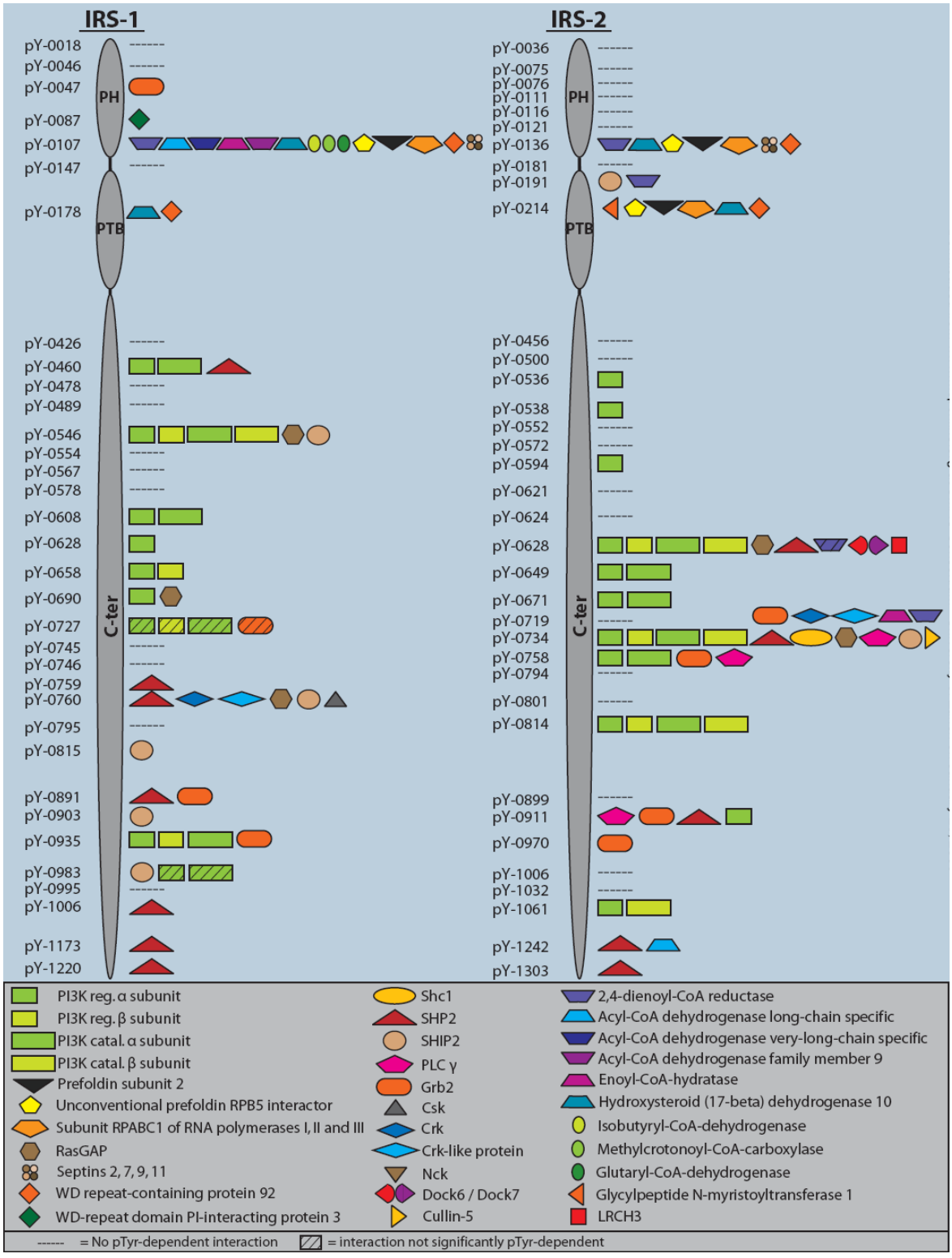

FIGURE A. 3: POTENTIAL P-TYR SITES ON IRS1 AND IRS2 AND BINDING PARTNERS ANALYSED BY PROTEOMICS (TAKEN FROM [27])

The phospho-Tyr interactomes of IRS1 and IRS2. Potential site-specific, phospho-Tyr-dependent interaction partners are indicated. Interaction partners were determined by pulldown approach in lysates of the murine muscle cell line C2C12 with phosphorylated vs. non-phosphorylated bait peptides, combined with quantitative proteomics.

A.1.4.3 Function of IRS proteins

The common view in literature is that IRS proteins act as adaptors linking membrane receptors to intracellular signalling pathways [26, 29, 37, 38]. Even though IRS1 and IRS2 are 75 % identical in their N-terminal domains and 35 % in their C-terminal parts, the two isoforms are not functionally interchangeable in insulin signalling. Depending on the tissue and extracellular stimuli, IRS1 and IRS2 play different roles in signal transduction.

Studies in *Irs1*$^{-/-}$ or *Irs2*$^{-/-}$ mice showed that defects caused by the lack of one isoform can not be completely rescued by the remaining isoform. Disruption of IRS1 in mice results in retarded growth and insulin resistance. However these mice did not develop diabetes as insulin secretion is increased to compensate for insulin resistance. IRS2 knockout mice show insulin resistance in liver and β-cell failure leading to type 2 diabetes [39, 40].

In pancreatic β-cells the role of IRS1 and IRS2 was analysed in a study overexpressing each isoform in isolated islets [41]. IRS2 but not IRS1 overexpression induced β-cell proliferation and decreased glucose-induced apoptosis. In addition IRS2 and not IRS1 improved insulin secretion. These findings are consistent with *in vivo* data. IRS2 knockout mice showed β-cell deficiency combined with peripheral insulin resistance leading to type 2 diabetes, whereas IRS1 knockout mice were able to compensate for insulin resistance by increasing insulin secretion [42].

Complementary roles of IRS1 and IRS2 downstream of insulin were also observed in the control of hepatic metabolism [43]. ShRNA was utilised to specifically knock down IRS1 or IRS2 in liver of wild type mice. Reduction of IRS1 expression lead to increased expression of gluconeogenic genes and decreased expression of glucokinase, linking IRS1 to hepatic glucose metabolism. Downregulation of IRS2 increased expression of important lipogenic genes showing that IRS2 is more closely linked to lipid metabolism in liver.

Distinct functions of IRS isoforms were also described in muscle. L6 myotubes were incubated in the presence of siRNA against either IRS1 or IRS2 [44]. Downregulation of IRS1 decreased insulin-induced actin-remodelling, glucose uptake and GLUT4 translocation and inhibited insulin-induced PKBα and PKBβ phosphorylation, indicating that IRS1 is important in glucose uptake. Downregulation of IRS2 inhibited insulin-induced phosphorylation of PKBβ without affecting other functions, suggesting that IRS2 has a minor role in glucose uptake in muscle. In contrast to IRS1 ablation, IRS2 reduction decreased insulin-induced ERK phosphorylation.

To sum it up, the choice of which IRS is recruited to the receptor is dependent on tissue, stage and extracellular stimuli (context). Furthermore, depending on the context, each IRS isoform can initiate several different downstream pathways. Beyond that, several receptors can recruit IRS proteins. The question arising is how specific signalling can be garanteed. We propose that the adapter-model is insufficient to explain the complexity in IRS-mediated insulin signalling and especially in generation of context-specific signalling outputs. In part A.1.6 we introduce our model, attempting to explain context-specificity.

A.1.5 IRS-interacting proteins

Several binding partners of IRS proteins have been described and most of them contain a SH2 domain that binds to phospho-Tyr motifs. PI3K, Grb2, Nck, Crk, Fyn, Csk, Ship and SHP2 all belong to this group. Some binding partners of IRS do not contain an SH2 domain, e.g. some integrins, Ca^{2+} ATPases (SERCA1 and SERCA2) and adaptor protein14-3-3 [45]. Some of the binding partners are described in more detail below.

Our group had identified new IRS-interacting proteins by the yeast 2-hybrid system [45]. Two of the identified binding partners were chosen and further analysed during this project, these were GRP78 and CGR19, described in part A.1.5.2 and A.1.5.3.

A.1.5.1 Previously known binding partners

A.1.5.1.1 Phosphatidylinositol-3 kinase (PI3K)

The regulatory subunit (p85) of PI3K contains two SH2 domains and can bind to phosphorylated YMXM and YXXM motifs in IRS1 [32]. Binding of the regulatory subunit of PI3K to IRS1 recruits the catalytic subunit p110 to the plasma membrane where it phosphorylates inositol phospholipids at the 3' position of the inositol ring, generating $PI(3,4)P_2$ or $PI(3,4,5)P_3$. $PI(3,4)P_2$ or $PI(3,4,5)P_3$ then serve as docking sites for several intracellular signalling proteins, forming signalling complexes at the plasma membrane. In this manner PKB is put in close proximity to phosphatidyl-dependent kinase1 (PDK1). PKB is phosphorylated by PDK1 and activated PKB then dissociates from the plasma membrane [46]. PKB has a variety of downstream target proteins controlling various cellular functions like gene transcription, protein synthesis, glucose metabolism and cell cycle.

PI3K does not only bind to IRS, but can be activated by directly binding to several receptor Tyr kinases, as well as by many other types of cell-surface receptors, including

some G-protein-coupled receptors (GPCRs). Whereas many growth factor receptors as e.g. PDGFR bind PI3K directly via phosphorylated Tyr sequences on the receptor itself, the IR and several cytokine receptors recruit IRS1 to activate PI3K [47].

The insulin signalling pathway is largely conserved in Drosophila melanogaster. As in mammals, the IRS homologue Chico links InR (IR homologue) to Dp110/p60 (PI3K homologue). However, in Drosophila melanogaster Dp110/p60 can also bind directly to InR. This interaction takes place at a C-terminal extension of the Drosophila InR that contains binding sites for Dp110/p60 and that is not present in vertebrate receptors [21].

A.1.5.1.2 Grb2

Growth factor receptor-bound protein 2 (Grb2) contains an SH2 domain which binds Tyr phosphorylated sequences, for example phosphorylated Tyr895 in IRS1 [48]. Two SH3 domains on Grb2 form complexes with proline-rich regions of other proteins. One of the SH3 domains of Grb2 can bind the guanine nucleotide exchange factor SOS (Son of Sevenless). The SOS-Grb2-IRS interaction brings SOS into close proximity with $p21^{ras}$, which is anchored to the plasma membrane by a farnesyl residue. SOS stimulates GDP/GTP exchange and thereby inactive $p21^{ras}$-GDP is converted to active $p21^{ras}$-GTP. $p21^{ras}$ itself activates ERK cascade, that plays an important role in mitogenic signalling pathways. In contrast to this important mitogenic function of insulin, the Ras-ERK pathway does not play a major role in the metabolic actions of insulin as glucose uptake and activation of glycogen synthase [49, 50].

A.1.5.1.3 SHP2

SHP2 (also known as SH-PTP2, PTP1D or Syp) is a phospho-Tyr phosphatase that contains two SH2 domains [50]. The IR and several growth factor receptors like EGFR and PDGFR bind SHP2. In addition, two phospho-Tyr motifs in the C-terminus of IRS1 and IRS2 bind to SHP2 [37]. The signalling pathways downstream of SHP2 are not well defined yet. When a catalytically inactive mutant of SHP2 was expressed, decreased insulin-induced Ras activation was observed in CHO-IR cells, indicating that activation of SHP2 positively regulates insulin-stimulated Ras/ERK activity [51]. In another study in 32D cells, the Tyr on IRS1 that bind to SHP2 were mutated. In contrast to a previous study, mitogenic signals trough the Ras/MAKP pathway were mediated normally in the presence of the mutated IRS1. However, Tyr phosphorylation of IRS1, PI3K binding and activation of protein synthesis were increased upon insulin stimulation. These findings

indicate that SHP2 attenuates IRS1 phosphorylation and downstream signalling in metabolic insulin actions [52].

A.1.5.2 GRP78

Glucose-regulated protein 78 (GRP78, also called BiP) is a heat shock protein 70 (HSP70) family member, however it is not induced under heat-shock. It contains an ATP-binding domain which is required for its chaperone function. GRP78 transiently interacts with hydrophobic sites of nascent proteins preventing missfolding of folding-intermediates.

GRP78 regulates the activation of the unfolded protein response (UPR) upon accumulation of unfolded or missfolded proteins in the ER lumen (ER stress). In unstressed cells, the luminal domain of the transmembrane proteins PERK (PKR-like endoplasmic reticulum kinase), IRE1 (inositol-requiring enzyme) and ATF6 (activating transcription factor 6) are bound to GRP78 and hence retained in their monomeric and inactive forms. Upon accumulation of unfolded proteins, GRP78 is released allowing the UPR transducers PERK and IRE1 to homodimerize, autophosphorylate and become active. Finally ER stress is transduced by downstream activation of multiple ER stress response genes. Release of GRP78 from ATF6 uncovers a targeting sequence directing it to the Golgi complex where it is cleaved yielding a free domain that acts as a transcription factor [53-55]. ER stress itself induces GRP78 expression [56].

ER stress has been shown to link obesity with deterioration of insulin action in type 2 diabetes. In two obesity mouse models (HFD-induced and *ob/ob*) expression of several ER stress indicators (PERK phosphorylation, c-Jun phosphorylation, GRP78 expression) was increased in liver and adipose tissue [56]. Additionally a recent study in nondiabetic humans correlated expression of ER stress markers of adipoyctes with BMI and percent fat of subjects [57]. In Fao cells ER stress (induced with tunicamycin or thapsigargin) promoted JNK-dependent IRS1 Ser phosphorylation, which finally inhibited insulin signalling [56].

We had identified amino acids 336-517 of rat GRP78 in a search for new proteins that bind to IRS2 in yeast 2-hybrid screens [45]. Later the interaction of this fragment with IRS2 and also with IRS1 was confirmed in GST-pulldown experiments with mammalian cell lysates. The binding between GRP78 and IRS might therefore constitute the physical link between ER stress and insulin resistance. To test for possible roles of GRP78 in insulin signalling, GRP78 was overexpressed under homeostasis or ER stress (Linha Xu, manuscript in preparation). In 3T3-L1 adiocytes under homeostasis, overexpression of

GRP78 decreased IR protein level and inhibited insulin-dependent ERK phosphorylation but increased PKB activation. Under ER stress, insulin-dependent PKB but not ERK activation was restored by overexpression of GRP78 (IR was not detectable). These and other findings clearly demonstrate that GRP78 can indeed regulate insulin signal transduction.

Our findings fit well with a recently published study confirming an important role for GRP78 in insulin signalling [58]: Hepatic overexpression of GRP78 in *ob/ob* mice improved insulin signalling and insulin sensitivity.

A.1.5.3 CGR19

Very little information is available about the function of cell growth regulator 19 (CGR19). It has been identified as a repressor of proliferation downstream of p53. CGR19 is a 331 amino acid long protein. The rat and human homologues are highly conserved with 85 % identity. A putative zinc-binding ring-finger domain is located at the C-terminus of the protein. Unlike in other ring-finger-containing proteins, no ring-finger-associated B-box domain is present in CGR19 [59]. The function of the ring-finger domain is unclear, it is discussed to mediate nucleic acid binding and protein-protein interactions [60].

Our unpublished results (M. McNamara) showed that CGR19 is expressed in 3T3-L1 adipocytes, where it was localised in or on the ER. Overexpression of CGR19 increased 2-deoxy-D-glucose uptake in 3T3-L1 adipocytes, whereas insulin-induced proliferation was repressed in CHO-IR cells.

A.1.6 Hypothesis and aims

A.1.6.1 Our hypothesis

As described above (part A.1.4.3.), IRS-dependent signalling is highly context-dependent and complex. We assume that the adapter-model (assuming IRS proteins acting as mere adapters linking membrane receptors to intracellular signalling) is insufficient to describe the molecular function of IRS proteins. Especially, the adapter-model can not explain how context-specific signalling outputs can be guaranteed. We propose that IRS proteins not only act as adaptors but also as integrators of signalling information. This integrator-model is explained in the following section and in Figure A.4.

Cells are constantly exposed to many different stimuli reflecting changes in their environment. Accordingly, we presume that the pool of IRS proteins within a cell is

exposed to different signals simultaneously. In order to permit context-specific signalling, IRS proteins have to integrate all these informations. This implies that IRS proteins are carriers of information instead of being mere adaptors. Integration of different stimuli depends on modification of *cis*-elements on IRS and their interaction with *trans*-acting protein complexes composed of downstream mediators. Our model describes stimulus-dependent modification of the *cis*-elements as coding, whereas the built up of specific protein complexes is viewed as decoding. The composition of the protein complexes reflects the context to which a cell is exposed at a given time. These binding complexes might contain known but also so far unknown proteins. Unknown proteins might confer specificity to signal transduction. Since the formation of binding complexes depends on the code and reflects a specific context, they are referred to as decoding complexes in this work.

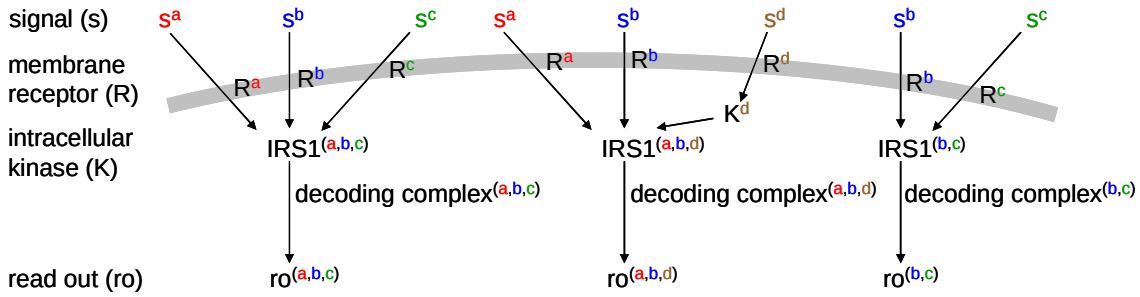

FIGURE A. 4: MODEL: IRS PROTEINS ACT AS INTEGRATORS OF SIGNALLING INFORMATION
Our hypothesis is that IRS proteins not only act as adaptors but also as integrators of signalling information. Different signals (s) stimulate IRS e.g. via membrane receptors (R) and their intracellular kinases (K). The combination of the incoming stimuli leads to specific modification of IRS (depicted as superscript letters). Depending on the code a specific decoding complex is formed on IRS. This context-specific decoding complex leads to a context-specific cellular read-out (ro).

As IRS proteins contain many Thr, Ser and Tyr residues whose phosphorylation state is known to modulate IRS-dependent signal transduction, we hypothesise that coding could depend on specific phosphorylation patterns (Figure A.5). Depending on the phosphorylation state, every Tyr, Ser, Thr position on IRS might be considered as a molecular binary switch that is either on or off (1/ 0). Combinations of all these single switches constitute a code.

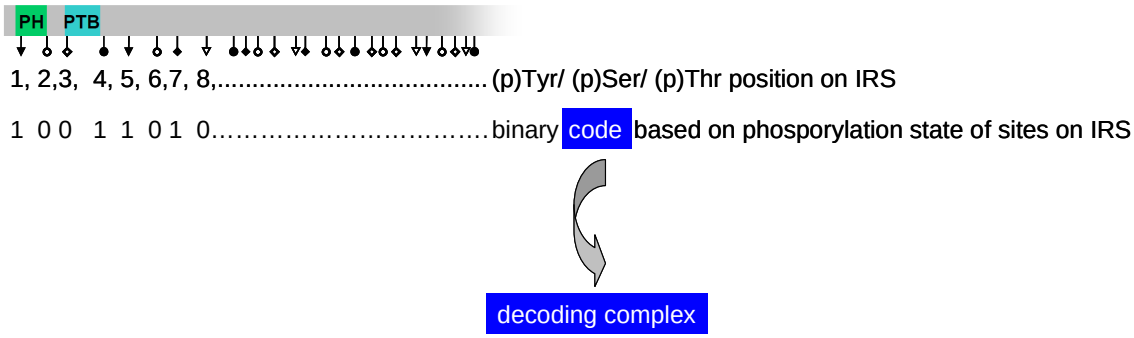

FIGURE A. 5: PHOSPHO-PATTERNS ON IRS COULD SERVE AS CODE FOR CONTEXT-SPECIFIC SIGNALLING

Context-specific encoding based on phosphorylation patterns of IRS. Circles represent Tyr, squares Ser and triangles Thr residues, respectively. Black symbols stand for phosphorylated (p), open symbols for non-phoshorylated residues. The model describes every Tyr, Ser, Thr position as a binary switch that is on or off (1/ 0) depending on the phosphorylation state. Combinations of all these single switches form a code, which is then read and translated by specific decoding complex to generate context-specific read-out.

To test our model, new IRS-binding partners that could be part of the decoding complexes to confer specificity were identified previously. A rat muscle cDNA library was screened using IRS2 as bait (yeast 2-hybrid system). In this way several new binding partners were indeed identified. Binding could later be confirmed in GST-pulldown assays and co-immunoprecipitations with lysates from chinese hamster ovary cells overexpressing the IR (CHO-IR) and from 3T3-L1 adipocytes [45]. Among the proteins identified in our screens were GRP78 and CGR19, which were both investigated in this study.

A.1.6.2 Objective of the study

The aim of the project was to define the postulated *cis-elements* on IRS and to test the existence of the postulated code. This included determination of the exact binding regions of the newly identified *trans-acting* factors CGR19 and GRP78 and the identification of stimulus-dependent phosphorylation patterns. A second goal was the identification of specific *trans-acting* decoding complexes composed of known and unknown factors.

A.1.7 From the IRS- to the IL-1β project

Many challenges such as technical and financial difficulties finally lead to the decision to stop the project. The second project in the group of Marc Donath allowed me to continue to work in a same field of research.

One connection between the two projects is that they involve both the analysis of specificity during signal transduction. The function of MyD88 as an adapter which binds to different receptors resembles the function of IRS. In both cases different receptors are linked to distinct specific cellular read-outs. A main issue connected to both projects is how cells can implement signal-specificity by using one adaptor (MyD88 or IRS) linking different membrane receptors to intracellular read-outs. This interesting question was, however, not directly addressed during the second project about the regulation of IL-1β.

A.2 Materials and methods

A.2.1 Molecular techniques and tools

A.2.1.1 Basic molecular biological techniques

Basic molecular experiments were performed using standard protocols [61, 62]. Variations and specifications are described below:

PCR amplified sequences or PCR-fragments after restriction digestion were purified using the Nucleo Spin Extract II kit (Macherey Nagel, Oensingen, Switzerland) or the PCR purification kit (Qiagen, Hombrechtikon, Switzerland). Product was eluated with 10 mM Tris at pH 7.5, instead of the supplied elution buffer. Eluates were concentrated by ethanol precipitation.

For cloning of plasmid DNA, *Escherichia Coli XL1blue* were used. Cells were grown in autoclaved and prewarmed LB medium (L-Broth, BIO 101, La Jolla, USA) at 37 ℃ and 260 rpm or they were plated on agar plates. Depending on the plasmid the appropriate antibiotic was added to the medium for selection. Midi- and Maxi-preps for amplification of the plasmid were performed with the Nucleobond AX kit (Macherey Nagel, Oensingen, Switzerland), a subsequent ethanol precipitation concentrated the plasmid.

A.2.1.2 Plasmid constructs

cDNA sequences used in this project encoded human IRS1, mouse IRS2, human GRP78 and rat CGR19. Unless otherwise noted the sequences and their numbering correspond to the sequence of the respective species.

A.2.1.2.1 Fusion of GRP78 and CGR19 fragments to GST in pGEX-4T-1

All GST-tagged sequences, GRP78(336-519)-GST, CGR19(wt)-GST, GST, used as a bait in pulldown assays were cloned into the prokaryotic expression vector pGEX-4T-1 (Stratagene Cloning System) by Brad Joblin. The map of the vector is shown in Figure A.6. The inserts were ligated into NotI and SalI sites of the vector.

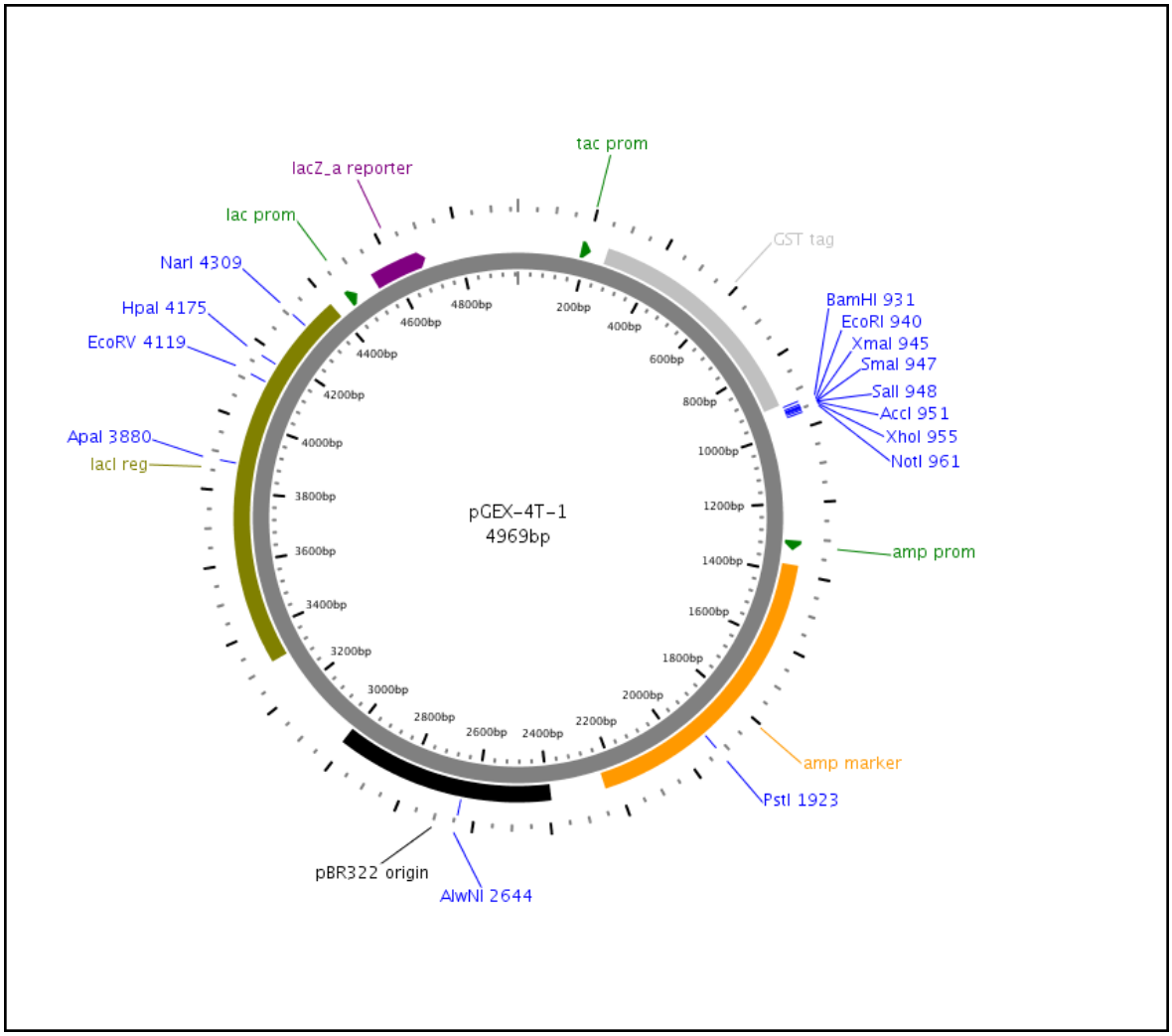

FIGURE A. 6: MAP OF PGEX4T-1 VECTOR

A.2.1.2.2 Fusion of IRS1 and IRS2 fragments to a myc-his-tag in pCT

All fragments tagged to myc-his or flag were cloned into transfer vector containing the cytomegalovirus promoter (pCMV-transfer A^+, pCT). The map of the vector is shown below in Figure A.7. IRS1 and IRS2 constructs with myc-his-tag were kindly provided by Linhua Xu. All the used fragments for immunoprecipitation and pulldown are listed in Table A.2, part A.2.1.2.5.

Recombinant adenoviruses for ectopic expression of the respective fragments were generated (see part A.2.2.2.2.).

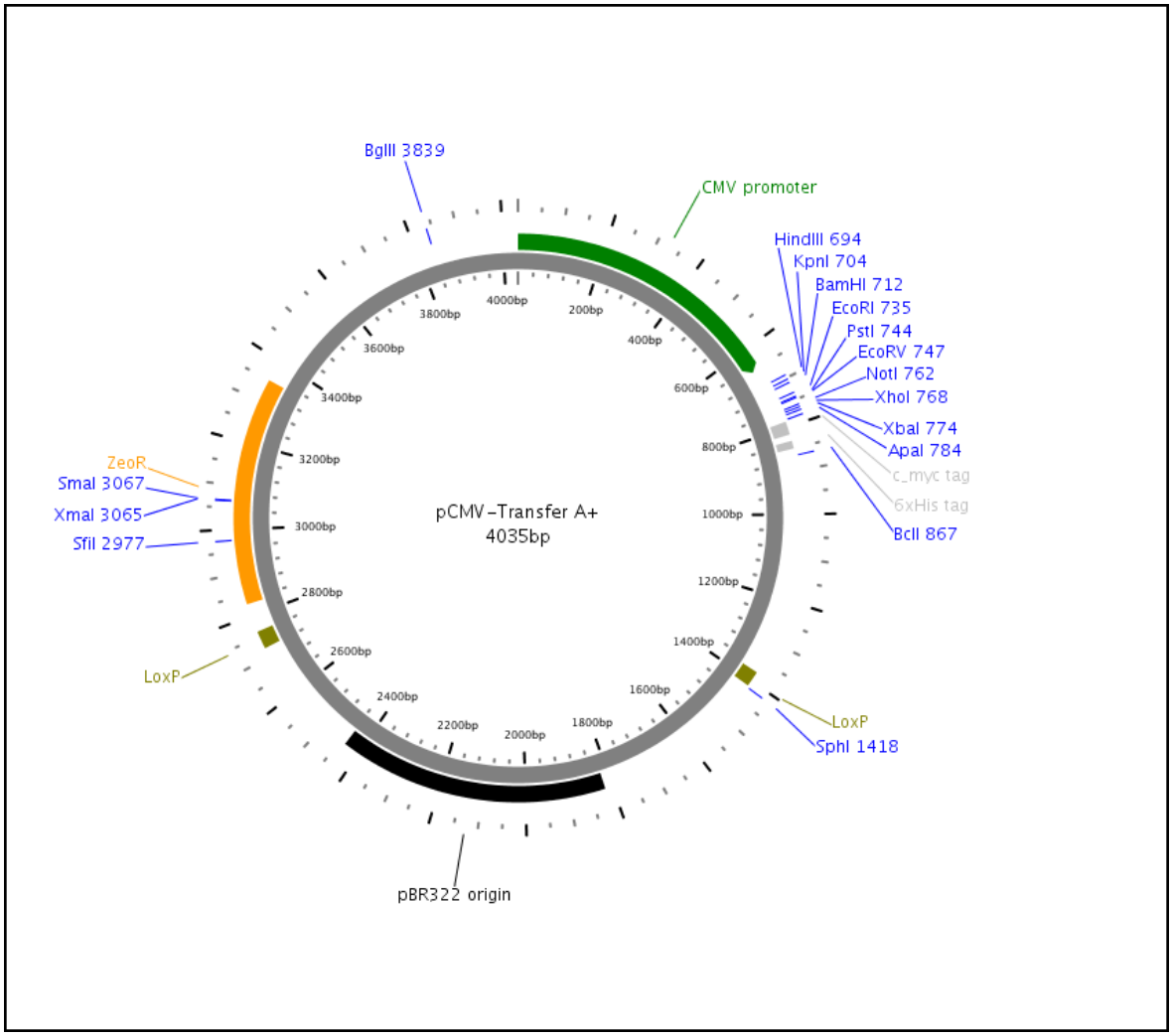

FIGURE A. 7: MAP OF PCMV-TRANSFER A$^+$ VECTOR

A.2.1.2.3 Fusion of GRP78 and CGR19 fragments to a flag-tag in modified pCT

At the beginning of this study, all IRS fragments and truncations of their interacting partners GRP78 and CGR19 were available as fusions with myc-his-tag. New fragments of GRP78 and CGR19 with flag-tag were generated with the following cloning strategy. All utilised synthetic oligonucleotides were ordered from Microsynth (Balgach, Switzerland), they are listed in Table A.1.

A first goal was to obtain a pCT vector with a flag-tag sequence. To this end an oligonucleotide with an EcoRI restriction site at the 5' end and a NotI site at the 3' end was ligated into pCT vector. This double-stranded oligonucleotide made with forward oligomer 9a and reverse oligomer 9b contained a start-codon, followed by a PvuI and a ClaI restriction site, a 3' flag-tag and a stop codon. In order to get the required fragment for the

newly synthesised vector containing a flag-tag, PCR was used to amplify the fragment. Primers that introduced a PvuI site at the 5' end and a ClaI site at the 3' site of the PCR-fragment were used. The resulting oligonucleotide was digested and ligated into the new vector. Combination of forward Primer 1 and reverse primer 2 lead to the fragment Cgr19(wt)-flag, primer 1 and 3 to Cgr19(delta Zn)-flag, primers 4 and 5 to Grp78(336-517)-flag, primers 4 and 6 to Grp78(336-367)-flag and primers 7 and 8 to Grp78(wt)-flag. Cloning of Grp78(wt)-flag did not succeed, and expression of Cgr19(delta Zn)-flag and Grp78(336-367)-flag was not detectable later in CHO-IR cells.

Nr.	Name	Sequence (5' to 3')	Intention/ position
9a	sb_flagfwd_9a	cggaattccaccatgcgatcggtcatcgatgattacaaggatgacga	} insertion of 3'flag in pCT
9b	sb_flagfwd_9b	atgcggccgctcagtcagttagctcttatcgtcgtcatccttgtaatc	
1	sb_cgr19fwd_1	gtcgatcggccgcagtgttcctggt	start CGR19 full-length
2	sb_cgr19rev_2	tgatcgatggaagtttctagtatgtcct	stop CGR19 full-length
3	sb_cgr19rev_3	tgatcgatctcctccaccgggtcc	stop CGR19 in front of zinc-finger
4	sb_grp78fwd_4	gtcgatcgcggtctactatgaagccc	start GRP78 at aa 336
5	sb_grp78rev_5	tgatcgatacccttgtcttcagctgt	stop GRP78 at aaS 517
6	sb_grp78rev_6	tgatcgattttaaccagttgctgaatctt	stop GRP78 at aa 376 (after hsp70 binding site)
7	sb_grp78fwd_7	gtcgatcgaagctctccctggtggc	start GRP78 full-length
8	sb_grp78rev_8	tgatcgatttctgctgtatcctcttca	stop GRP78 full-length without KDEL
11	sb_irs1_1013fwd_11	ttggatccgctgacatgcgaacagg	start IRS1 aa 1013, 5' BamHI
12	sb_irs1_1064fwd_12	ttggatcccaaggacctgggggca	start IRS1 aa 1064, 5' BamHI
13	sb_irs1_1169rev_13	ataagcttaagccccacacagtttgg	stop IRS1 aa 1169, 5' HindIII, stop
14	sb_irs1_1119rev_14	ataagcttaaaagggcactgtgttgc	stop IRS1 aa 1119, 5' HindIII, stop
15	sb_irs1_1093rev_15	ataagcttattgtgggtctgcacgga	stop IRS1 aa 1093, 5' HindIII, stop
-	T3	ttaaccctcactaaagg	e.g. start IRS1 aa 974

TABLE A. 1: PRIMERS AND OLIGONUCLEOTIDES FOR CLONING OF FRAGMENTS WITH FLAG-TAG

Primers and oligonucleotides 1-9 were used for cloning of flag-tagged CGR19 and GRP78 fragments in pCT. Primers 11-15 and T3 were used for cloning of flag-tagged IRS1 fragments in pCMV-Tag2B.

A.2.1.2.4 Fusion of IRS fragments to flag in pCMV-Tag2B

Region covering amino acids 933-1242 of IRS1 was broken down into smaller fragments. Truncations IRS1(933-1242)-flag, IRS1(1081-1242)-flag, IRS1(933-1080)-flag, IRS1(933-1169)-flag and IRS1(974-1169)-flag already existed at the beginning of the study and were kindly provided by Markus Niessen. As these truncations were inserted into pCMV-

Tag2B vector, this vector was used for cloning of several shorter IRS1 fragments fused to flag. The map of pCMV-Tag2B is depicted in Figure A.8.

All truncations were derived from IRS1(974-1169)-flag. In short, respective fragments were generated by PCR as described below and inserted into *pCMV-Tag2B* digested with BamHI and HindIII (Table A.1, primers 11-15 and T3).

Primers T3 and 14 lead to fragment IRS1(974-1119)-flag, primers T3 and 15 to IRS1(974-1093)-flag, primers 11 and 13 to IRS1(1013-1169)-flag, primers 12 and 13 to IRS1(1064-1169)-flag, primers 11 and 14 to IRS1(1013-1119)-flag, primers 11 and 15 to IRS1(1013-1093)-flag and primers 12 and 14 to IRS1(1064-1119)-flag. Combination of primer T3 and 13 produces fragment IRS1(974-1169)-flag, that contained a new stop codon right after the coding sequence, unlike the starting IRS1 fragment with the same sequence.

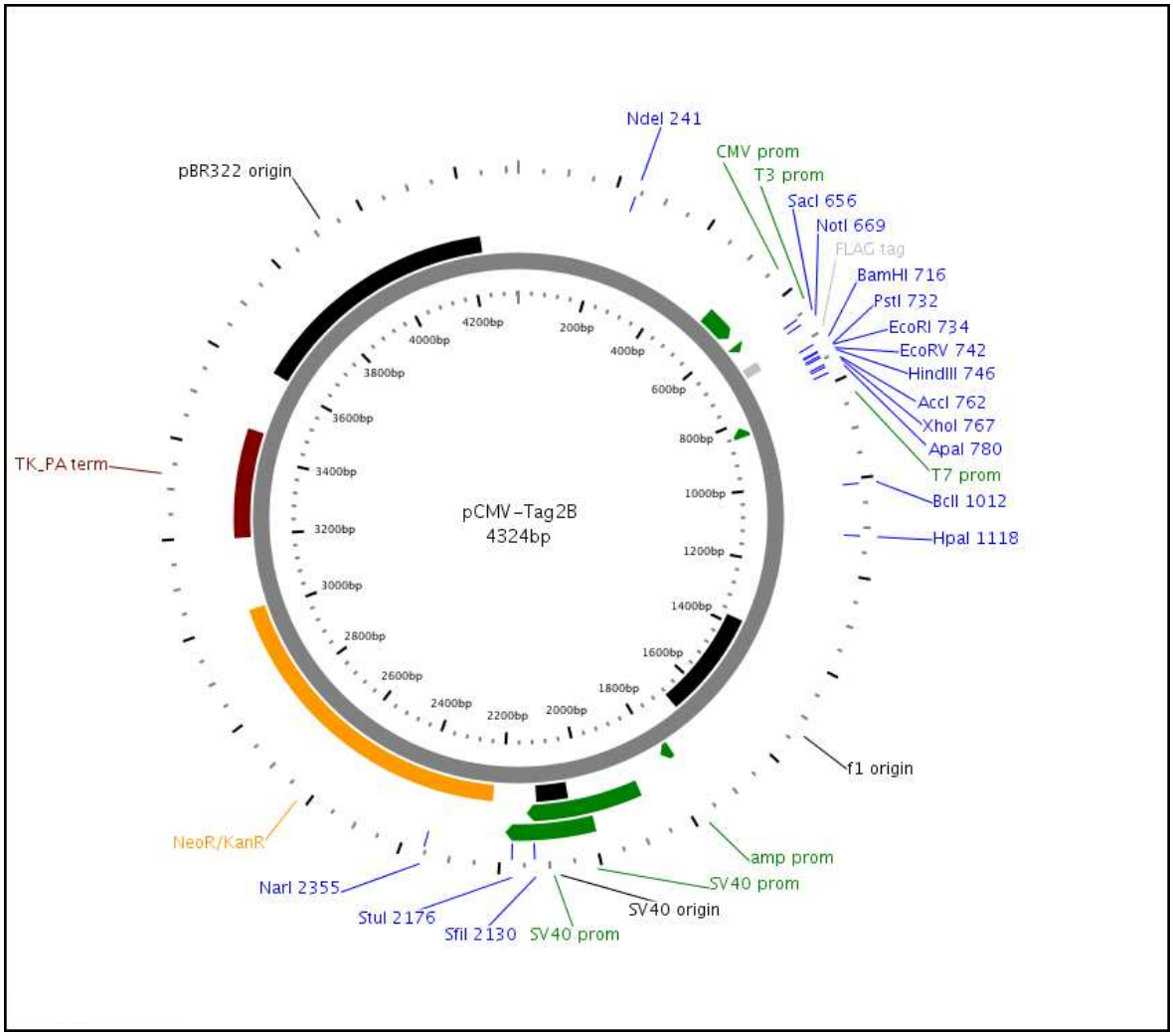

FIGURE A. 8: MAP OF PCMV-TAG2B VECTOR

A.2.1.2.5 Overview over all fragments used in this study

	protein fragment	tag	plasmid
IRS1	IRS1(wt, 1-1242)	myc-his	pCT
	IRS1(1-121/270-1242)		
	IRS1(1-1030)		
	IRS1(1-974)		
	IRS1(1-517)		
	IRS1(1-271)		
	IRS1(1-121)		
	IRS1(148-1242)		
	IRS1(270-1242)		
	IRS1(270-1030)		
	IRS1(270-974)		
	IRS1(270-517)		
	IRS1(974-1242)		
	IRS1(933-1242)	flag	pCMV-Tag 2B
	IRS1(933-1080)		
	IRS1(933-1169)		
	IRS1(1081-1242)		
	IRS1(974-1169)		
	IRS1(974-1119)		
	IRS1(974-1093)		
	IRS1(1013-1169)		
	IRS1(1013-1119)		
	IRS1(1013-1093)		
	IRS1(1064-1169)		
	IRS1(1064-1119)		
IRS2	IRS2(wt)	myc-his	pCT
	IRS2(PH)		
	IRS2(PTB)		
	IRS2(1-359)		
	IRS2(1-170)		
	IRS2(120-end)		
	IRS2(187-310)		
	IRS2(560-1321)		
GRP78	Grp78(336-519)	GST	pGEX4T-1
	Grp78(wt)	myc-his	pCT
	Grp78(336-517)		
	Grp78(336-517)	flag	
	Grp78(336-367)		
CGR19	Cgr19(wt)	GST	pGEX4T-1
	Cgr19(wt)	flag	pCT
	Cgr19(delta Zn)		

TABLE A. 2: PROTEIN FRAGMENTS USED FOR THIS STUDY

A.2.1.3 DNA analysis

For sequencing, plasmids were sent to Microsynth AG. Webcutter [63] was used to search for suitable restriction sites. Sequence search and alignments were performed with NCBI Blast [64]. Molecular weights of proteins were calculated using “Composition/molecular weight” [65]. Several proteomics and sequence analysis tools (e.g. DNA to protein translation, structure analysis, alignments) were provided by EXPASY [66].

A.2.1.4 Adenoviral vectors

Adenoviral constructs for expression of fusion proteins in CHO-IR cells were generated previously by Thomas Trüeb and Linhua Xu [41]. In brief, a sequence of interest was cloned between flanking LoxP sites in transfer vector containing the cytomegalovirus promoter (pCT) and a Zeocine resistance sequence allowing selection. Recombination between *pReceiver* (encoding the adenoviral genome) and pCT was achieved by co-transfection of *E.coli BM25* cells expressing Cre recombinase. Recombination product was amplified and isolated from *E. coli*. Mammalian HEK293 cells were then used for amplification of the adenovirus particles (see part A.2.2.2.2, Amplification of adenovirus).

A.2.2 Mammalian cell lines

A.2.2.1 Chinese hamster ovary cells expressing insulin receptor (CHO-IR)

Chinese Hamster Ovary cells stably transfected with a plasmid coding for the human insulin receptor (CHO-IR) were kindly provided by of Jeffery E. Pessin (Iowa City, USA).

A.2.2.1.1 Culture conditions

CHO-IR cells were maintained at 37 ℃ under 5 % CO_2 in F-12 (Ham) nutrient mixture supplemented with 10 % (v/v) FCS, 100 U/ml penicillin, 100 µg/ml streptomycin and 1 mM L-glutamine. Cells were splitted when they reached about 80 % confluence. All cell culture media and reagents were purchased from Gibco BRL (Invitrogen, Basel, Switzerland), unless otherwise stated.

A.2.2.1.2 Adenovirus-mediated expression of constructs

CHO-IR cells were grown on 10 cm-diameter-plates till about 70 % confluence. One plate was generally infected with viral particles at a multiply of infection (moi) of about 50. The

medium was changed before infection and about 16 hours after addition of the virus. Then cells were kept for another 12 hours at 37 ℃.

A.2.2.1.3 Lipofectamine-mediated expression of constructs

CHO-IR cells were grown on 10 cm-diameter-plates to 70 % confluency. For each plate 20 µg DNA was dissolved in 660 µl reduced serum medium OPTI-MEM I. Separately 40 µl Lipofectamin 2000 (Invitrogen) was mixed with 624 µl OPTI-MEM (ratio Optimem:Lipofectamin was 15,6:1 and DNA:Lipofectamin [µg/µl] was 1:2) . After 5 minutes at room temperature DNA/OPTI-MEM and OPTI-MEM/Lipofectamin solutions were carefully mixed by pipetting up and down and kept at room temperature for another 15 minutes to allow formation of micelles. CHO-IR cells were washed with PBS, then 8,5 ml OPTI-MEM was added per plate. The DNA/Lipofectamin/OPTI-MEM mixture was added to the plate and it was incubated for two hours at 37 ℃. Additional 5 ml growth medium were then added to the cells and they were incubated over night at 37 ℃. Next day medium was changed and cells were kept at 37 ℃ over night again. Cells were then scraped from the plate and either stored at -75 ℃ or lysed immediately (see below).

A.2.2.1.4 Cell lysis and protein determination

Cells were washed three times with PBS. 1 ml lysis buffer per 10 cm-diameter-plate (50 mM HEPES pH 7.5, 140 mM NaCl, 0.5 % Triton X-100, 1 mM PMSF, 10 mM NaF, 1 mM $Na_2H_2P_2O_7$, 1 mM Na_2O_4V, 3 µg/ml aprotinin, 3 µg/ml leupeptin) was added and cells were completely detached with a scraper. Lysis was completed by transferring cells to an Eppendorf tube and rotating them at 4 ℃ for at least half an hour. Centrifugation at 17'500 g for 10 minutes at 4 ℃ cleared the lysate. Supernatant was transferred into a fresh Eppendorf tube. If required total protein concentration was measured using the bicinchoninic acid assay (BCA) kit from Pierce (Rockford, USA). Expression of transgenes was assessed by SDS-PAGE and Western blot analysis.

A.2.2.2 Human embryonic kidney cells (HEK293)

Human embryonic kidney cells (HEK293) were provided by the research laboratory for Calcium Metabolism of Balgrist hospital (Zürich, Switzerland).

A.2.2.2.1 Culture condition

HEK293 cells were grown at 37 ℃ under 5 % CO_2 in D-MEM (Invitrogen, Basel, Switzerland) without sodium pyruvate, supplemented with 10 % fetal calf serum (FCS), 100 U/ml penicillin, 100 µg/ml streptomycin and 3.97 mM L-glutamin and 25 mM D-glucose.

A.2.2.2.2 Amplification of adenovirus

HEK293 were cultured in 75 cm^2 flasks (70 % confluence) and infected with adenoviral particles (moi=1). After about 50 % of cells had detached (2-3 days), cells were harvested. Using a scraper cells were detached, transferred into a 50 ml corning tube, centrifuged at 70 g for 5 minutes and redissolved in 2 ml of sterile D-MEM/ 2 % HEPES (pH 7,2 – 7,5, Invitrogen, Basel, Switzerland). After four consecutive freeze-thaw cycles (liquid nitrogen/ water bath), lysates were cleared at 1'570 g or 10 minutes at 4 ℃.

The supernatant contained infectious particles, and was stored at 4 ℃ or, for long term storage, as a glycerol stock at -20 ℃. Virus titer s were about 10^8 till 10^9 particles per ml.

A.2.3 Production of GST-fusion proteins

A.2.3.1 Expression of recombinant proteins

Recombinant GST-tagged proteins were produced in *Escherichia Coli BL21 (DE3)* transfected with the respective pGEX plasmid (Amersham Pharmacia Biotech, Uppsala, Sweden). Cells were grown in autoclaved and prewarmed LB-medium (L-Broth, BIO 101, La Jolla, USA) containing 200 µg/ml ampicillin. Cultures were shaken at 260 rpm at 37 ℃. Optical density (OD) at wavelength of λ = 600 nm was measured to assess growth. At OD between 0.4 and 0.8 recombinant protein expression was induced by addition of the non-metabolisable tag-promoter-inducer IPTG (isopropyl β-D-1 thiogalactopyranoside) at a concentration of 0.5 mM. After another four hours the bacteria were harvested. Bacterial cell pellets were either stored at -75 ℃ for later use or cells were lysed immediately.

A.2.3.2 Cell lysis

In order to achieve a high concentration of soluble fusion protein different lysis procedures (e.g. with different buffers, enzymatically versus mechanically) were tested. The challenge was to release the protein from insoluble inclusion bodies in the pellet. Finally a buffer containing of 50 mM Tris/HCl (pH 8), 10 mM EDTA, 0.5 mM PMSF and 6 M Urea was chosen for cell lysis. About 6 ml lysis buffer were used per gram of bacterial pellet. The lysate was sonicated to reduce viscosity and centrifuged. To renature the protein urea was gradually removed from the cleared lysate by dialysis at 4 ℃. Dialysis buffer contained stepwise 4 M Urea/ 200 mM NaCl, 3 M Urea/ 200 mM NaCl, 2 M Urea, 0.75 M Urea, 0.25 M Urea and 0 M Urea. GST-fusion protein production was assessed on SDS-PAGE. The renatured GST-fusion protein was later used for GST-pulldown (see chapter A.2.5.3).

A.2.4 Western blot analysis

A.2.4.1 Antibodies

Target	Species	Dilution Western	Catologue nr.	Company
Aktin	mouse	1:1'000	MAB1501	Millipore
Cbl	mouse	1:1'000	05-4	Upstate
flag	mouse	1:3'000	F-3165	Sigma-Aldrich
flag	rabbit	1:1'000	F-7425	Sigma-Aldrich
Grb2	rabbit	1:1'000	sc-255	Santa Cruz Biotechnology
GRP78	goat	1:1'000	sc-1051	Santa Cruz Biotechnology
his	mouse	1:3'000	clone His17	Anawa
IR (β chain)	rabbit	1:1'000	sc-711	Santa Cruz Biotechnology
IRS1	mouse	1:200	I 17820	Transduction Laboratories
IRS1	rabbit	1:200	sc-559	Santa Cruz Biotechnology
IRS2	goat	1:1'000	sc-1556	Santa Cruz Biotechnology
myc	mouse	1:50	-	own
p-Tyr	mouse	1:1500	u 05-321	Upstate
p85 (PI3K)	rabbit	1:5'000	u 06-195	Upstate
p-Thr	mouse	1:50	P-3555	Sigma-Aldrich
Shc	rabbit	1:1'000	sc-1695	Santa Cruz Biotechnology
SH-PTP2	rabbit	1:200	sc-280	Santa Cruz Biotechnology

TABLE A. 3: PRIMARY ANTIBODIES FOR WESTERN BLOTTING

Target	Species	Dilution Western	Catologue nr.	Company
goat	donkey	1:3'000	sc-2020	Santa Cruz Biotechnology
mouse	goat	1:3'000	sc-2005	Santa Cruz Biotechnology
rabbit	goat	1:3'000	170-6515	Biorad

TABLE A. 4: SECONDARY ANTIBODIES FOR WESTERN BLOTTING

A.2.4.2 SDS-PAGE

Minigels were prepared according to standard protocol [62] and run in BioRad chambers with SDS running buffer (250 mM Tris base, 2,5 M glycine, 1 % SDS). NuPAGE 4-12 % gradient Bis-Tris Gels (Invitrogen, Basel, Switzerland) were bought and run in chambers (Invitrogen System) according to manufacturers' instructions. For both gel-systems SDS-reducing buffer was prepared according to Laemmli, see reference [62]. For CHO-IR cell lysates the buffer was diluted to a final concentration of 1x, when proteins were detached from beads after co-immunoprecipitation or GST-pulldown experiments the buffer was used undiluted (4x). Heating at 90 ℃ for 5 minutes and subsequent cooling on ice denatured the proteins. SDS-PAGE Broad Range Marker (Biorad, Reinach, Switzerland) was used.

A.2.4.3 Staining SDS-PAGE with Coomassie brilliant blue

Staining solution contained 0.25 % (w/v) Coomassie Brilliant Blue R250 (Biorad, Reinach, Switzerland) in 45 % water/ 45 % methanol/ 10 % glacial acetic acid. Gels were destained to visualize the protein bands in 45 % water/ 45 % methanol/ 10 % glacial acetic acid.

A.2.4.4 Immunoblotting

Proteins were transferred to Hybond-P PVDF membranes (GE Healthcare Bio Sciences, Otelfingen, Switzerland) using the Invitrogen chambers according to the instructions given by the company. Prior to incubation with antibody the membranes were blocked with 2 % w/v milk powder (Biorad, Reinach, Switzerland) in TBS-T (250 mM Tris/HCl pH7.5, 1.5 M NaCl, 0.05 % Tween-20) for 30 minutes at 37 ℃. Mem branes were then incubated in the presence of primary and subsequent by secondary antibodies diluted in blocking solution. Antibodies and the dilutions are indicated in part A.2.4.1, Table A.3 (primary antibodies) and Table A.4 (secondary antibodies). After each antibody incubation step the membranes were washed with TBS-T (3 times for at least 10 minutes at room temperature). Finally the membranes were incubated with Lumi-light Western Blotting substrates 1 and 2 (Roche Diagnostic, Rotkreuz, Switzerland) and signals were detected using a Fuji LAS-3000 system and Aida Software (Raytest, Germany).

A.2.4.5 Silver staining

Mini gels were stained using the SilverQuestTM Silver Staining Kit (Invitrogen, Basel, Switzerland) according the manufacturer's instructions.

A.2.5 Pulldown experiments

For Co-immunoprecipitation, GST-pulldown and Ni-NTA purification experiments several different procedures varying in buffer composition, incubation time, washing frequency, protein and bead concentration/volumes were tested. The below-mentioned protocols turned out to be the most suitable ones.

A.2.5.1 Beads

Glutathione Sepharose™ 4 Fast Flow beads (GE Healthcare Bio Sciences, Otelfingen, Switzerland) were used for GST-pulldown assays.

Co-immunoprecipitations were performed using Protein G Sepharose™ 4 Fast Flow or rpm Protein A Sepharose™ Fast Flow (both GE Healthcare Bio Sciences, Otelfingen, Switzerland). In addition to these sepharose beads trisacryl GF-2000 beads with immobilised protein A (Pierce, Rockford, USA) were also used. Less unspecific binding was observed to trisacryl GF-2000 beads than to rpm Protein A Sepharose™ Fast Flow.

For purification of his-tagged protein, Ni-NTA agarose beads from Qiagen (Hombrechtikon, Switzerland) were used.

A.2.5.2 Co-immunoprecipitation (co-IP)

CHO-IR cells (10 cm-diameter-plate) overexpressing tagged fusion proteins were lysed in 1 ml lysis buffer containing 50 mM HEPES pH 7.5, 140 mM NaCl, 0.5 % Triton X-100, 1 mM PMSF, 10 mM NaF, 1 mM $Na_2H_2P_2O_7$, 1 mM Na_2O_4V, 3 µg/ml aprotinin, 3 µg/ml leupeptin. Protein content in lysates was determined by BCA and aliquots containing between 100 - 500 µg total protein were used per experiment. 2-3 µg of primary antibody were mixed with 400 µl of lysate. The mixture was incubated at 4 °C on a rotating wheel for at least four hours or over night. Protein A or G beads were washed three times with CHO-IR lysis buffer prior to blocking with 1 % BSA in CHO-IR lysis buffer for 30 minutes till one hour at 4 °C. Beads were washed again twice with CHO-IR lysis buffer. 15 µl of the washed beads were added per tube and the mixture was incubated for four hours at 4 °C on a rotating wheel. The beads were washed three times with CHO-IR lysis buffer, once with 1 % BSA in CHO-IR lysis buffer (for at least half an hour on the rotating wheel at 4 °C), once again with CHO-IR lysis buffer and twice with PBS. Centrifugation for 2 minutes at 3000 g allowed collection of the beads between washing steps. The last wash solution was aspirated as completely as possible. The proteins were detached from the beads by adding 50 µl of 4x SDS sample buffer (see part A.2.4.2.) and boiling at 90 °C for 5

minutes followed by cooling on ice. The mixture was centrifuged and the supernatant was transferred into a fresh Eppendorf tube and analysed by SDS-PAGE and immunoblotting.

A.2.5.3 GST-pulldown

GST-fusion proteins were produced in *E. coli* as described in part A.2.3. Beads were washed five times with PBS and blocked in a solution of 1 % BSA in PBS for 30 minutes at 4 °C on a rotating wheel. After two more PBS washing steps the beads were equilibrated in *E. coli* lysis buffer. Per gram of original bacterial pellet 500 µl of 1:1 slurry:beads solution were used. As the volume of the dialysate was 6 ml per g of bacterial pellet, the dialysate was incubated stepwise with the glutathione beads: in a 2 ml Eppendorf tube 2 ml of the dialysate were consecutively added to the same beads and incubated for 2 hours or over night at 4 °C with rotation. Beads were finally collected by centrifugation for 5 minutes at 500 g at 4 °C and supernatant was aspirated. Beads were washed five times with PBS and were then stored up to some days in PBS (the same volume than beads). The amount of GST-fusion protein on the beads was assessed by SDS-PAGE and Coomassie staining. Usually, only a small fraction of the total fusion protein in the dialysate was binding to the glutathione beads.

Appropriate amounts of immobilised GST-fusion protein were equilibrated twice with CHO-IR lysis buffer and distributed to fresh tubes for the GST-pulldown experiment; at least 800 ng of fusion protein were used per tube (about 15 µl beads). After centrifugation, the buffer was removed from the beads and the cleared lysate of CHO-IR cells containing myc-tagged protein-prey (see part A.2.2.1.4) was added. Samples were incubated for 4 hours at 4 °C on a rotating wheel. Beads were collected by centrifugation and washed once with CHO-IR lysis buffer and 5 times with PBS. One or two wash steps lasted for 30 minutes on the beads to allow diffusion of unspecifically bound proteins. After the last wash step the buffer was aspirated off as completely as possible and SDS reducing buffer (see part A.2.4.2) was added. Samples were boiled at 95 °C for 5 minutes and immediately cooled on ice-water. The protein-containing supernatant was separated from the beads by centrifugation and analysed by SDS-PAGE and Western blotting.

A.2.5.4 Affinity purifications using Ni-NTA under native conditions: co-pulldown

10^7 CHO-IR cells (one 10 cm dish) overexpressing the respective fusion protein(s) were lysed in 700 µl lysis buffer. The composition of the buffers for this experiment is listed in Table A.5. Lysates were cleared by centrifugation at 17'500 g for 10 minutes at 4 °C. Ni-

NTA beads were washed three times with water and five times with lysis buffer. 30 µl beads were added to 600 µl cleared CHO-IR lysate followed by incubation by a rotating wheel at 4 °C for 2 to 4 hours. The beads were then collected by centrifugation (1 minute at 3'000 g) and washed seven times with lysis buffer. The third wash step contained 1 % BSA and was performed for 30 minutes at 4 °C with rotation. Elution buffer containing 400 mM imidazole was added, mixed and incubated for two minutes to elute his-tagged proteins and binding partners (three times 50 µl buffer). The eluate was analysed by SDS-PAGE and Western blotting.

Lysis buffer	**Elution buffer**
50 mM NaH_2PO_4/Na_2HPO_4 0.5 % Nonidet P40 300 mM NaCl 10 mM imidazole 1 mM PFSF/PM 3 µg/ml leupeptin 3 µg/ml aprotein 10 mM NaF 1 mM $Na_2H_2P_2O_7$ 1 mM Na_3O_4V pH set to 8	50 mM NaH_2PO_4/Na_2HPO_4 0.5 % Nonidet P40 300 mM NaCl 400 mM imidazole pH set to 8

TABLE A. 5: BUFFERS FOR NI-NTA CO-PULLDOWN

A.2.5.5 Affinity purifications using Ni-NTA under denaturing conditions: purification

10^7 CHO-IR cells (one 10 cm-dish) were lysed in 700 µl lysis buffer for at least one hour at 4 °C. The composition of all the buffers for this experiment is listed in Table A.6. Lysates were cleared by centrifugation at 17'500 g for 10 minutes at 4 °C. Urea was added to a final concentration of 6 M and imidazole was added to a final concentration of 10 mM. The pH was adjusted to 8. Samples were incubated for 10 minutes on ice. At the same time Ni-NTA beads (see part A.2.5.1) were washed four times with wash buffer A. Subsequently 30 µl of the beads were added to the lysate and incubated for two hours at 4 °C on a rotating wheel. Beads were collected by a short centrifugation at 3'000 g and washed once with wash buffer A and twice with wash buffer B. The his-tagged protein was eluted by stepwise increasing imidazole concentration. Consecutively 100 µl of elution buffer (EB) 40, 100 µl EB60, 100 µl EB80, 100 µl EB100, 100 µl EB250, 200 µl EB250 and 200 µl EB250 was added to the beads, mixed well and incubated for 2 minutes. The

last elution buffer was incubated for 1 hour on a rotating wheel at 4 ℃. All eluates were analysed separately with SDS-PAGE and silver staining.

Lysis buffer	**Wash buffer A**	**Wash buffer B**	**Elution buffer X (X = 40, 60, 80, 100, 250)**
50 mM NaH_2PO_4/ Na_2HPO_4	50 mM NaH_2PO_4/ Na_2HPO_4	50 mM NaH_2PO_4/ Na_2HPO_4	50 mM NaH_2PO_4/ Na_2HPO_4
50 mM HEPES	50 mM HEPES		
0.5 % Triton X-100	0.5 % Triton X-100	0.5 % Triton X-100	0.5 % Triton X-100
300 mM NaCl	300 mM NaCl	300 mM NaCl	300 mM NaCl
1 mM PMSF/PM	1 mM PMSF/PM		
3 mg/ml leupeptin	3 mg/ml leupeptin		
3 mg/ml aprotein	3 mg/ml aprotein		
10 mM NaF	10 mM NaF		
1 mM $Na_2H_2P_2O_7$	1 mM $Na_2H_2P_2O_7$		
1 mM Na_3O_4V	1 mM Na_3O_4V		
	6 M urea	6 M urea	6 M urea
	10 mM imidazole	20 mM imidazole	x mM imidazole
pH set to 8	pH set to 8	pH set to 8	pH set to 8

TABLE A. 6: BUFFER FOR NI-NTA PURIFICATION OF HIS-TAGGED PROTEIN

A.2.5.6 Analysis of results from binding assays

Binding in GST-pulldown and Co-immunoprecipitation experiments was evaluated taking the different expression levels of the fusion proteins into account. The amount of protein in the eluate was always compared to the amount of this protein in the lysate at the start of the experiment to estimate binding intensities. To compare between different assays the mean binding intensity of all the single assays with the same fragment was calculated.

A.3 Results

Based on our hypothesis that IRS proteins act as integrators of signalling information and that context-specific signal transduction could depend on an interplay of *cis-elements* on IRS with recently identified *trans-acting* factors, we aimed at defining these *cis-elements* on IRS (see part A.1.6, hypothesis and aims) based on previously identified binding partners. This included the elucidation of the regions required for binding between IRS1/2 and the newly identified binding proteins GRP78 and CGR19.

A.3.1 Constructs for binding assays

We wanted to map binding between IRS1/2 and GRP78 and between IRS1/2 and CGR19 in GST-pulldown, Co-immunoprepipitations and Ni-NTA co-pulldowns. Truncations of IRS and candidate proteins GRP78 and CGR19 were fused to different tags for these binding assays. An overview over the different constructs is shown in Figure A.9. The cloning strategy is described in part A.2.1.2, Materials and Methods. Several constructs already existed at the beginning of the study, others were newly generated.

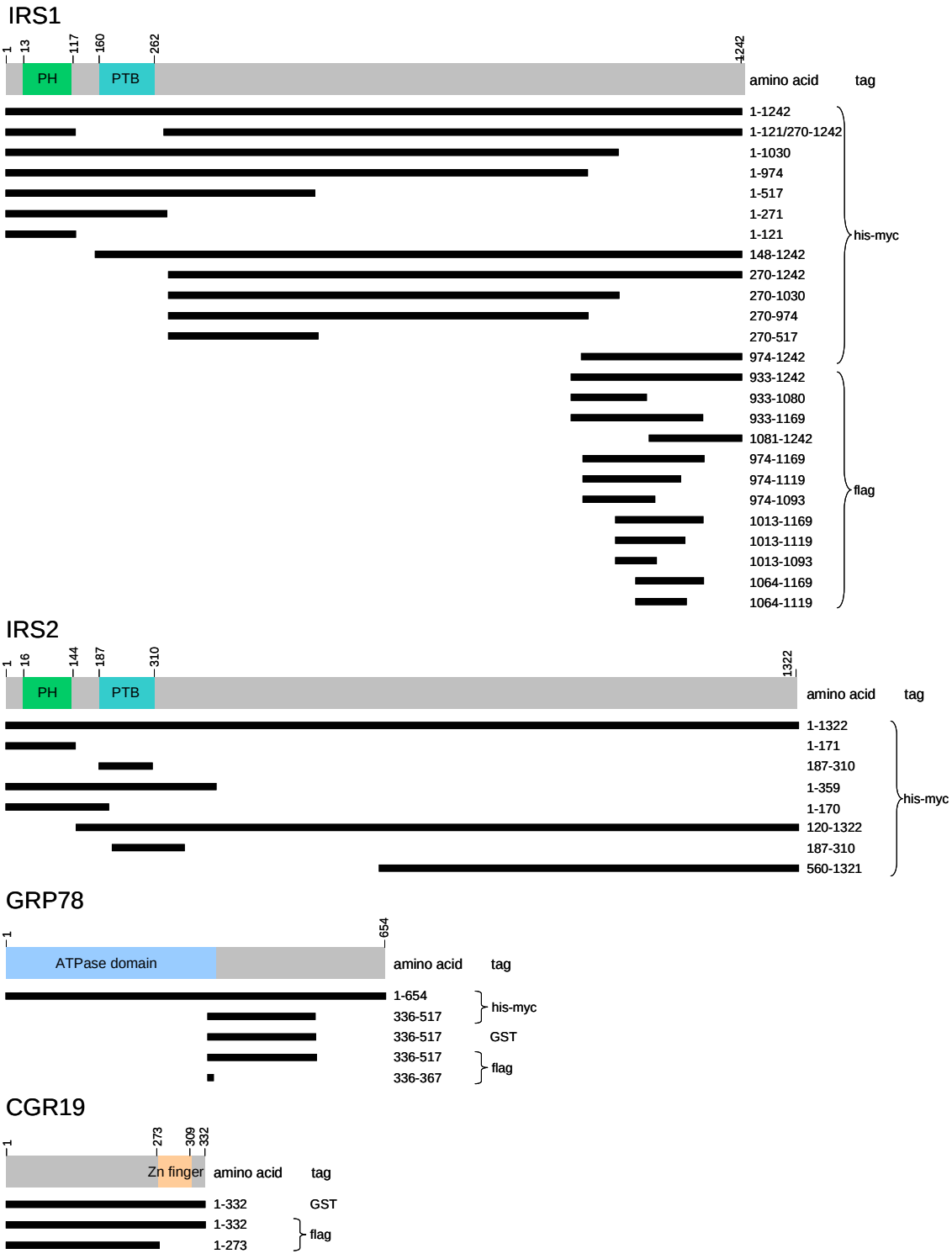

FIGURE A. 9: FRAGMENTS OF IRS1, IRS2, GRP78 AND CGR19

Grey bars illustrate full-length wild type proteins, black bars represent the amino acid sequences of the fragments that were used for GST-pulldown, Co-immunoprecipitations and Ni-NTA co-pulldown experiments (sequences: IRS1 human, IRS2 mouse, GRP78 human, CGR19 rat).

A.3.2 Determination of binding regions

A.3.2.1 Binding sites on IRS1 that bind to GRP78

A.3.2.1.1 Confirmation that binding sites must be present on IRS1(270-517) and IRS1(974-1242)

Two binding regions on IRS1 that bind GRP78 had been previously identified by Brad Joblin [45] and Anja Egli [67]: One between aa 270-517 and one between aa 974-1242. In the course of this study we successfully confirmed these findings by GST-pulldown and co-IP experiments.

A.3.2.1.2 C-terminal binding site: IRS1(1013-1119)

In co-IP and Ni-NTA co-pulldown experiments, the C-terminal binding site was more precisely mapped, starting from IRS1(974-1242). Results are summarised in Figure A.10.

As GRP78 often binds unspecifically to sepharose/ agarose beads, we decided to bind GRP78-myc-his to the beads and then to perform Ni-NTA co-pulldown or co-IP in the presence of flag-tagged IRS1 fragments. All the truncations that were used for mapping of the C-terminal binding site on IRS1 are shown in Figure A.10. IRS1(933-1242)-flag was tested first together with IRS1(1081-1242)-flag, IRS1(933-1080)-flag, IRS1(933-1169)-flag and IRS1(974-1169)-flag. IRS1(974-1169)-flag was the shortest fragment that was co-pulled down. A representative Ni-NTA Co-pulldown experiment is shown in Figure A.11. As expected, the two longer fragments IRS1(933-1242)-flag and IRS1(933-1169)-flag were also co-pulled down. The fact that the two fragments IRS1(933-1080)-flag and IRS1(1081-1242)-flag were not co-pulled down in this assay (and only weakly in other experiments) suggested that binding could occur in the region around aa 1081, the break point between the two fragments (indicated in green in Figure A.10). Hence IRS1(974-1169)-flag was broken down into smaller truncations (cloning details see part A.2.1.2.4) around aa 1081: IRS1(974-1119)-flag, IRS1(974-1093)-flag, IRS1(1013-1169)-flag, IRS1(1064-1169)-flag, IRS1(1013-1119)-flag, IRS1(1013-1093)-flag and IRS1(1064-1119)-flag. While IRS1(1064-1119)-flag was probably to small to be detected in SDS PAGE gel, the remaining fragments were indeed expressed in CHO-IR cells. A preliminary Ni-NTA co-pulldown experiment with GRP78-myc-his only co-pulled down fragment IRS1(1013-1119)-flag. The project was stopped before this experiment could be repeated and hence the notion that there is a binding site for GRP78 on IRS1(1013-1119) needs confirmation.

An overview of the regions on IRS1 binding to GRP78 is shown in Figure A.15, where the newly revealed C-terminal binding fragment IRS1(1013-1119) is shown as a dashed ellipse.

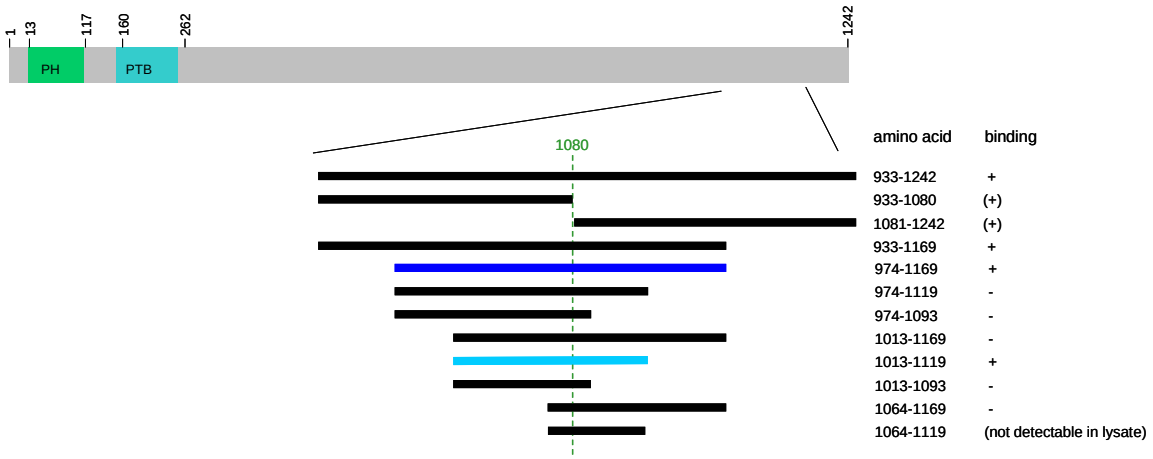

FIGURE A. 10: C-TERMINAL FLAG-TAGGED IRS1 FRAGMENTS FOR MAPPING OF GRP78 BINDING SITE(S)

Grey bar illustrates full-length wild type IRS1, black bars represent the amino acid sequences of the fragments that were used for C-terminal mapping experiments. + represents binding, (+) weak or no binding, - means no binding (preliminary results). Dark blue represents the smallest C-terminal binding fragment (confirmed in several experiments), light blue stands for a more precise mapping fragment revealed in a preliminary experiment.

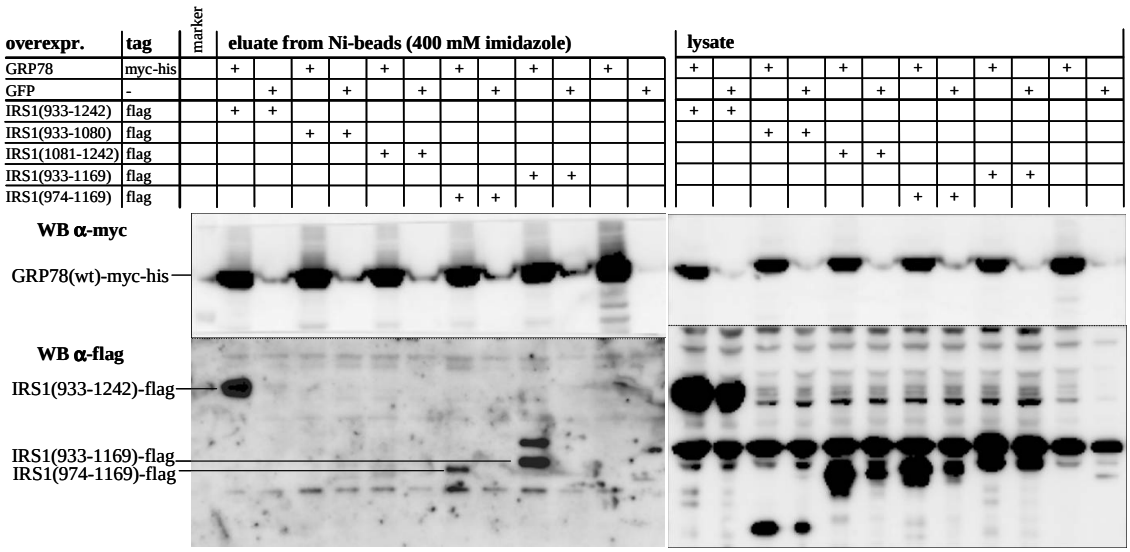

FIGURE A. 11: WESTERN BLOT SHOWING NI-NTA CO-PULLDOWN OF GRP78-MYC-HIS WITH C-TERMINAL IRS1-FLAG FRAGMENTS

Lysates from CHO-IR cells overexpressing the indicated C-terminal flag-tagged IRS1 fragments and GRP78-myc-his (or GFP control) were incubated in the presence of Ni-NTA beads. Eluates from the beads were analysed by Western blotting with α-flag antibody to detect co-pulled down IRS1 fragments.

A.3.2.1.3 Sequence analysis of IRS1(974-1169)

As described, IRS1(974-1169) was the smallest C-terminal binding fragment confirmed in several experiments. It is co-linear with IRS1(1013-1119). These GRP78-binding regions were analysed for the presence of special features in their sequence. Ser, Thr and Tyr residues are highlighted in the sequence in Figure A.12. The smallest fragment (aa 1013-1119) contained no Tyr residue. Strikingly many sites were Ser residues, 16 % of all amino acids in IRS1(974-1169) and as well as in IRS1(1013-1119). In addition, the calculated isoelectric point (pI) was high for both fragments, it was 9.6 for aa 974-1169 and 11.1 for aa 1013-1119 [66]. Sequence pattern search was performed with “Pattern search tool” from PIR [68], predicted patterns are underlined in Figure A.12. In IRS1(1013-1119) four sites were predicted: a PKC phosphorylation site, a N-myristoylation site, a N-glycosylation site and a cAMP-/ cGMP-dependent protein kinase phosphorylation site.

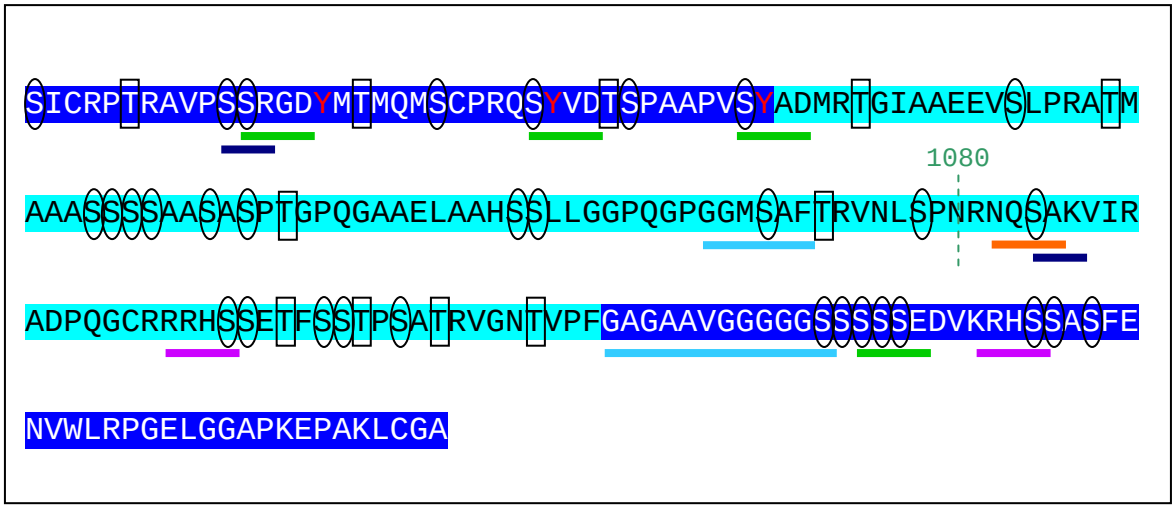

FIGURE A. 12: AMINO ACID SEQUENCE OF SMALLEST BINDING FRAGMENT IRS1(974-1169)
C-terminal amino acid sequence of IRS1 that binds to GRP78. The whole sequence (dark blue and light blue) corresponds to IRS1(974-1169), the light blue sequence to IRS1(1013-1119). Ser residues are indicated by ellipses, Thr by rectangles and Tyr in red letters. Underlined in green are casein kinase (CK) II phosphorylation sites, in dark blue PKC phosphorylation sites, in light blue an N-myristoylation site, in orange a N-glycosylation site, and in violet cAMP-/ cGMP-dependent protein kinase phosphorylation sites (all sequence patterns were predicted from “Pattern search tool” from PIR, [68]).

As GRP78 binds to IRS1 and IRS2, we tested whether sequences in IRS2 showed similarity to IRS1(1013-1119) indicating possible binding sites. IRS1(1013-1119) was compared to full length IRS2 by the “Alignment tool” from PIR [68]. IRS2(1062-1156) was found and alignment to IRS1(1013-1119) showed 42 % identical amino acids (Smith-

Waterman algorithm [68]: Z-score=238.7, E-value=1.7e-11, Smith-Waterman score=198, similarity 65 %). The alignment is shown in Figure A.13. Alignment of the 26 aa long stretch between IRS1(1082-1107) and IRS2(1119-1144) contains 25 similar and 22 identical residues in close proximity to aa 1080 in IRS1 (see Figure A.13, red rectangle).

We searched for kinase-specific phosphorylation sites in IRS1(1013-1119) and IRS2(1062-1156) using the online tool “NetPhosK” [69]. It was predicted that Ser1100 in IRS1 and Ser1137 in IRS2 were predicted to be phosphorylated by PKA, Ser1101/ Ser1138 by PKB and Thr1103/ Thr1140 by PKC (indicated in Figure A.13). Interestingly, these sites are located in IRS1(1082-1107) respectively IRS2(1119-1144) as well. The only predicted common pattern in the respective regions of IRS1 and IRS2, the cAMP-/ cGMP-dependent protein kinase phosphorylation site, was also found in IRS1(1082-1107)/ IRS2(1119-1144) (Figure A.13, violet underlined). Interestingly, only 9 (out of 25) Ser and Thr sites were conserved in IRS1(1013-1119) and IRS2(1062-1156). However 6 of these Ser/ Thr sites are located in IRS1(1082-1107) / IRS2(1119-1144), the part with highest similarity.

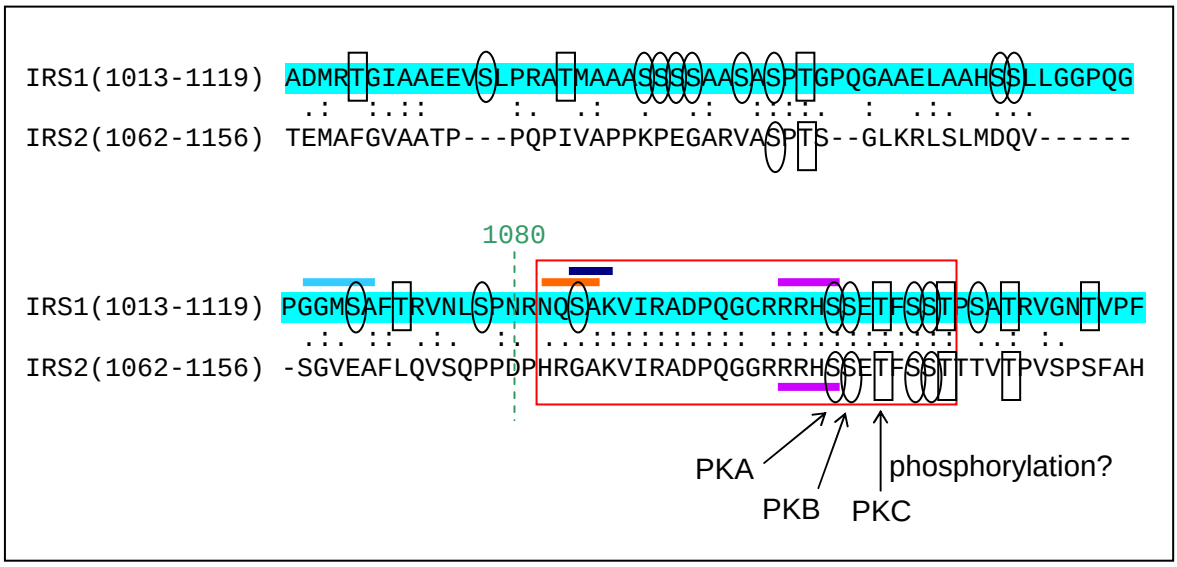

FIGURE A. 13: ALIGNMENT OF IRS1(1013-1119) AND IRS2(1062-1156)
The smallest binding fragment IRS1(1013-1119) was aligned to full-length IRS2. The region in IRS2 sharing the highest number of identical residues (42 %) with IRS1(1013-1119) spanned aa (1062-1156). Within this alignment, IRS1(1082-1107) and IRS2(1119-1144) shows highest similarity, indicated by a red rectangle. Ser residues are indicated by ellipses and Thr by rectangles. Dark blue represents PKC phosphorylation site, light blue N-myristoylation site, orange N-glycosylation site, violet cAMP-/ cGMP-dependent protein kinase phosphorylation site. Arrows indicate phosphorylation sites predicted with the highest probability from “NetPhosK” online tool [69].

A.3.2.1.4 Comparison of IRS1(270-517) and IRS1(974-1169)

To test whether the two binding regions for GRP78 on IRS1 share conserved sequences, IRS1(974-1169) was aligned to the N-terminal binding region IRS1(270-517) (Figure A.14). The overlapping stretch showed only 24.5 % identity, however higher than for two randomly chosen sequences (Smith-Waterman algorithm [68]: Z-score=100.4, E=0.00088, Smith-Waterman score=83, similarity 51.0 %). Conserved sites were concentrated in the C-terminal part of IRS1(974-1169), between aa1140-1145.

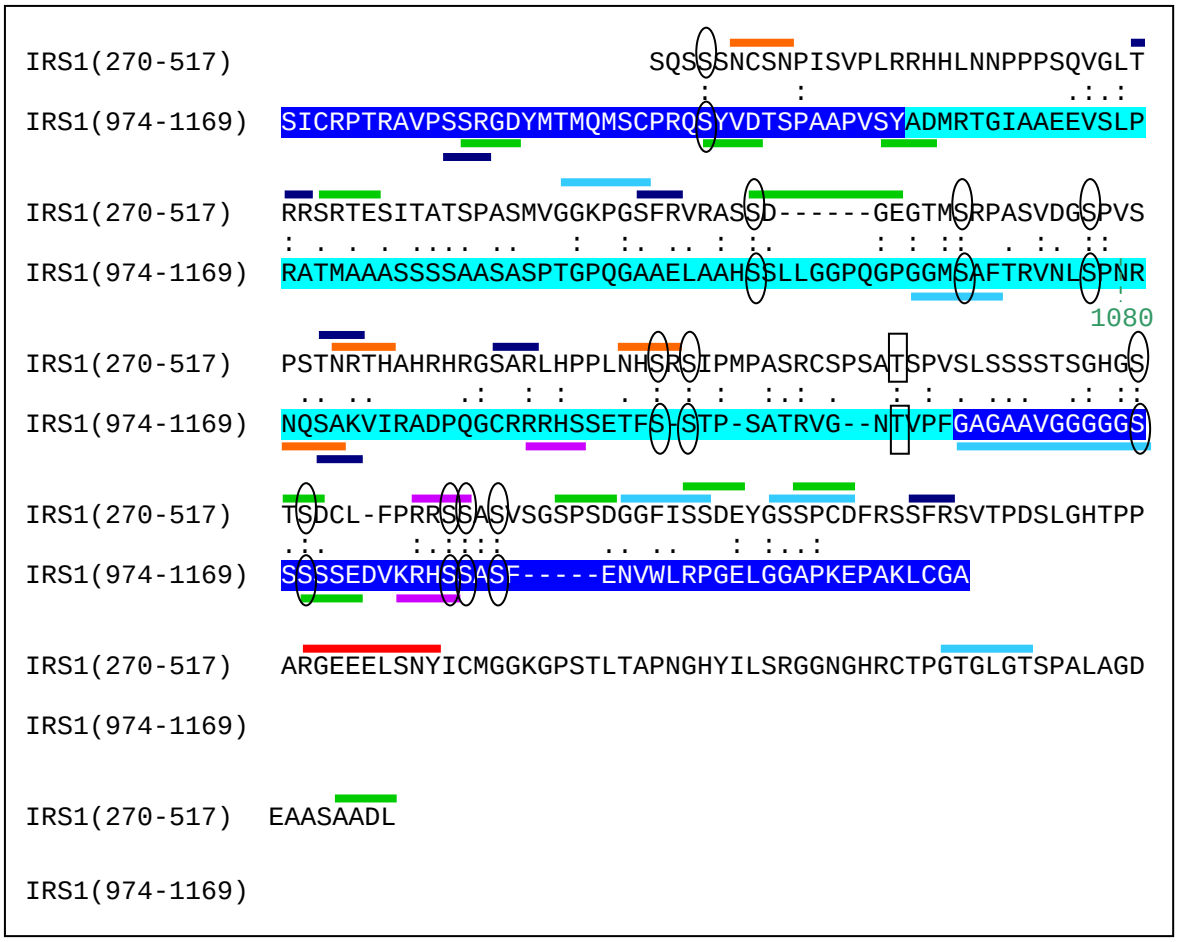

FIGURE A. 14: ALIGNMENT OF IRS1(270-517) AND IRS1(974-1169)
The smallest confirmed C-terminal binding fragment IRS1(974-1169) was aligned to N-terminal binding region IRS1(270-517) to analyse for sequence homology [68]. The dark blue together with the light blue sequence corresponds to aa974-1169, the light blue to aa1013-1119, respectively. The overlapping stretch showed 24.5 % identity as indicated by colon [68]. Common Ser residues are indicated by ellipses and common Thr with rectangles. Underlined in green are casein kinase (CK) II phosphorylation sites, in dark blue PKC phosphorylation sites, in light blue N-myristoylation sites, in orange N-glycosylation sites, in violet cAMP-/ cGMP-dependent protein kinase phosphorylation sites and in red a Tyr phosphorylation site (all sequence patterns were predicted from “Pattern search tool” from PIR [68]).

IRS1(974-1169) was also aligned to IRS1(1-973), the N-terminal remainder of IRS1. Interestingly, IRS1(266-435) was identified, a segment collinear with IRS1(270-517) (Smith-Waterman algorithm [68]: Z-score=94.9, E-value=0.0018, Smith-Waterman score: 88, identity 23.7 %, similarity 49.7 %).

Sequence patterns such as PKC phosphorylation sites, N-myristoylation sites, N-glycosylation sites, a cAMP-/ cGMP-dependent protein kinase phosphorylation sites and a Tyr phosphorylation site were predicted on IRS1(974-1169) and IRS1(270-517) [68]. Due to overall low sequence similarity, it is difficult to decide whether the sites are conserved or not. Noticeable is a cAMP-/ cGMP-dependent protein kinase phosphorylation sites in region with higest similarity, in IRS1(409-415) and IRS1(1139-1145).

A.3.2.1.5 Overview of the binding sites on IRS1 that bind to GRP78

Binding regions for GRP78 on IRS1 were identified between aa 270-517 and aa 974-1169. The C-terminal binding region aa 974-1169 was more precisely mapped and preliminary results indicated that binding takes place between aa 1013-1119. A summary of the location of these binding sites is shown in Figure A.15.

FIGURE A. 15: REGIONS ON IRS1 THAT BIND TO GRP78
The regions on IRS1 that bound to GRP78 are illustrated with blue ellipses, dashed ellipse indicates that region is not confirmed yet (aa 1013-1119). Binding regions lie between aa 270-517 and aa 974-1169.

A.3.2.2 Binding site in GRP78 that binds to IRS1

Binding of GRP78(336-517) to IRS1 and IRS2 had been previously defined by Brad Joblin. This study confirmed these findings. One smaller construct GRP78(336-376)-flag containing the Hsp70 domain was generated, but due to its small size the encoded protein could not be detected in SDS PAGE. Figure A.16 illustrates the region on GRP78 that bound to IRS1.

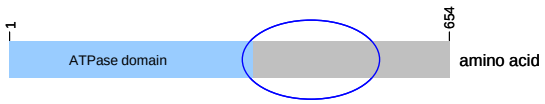

FIGURE A. 16: REGION ON GRP78 THAT BOUND TO IRS1
The region on GRP78 that bound to IRS1 is illustrated with a blue ellipse, binding region lies between aa 336-517.

A.3.2.3 Binding between IRS1 and CGR19

The binding sites for CGR19 on IRS1 were mapped by GST-pulldown experiments using the CGR19-GST fusion protein. Figure A.17 shows a representative GST-pulldown experiment in which CGR19(wt)-GST was bound to glutathione beads. Strong co-precipitation was detected for full-length IRS1-myc-his, IRS1(1-271)-myc-his and IRS1(270-974)-myc-his. All mapping experiments together revealed that CGR19 binds to one N-terminally located region on IRS1 comprising the domains PH/ PTB and to a second region between aa 517-974. An overview is given in Figure A.18.

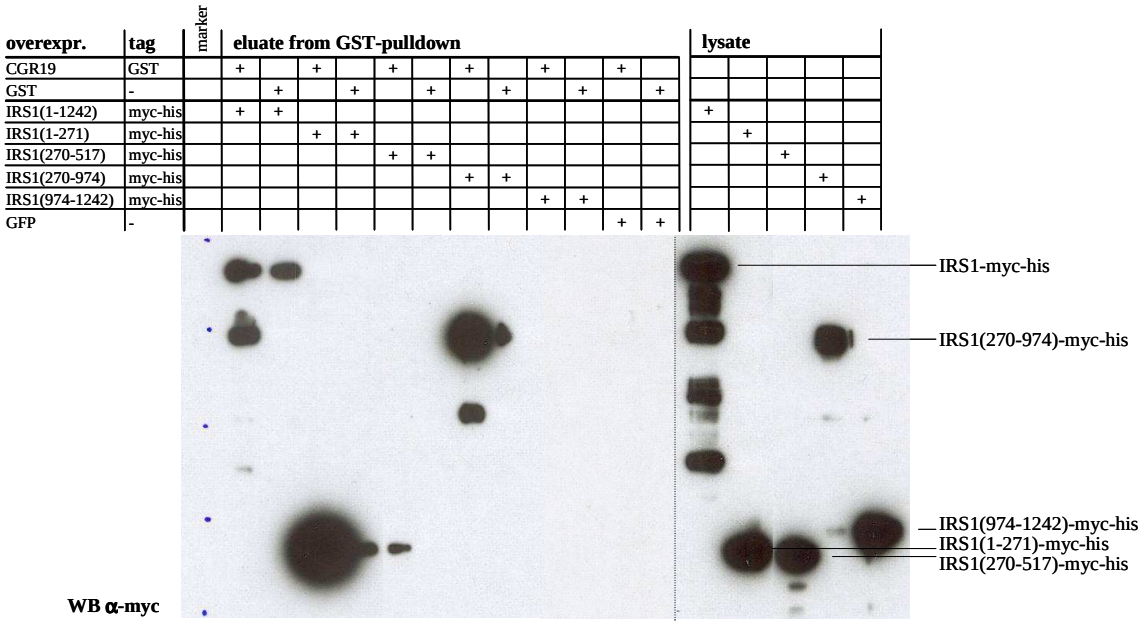

FIGURE A. 17: WESTERN BLOT ANALYSIS OF A GST-PULLDOWN EXPERIMENT WITH CGR19(WT)-GST AND IRS1-MYC-HIS FRAGMENTS

Lysates from CHO-IR cells overexpressing the indicated IRS1 fragments (or GFP control) were incubated with CGR19-GST (or GST control) bound to gluthathione beads. Eluates from the beads were analysed by Western blotting with α-myc antibody to detect co-pulled down IRS1 fragments.

For further mapping Ni-NTA co-pulldown with all our myc-his-tagged IRS1 fragments was planned. To this end, CGR19 was fused to a flag-tag. Mapping was not followed up as the project was stopped at that time point. Due to the same reason the binding sites of IRS1 on CGR19 were not determined.

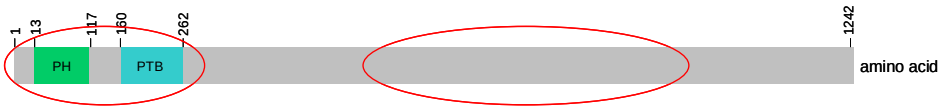

FIGURE A. 18: REGIONS ON IRS1 THAT BOUND TO CGR19
The regions on IRS1 that bound to CGR19 are illustrated with red ellipses. Binding regions span aa 1-271 and aa 517-974.

A.3.3 Purification and enrichment of IRS1-myc-his

We had postulated (see A.1.6, hypothesis and aims) that different patterns of phosphorylated and unphosphorylated Thr, Ser and Tyr residues on IRS must exist dependent on combinations of stimuli. Using 2D gel electrophoresis we wanted to visualise these different phosphorylation patterns. Differently phosphorylated isoforms of IRS1 with distinct isoelectric points are expected to be separable in 2D gel.

CHO-IR cells were transfected with adenovirus encoding IRS1-myc-his. In first experiments cells were stimulated with insulin to induce phosphorylation. For later experiments it was planned to combine different stimuli as e.g. insulin and IGF-1. After stimulation, cells were lysed and IRS1-myc-his was purified using Ni-NTA beads.

For Ni-NTA purifications different conditions were tested e.g. varying buffer composition, incubation time, washing frequency, protein and bead concentrations/ volumes. The whole process was performed with batch incubation or with columns. In addition, his-tagged IRS1 was bound to the matrix under denaturing or under native condition. One of the effective purification protocols is described in part A.2.5.5. In short, CHO-IR cells overexpressing IRS1-myc-his were lysed under denaturing conditions (6 M urea). Lysates were mixed with Ni-NTA beads. After washing, the his-tagged protein was eluted from the beads by stepwise increasing imidazole concentrations. A silver-stained SDS-PAGE of a representative IRS1-myc-his purification experiment is shown in Figure A.19.

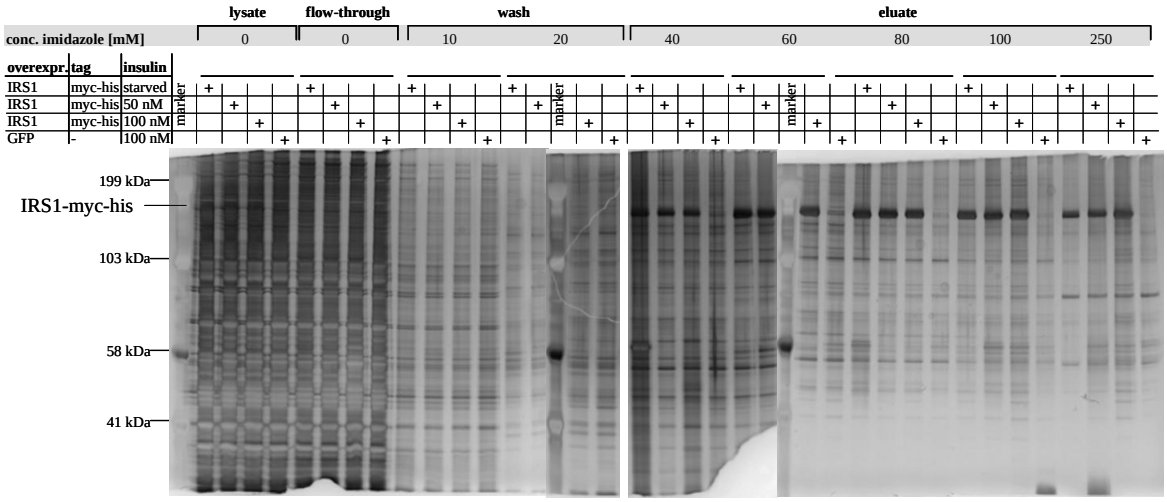

FIGURE A. 19: SILVER STAINING AFTER SDS-PAGE OF NI-NTA PURIFICATION OF IRS1-MYC-HIS

CHO-IR cells overexpressing IRS1-myc-his or GFP (negative control) were stimulated with insulin (50 nM or 100 nM) to induce phosphorylation. Cells were lysed under denaturing conditions (lysate) and lysate was incubated with Ni-NTA beads to pulldown IRS1-myc-his. Beads were washed with increasing imidazole concentration (wash), finally IRS1-myc-his was eluted stepwise with 40, 60, 80, 100 and 250 mM imidazole (eluate). Size of IRS1-myc-his protein band and marker bands are indicated.

Western blotting with α-myc antibody confirmed that the protein that bound to the Ni-NTA beads and that was stained prominently in silver staining (see Figure A.19, MW around135 kDa) was IRS-myc-his. A Western blot analysis of fractions of a purification experiment is depicted in Figure A.20. IRS1-myc-his was present in the CHO-IR cell lysate, whereas in the flow-through after the incubation with the Ni-NTA beads the amount of protein was below the detection limit. In the eluate IRS1-myc-his was detected.

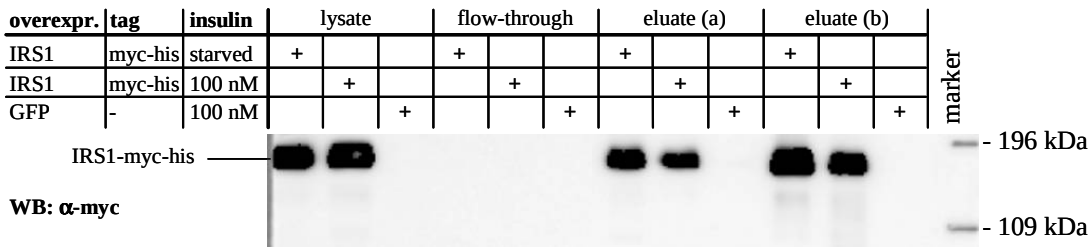

FIGURE A. 20: WESTERN BLOT ANALYSIS OF A NI-NTA PURIFICATION OF IRS1-MYC-HIS

CHO-IR cells overexpressing IRS1-myc-his or GFP (negative control) were stimulated with 100 nM insulin or starved. Cells were lysed under denaturing conditions and lysates were incubated with Ni-NTA for pulldown of IRS1-myc-his. After washing, bound proteins were eluted and analysed by Western blotting using α-myc antibody. Elution buffer contained 400 mM imidazole, (a) represents first and (b) the second elution.

In a next step it was tested whether phosphorylated IRS1-myc-his would bind to the Ni-NTA beads. Eluates (fraction eluated with elution buffer EB100, see part A.2.5.5 Ni-NTA under denaturing conditions: purification) from Ni-NTA purifications of insulin-stimulated and starved CHO-IR cells overexpressing IRS1-myc-his were analysed by Western blotting (Figure A.21). With an α-IRS1 antibody it was confirmed that the binding protein was IRS1. α-myc and α-his antibodies visualised the same band. The α-pTyr antibody revealed that Tyr phosphorylated IRS1-myc-his bound to the Ni-NTA beads. As expected, when cells were stimulated with 100 nM insulin, more Tyr phosphorylated IRS1-myc-his was pulled down than from lysates from starved CHO-IR cells.

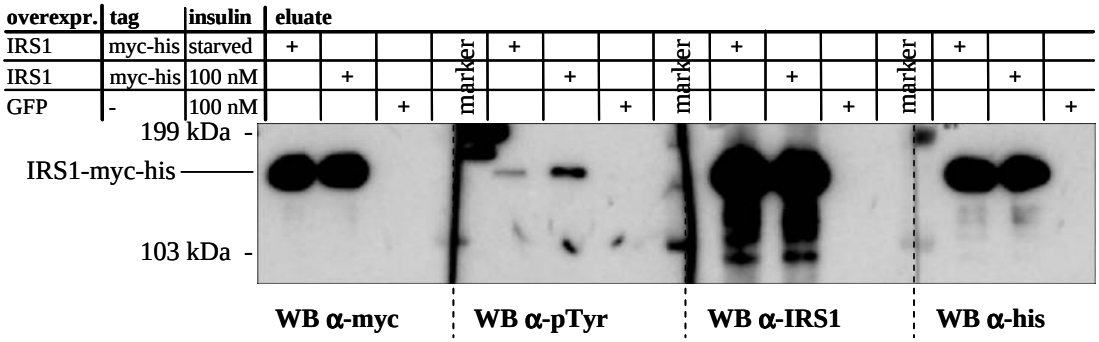

FIGURE A. 21: WESTERN BLOT ANALYSIS OF ELUATES OF A NI-NTA PURIFICATION
Eluate from Ni-NTA purification of IRS1-myc-his from cell lysate was analysed by Western blot (WB) with α-myc, α-pTyr, α-IRS1 and α-his. Before lysis CHO-IR cells were stimulated with 100 nM insulin for x minutes or starved. GFP overexpression was used as negative control. Size of IRS1-myc-his protein band and marker are indicated.

Purified IRS1-myc-his was analysed by two-dimensional gel electrophoresis in collaboration with Dr. Heinz Troxler and Peter Kleinert from the Clinical Chemistry and Biochemistry (mass spectrometry facility, Kinderspital Zürich). The large size of the IRS1-myc-his (also containing many phosphorylation sites) was a challenge for two-dimensional gel electrophoresis. We did not succeed with this method in time.

A.4 Discussion

A.4.1 Regions mediating binding between IRS1 and GRP78

Based on our hypothesis that IRS proteins not only act as adaptors but also as integrators of signalling information, we proposed that the molecular function of IRS proteins depends on an interplay of *cis-elements* on IRS with yet unknown *trans-acting* factors. One aim of the project was to define such regulatory *cis-elements* on IRS by mapping the binding sites of GRP78 and CGR19, two previously identified new interaction partners.

We found that GRP78 binds to IRS1(270-517) and IRS1(974-1169). Because binding sites for GRP78 on IRS1 were most accurately mapped in this study (aa 974-1169), they will be the main focus of this discussion. Binding between IRS1 and CGR19 is shortly discussed in part A.4.2.

A.4.1.1 Sequence analysis of IRS1(974-1169)

The smallest fragment of IRS1 that bound to GRP78 spans aa 974-1169, and preliminary data even indicated region aa 1013-1119. Surprisingly preliminary experiments showed no binding for IRS1(1013-1169) and IRS1(974-1119), whereas the shorter IRS1(1013-1119) binds to GRP78 (see Figure A.10). One possible explanation is that the extensions in either IRS1(1013-1169) or IRS1(974-1119) affect folding of the whole fragment such that the binding site is masked. Alternatively, inhibitory domains might be located in IRS1(1013-1169) and IRS1(974-1119) but not in IRS1(974-1119). It can also not be excluded, however, that binding of GRP78 to IRS1(1013-1119) is an artefact. However, the pilot experiments which were performed will have to be repeated in order to confirm or dismiss our results.

The finding that IRS1(933-1242)-flag and IRS1(933-1169)-flag were co-pulled down in Ni-NTA assays while IRS1(933-1080)-flag and IRS1(1081-1242)-flag were not (or only weakly) suggested that the binding region could stretch across the break point between the two latter fragments, around aa 1080 (overview see Fig. A.10).

Sequence analysis of IRS1(1013-1119) predicted a PKC phosphorylation site (aa 1084), a N-myristoylation site (aa 1067/1068), a N-glycosylation site (aa 1082) and a cAMP-/ cGMP-dependent protein kinase phosphorylation site (aa 1100) (Figure A.13).

Generally N-glycosylation is important for correct folding and oligiomerization of some proteins. However, N-glycosylation of IRS has not been described yet in literature. The

functions of the N-glycosylation sites of the IR (18 possible sites) were tested by site-directed mutagenesis [70]. It was shown that deletion of some N-glycosylation sites did not have any effect, whereas others had detrimental effects on cell surface expression, processing, insulin binding or autophosphorylation. In contrast to N-glycosylation, more knowledge exists about O-glycosylation of IRS1 and IRS2. O-glycosylation negatively influences insulin signalling [35]. In 3T3-L1 adipocytes increased levels of O-GlcNAc lead to increased O-glycosylation of IRS1 and attenuated activation of PKB and GSK-3β decreasing glucose uptake [71]. Myristoylation adds a lipid anchor targeting proteins to plasma membrane. It is conceivable that myristoylation directs IRS to the plasma membrane where it can interact with the activated IR. However, no investigation about myristoylation of IRS is published so far.

Prediction of kinase-specific phosphorylation sites in IRS1(974-1169) calculated highest probability for Ser1100 (phosphorylated by PKA), Ser1101 (by PKB) and Thr1103 (by PKC) (Figure A.13). Deletion constructs will have to be generated in order to determine if these sites are relevant for binding to GRP78. Ser1101 phosphorylation was identified to negatively regulate insulin signalling [72, 73]. However, PKB was not reported to affect this site. It was shown that PKCθ phosphorylated Ser1101 hereby blocking IRS1 Tyr phosphorylation and activation of the PKB pathway [73]. Ser1101 phosphorylation in muscle cells was induced by insulin, phorbol esters, TNFα and free fatty acids [73]. A recent study reported that S6K1 (ribosomal protein S6 kinase 1) phosphorylates Ser1101 of IRS1 in vitro [72]. Additionally the authors demonstrated that infusion of amino acids in humans leads to activation of S6K1, phosphorylation of Ser1101, reduced IRS1 function and insulin resistance in muscle [72]. Another study described significantly increased phosphorylation of Ser1101 in muscle biopsies from healthy volunteers after insulin stimulation [74]. In the same study, phosphorylation of Ser1100 was unchanged. Incidence and function of Thr1103 phosphorylation was not published so far.

Downstream signalling components often bind to phosphorylated Tyr residues on IRS. However, IRS1(974-1169) contains only three Tyr residues and not one is located within IRS1(1013-1119) (amino acid sequences in Figure A.12). Supposing that IRS1(1013-1119) is indeed the minimal fragment binding to GRP78 therefore excludes a role for Tyr residues. While only three Tyr residues are contained in IRS1(974-1169), 16.3 % of all amino acids in this sequence are Ser residues, in IRS1(1013-1119) the Ser content is 15.9 %. These ratios are around twice the average content for Ser found in eukaryotic proteins of 8 % [28]. In IRS1(974-1169) 5.6 % of the sites were Thr, in IRS1(1013-1119)

7.5 %. Both values are similar or slightly higher compared to the average occurrence (5.7 %).

A.4.1.2 Sequence comparison between IRS1(974-1169) and IRS1(270-517)

The two regions in IRS1 with affinity for GRP78, IRS1(974-1169) and IRS1(270-517), were compared to each other to test for sequence homology. The alignment (Figure A.14) showed only 24.5 % identity, however higher than for two randomly chosen sequences. The C-terminal binding sequence IRS1(974-1169) was also compared to the N-terminal remainder of IRS1 (aa 1-973). Interestingly, the sequence showing highest similarity spanned region IRS1(266-435), a region that is comprised (with a short N-terminal extension) in region IRS1(270-517) (Smith-Waterman algorithm [68]: identity 23.7 %, similarity 49.7 %, E-value=0.0018). The E-value is a measure for significance. The low E-value of 0.0018 indicates that IRS1(266-435) is indeed similar to IRS1(974-1169).

PKC phosphorylation sites, N-myristoylation sites, N-glycosylation sites, a cAMP-/ cGMP-dependent protein kinase phosphorylation sites and Tyr phosphorylation sites were predicted for IRS1(974-1169) and IRS1(270-517) by “Pattern search tool” (PIR [68]). Interestingly a cAMP-/ cGMP-dependent protein kinase phosphorylation site is found in IRS1(409-415) and IRS1(1139-1145), the region with higest similarity. These finding might indicate that binding to GRP78 is mediated by this highly similar region IRS1(409-415) and IRS1(1139-1145). However, other findings that are discussed later (see A.4.1.4) indicate that IRS1(974-1169) and IRS1(270-517) comprise two distinct sites for binding to two sites on GRP78.

A.4.1.3 Does IRS2 contain a region with homology to IRS1(974-1169)?

Because GRP78 was also found to bind to IRS2 we speculated that some sequence elements contained in IRS1(1013-1119) are also present in IRS2. To search for these homologous sequences, full length IRS2 and IRS1(1013-1119) were aligned to each other. We found that IRS2(1062-1156) was 42 % identical to IRS1(1013-1119) (Figure A.13). Within the aligned sequences IRS1(1085-1107) and IRS2(1122-1144) were 95.6 % identical. Furthermore, almost all conserved Ser and Thr residues were located in these regions.

As our constructs encode human IRS1 and mouse IRS2, the above described alignment was performed with human IRS1(1013-1119) and mouse full length IRS2. To check for sequence differences, human IRS1(1013-1119) was aligned with human full length IRS2 as well. The found overlap was the same and showed virtually the same amount of

identical sites (43 %). Mouse IRS2(1122-1144) that contained 95.6 % identical amino acids to the corresponding sequence IRS1(1085-1107) was even completely conserved in the human IRS2 sequence. As mentioned in the result part, unless otherwise noted the sequences and the numbering correspond to human IRS1 and to mouse IRS2.

When searching for common sequence patterns, one cAMP-/cGMP-dependent protein kinase phosphorylation site was predicted for IRS1(1013-1119) and IRS2(1062-1156), respectively ($IRS1_{Ser1100}$ and $IRS2_{Ser1137}$). Kinase-specific phosphorylation sites were also predicted with another search tool (NetPhosK [69]). Interestingly, the sites that were predicted with the highest probability for kinase-specific phosphorylation are present in IRS1(1013-1119) as well as in IRS2(1062-1156) (Figure A.13: $IRS1_{Ser1100}$/ $IRS2_{Ser1137}$ by PKA, $IRS1_{Ser1101}$/ $IRS2_{Ser1138}$ by PKB and $IRS1_{Thr1103}$/ $IRS2_{Thr1140}$ by PKC). Residues $IRS1_{Ser1100}$/ $IRS2_{Ser1137}$ are predicted by pattern search ("Pattern search tool", PIR [68]) as well as by kinase-specific phosphorylation sites ("NetPhosK" [69]) search. This finding is consistent as PKA is a cAMP-dependent protein kinase that is activated by the binding of two cAMP molecules to specific areas at each regulatory subunit of the enzyme. If later experiments should show that GRP78 binds to IRS2(1062-1156), the involvement of the three phosphorylation sites should be tested by deletion/mutation.

The less precisely mapped binding site IRS1(270-517) was also aligned to full length IRS2. We found that IRS2(303-566) was 46.1 % identical to IRS1(270-517) (Smith-Waterman algorithm [68]: Z-score=360.7, E-value=2.5e-33, Smith-Waterman score=516, similarity 60.1 %). Higher number of identical amino acids was found between corresponding regions in IRS1 and IRS2 than between IRS1(270-517) and IRS1(974-1169).

A.4.1.4 Binding sites IRS1(270-517) and IRS1(974-1242) in functional assays

If the interaction between GRP78 and IRS affects insulin signalling was tested by Linhua Xu (Linhua Xu, manuscript in preparation). She analysed insulin signalling in CHO-IR cells and in 3T3-L1 adipocytes overexpressing IRS1(270-517), IRS1(974-1242) or both fragments together, respectively. Only co-overexpression of IRS1(270-517) and IRS1(974-1242) was able to counteract ER stress-dependent inhibition of insulin signalling. On the one hand these findings indicate that the interaction between IRS1 and GRP78 inhibits insulin signalling. On the other hand, these results also indicate that the two sites in IRS1 are not equivalent and that two different sites on GRP78 bind to two different sites in IRS1. The latter fits well with the finding that homology was low between

IRS1(270-517) and IRS1(974-1242) and that sequence pattern search did not predict any known common pattern.

An additional finding by Xu and Niessen was that co-overexpression of IRS1(270-517) and IRS1(974-1242) was necessary to reverse the reduction of adiponectin secretion under ER stress in 3T3-L1 adipocytes. This shows that bindig between GRP78 and IRS1 has an influence on functional read-outs and hence confirms that binding is indeed important for insulin signalling *in vivo*.

A.4.1.5 Compartmentalisation of binding between IRS1 and GRP78

Binding between IRS1 and GRP78 was analysed by co-immunoprecipitation, GST-pulldown experiments and co-purification on nickel-agarose. All of these techniques represent *in vitro* methods. Under such conditions, even proteins from different cellular compartments come in close proximity and thus have the possibility to interact.

One important question therefore is in which compartment of the cell binding can take place *in vivo*. In 3T3-L1 adipocytes IRS1 was preferentially found in the intracellular membrane compartment and only to a lesser extent in cytosol. After insulin-stimulation, it translocated to the cytosol [75]. GRP78 is a chaperone protein and most likely located in the ER lumen. However, it was reported that beside the localisation in the ER lumen, a subpopulation of GRP78 exist as an ER transmembrane protein [76]. Additionally, a study showed that IRS was localized at intracellular membranes, in particular ER membranes [77]. Furthermore this study demonstrated co-localization of IRS1 with GRP78 by confocal microscopy [77]. These findings indicate that GRP78 and IRS1 interact at the ER membrane.

A.4.1.6 Challenges due to the methodology

One difficulty in the mapping of binding sites for GRP78 is the fact that it is a chaperone and therefore expected to interact with many proteins. It is conceivable that some protein fragments of IRS1 used in our experiments were bound by GRP78 because they were recognised as improperly folded and not because they contain “specific” binding sites for GRP78. Another complication concerning GRP78 was that it showed unspecific binding to sepharose and agarose beads in some binding assays.

A general disadvantage of the used mapping techniques is that the proteins might loose their secondary and tertiary structures when shortened (deletion anaylsis). As many protein-protein interactions are mediated by secondary and tertiary structures, some binding sites might not be recognised anymore when small fragments are tested for

binding. Other methods with less influence on folding should be considered. Random mutagenesis could be applied for full-length IRS1 or for defined fragments to locate amino acids involved in binding.

A.4.2 Regions mediating binding between IRS1 and CGR19

Binding regions for CGR19 were determined to span IRS1(1-271) and IRS1(517-974). The binding sites of CGR19 and GRP78 are located within different regions of IRS1. The N-terminal binding site of CGR19 includes the PH/PTB region (aa 13-262). The PH domain mediates binding to the plasma membrane, the PTB domain is involved in insulin receptor binding. It is conceivable that binding of CGR19 within this PH/PTB region could impede binding of IRS1 to the activated receptor and hence inhibit insulin signalling. The literature about CGR19 and its functions is very poor. Our preliminary results about the effect of CGR19 overexpression on glucose uptake and proliferation were contradictory (M. McNamara, unpublished).

In future, also the compartmentalisation of binding between IRS1 and CGR19 in the intact cell will have to be investigated. The localisation of CGR19 has not been described yet in literature. Our preliminary data showed that CGR19 was localised in or on the ER in 3T3-L1 adipocytes (M. McNamara, unpublished).

A.4.3 Determination of stimulus-dependent regulatory regions on IRS1

To detect stimulus-dependent phosphorylation on IRS1, it was planned to apply mass spectroscopy (MS). We succeeded in the purification and enrichment of IRS1-myc-his using Ni-NTA pulldown assays and we could show that Tyr phosphorylated IRS1 protein was also pulled down (Figure A.21). Unfortunately we were not able to find appropriate collaborators for the required MS analysis. We therefore decided to visualize stimulus-dependent phosphorylation patterns on IRS by 2D- gelelectrophoresis in collaboration with Dr. Heinz Troxler and Dr. Peter Kleinert (Kinderspital Zurich, Clinical Chemistry). However, because IRS1 is a very large and basic molecule 2D-gelelectrophoresis proved to be a challenge and we did not succeed within the available time frame.

Another aim of my project was the identification of stimulus-dependent specific signalling complexes assembled on IRS. It was planned to analyse these IRS binding partners by MS analysis after co-purification of IRS1-myc-his on nickel-agarose under native conditions. Before these experiments were started, we had to decide to stop this project.

A.5 References

[1] M.E. Daly, C. Vale, M. Walker, A. Littlefield, K.G. Alberti, J.C. Mathers, Acute effects on insulin sensitivity and diurnal metabolic profiles of a high-sucrose compared with a high-starch diet, *Am J Clin Nutr* 67 (1998) 1186-1196.

[2] S. Lund, A. Flyvbjerg, G.D. Holman, F.S. Larsen, O. Pedersen, O. Schmitz, Comparative effects of IGF-I and insulin on the glucose transporter system in rat muscle, *Am J Physiol* 267 (1994) E461-466.

[3] D.R. Clemmons, Involvement of insulin-like growth factor-I in the control of glucose homeostasis, *Curr Opin Pharmacol* 6 (2006) 620-625.

[4] G.I.B.e. S. Seino, Pancreatic Beta Cell in Health and Disease, Springer, Shinano, Japan, 2008.

[5] J.C. Henquin, C. Boitard, S. Efendic, E. Ferrannini, D.F. Steiner, E. Cerasi, Insulin secretion: movement at all levels, *Diabetes* 51 Suppl 1 (2002) S1-2.

[6] P. Rorsman, L. Eliasson, E. Renstrom, J. Gromada, S. Barg, S. Gopel, The Cell Physiology of Biphasic Insulin Secretion, *News Physiol Sci* 15 (2000) 72-77.

[7] World Health Organisation (WHO), http://www.who.int/diabetes/en/, cited 2. February 2009.

[8] M.Y. Donath, J.A. Ehses, K. Maedler, D.M. Schumann, H. Ellingsgaard, E. Eppler, M. Reinecke, Mechanisms of beta-cell death in type 2 diabetes, *Diabetes* 54 Suppl 2 (2005) S108-113.

[9] M.Y. Donath, J.A. Ehses, Type 1, type 1.5, and type 2 diabetes: NOD the diabetes we thought it was, *Proc Natl Acad Sci U S A* 103 (2006) 12217-12218.

[10] K. Paz, R. Hemi, D. LeRoith, A. Karasik, E. Elhanany, H. Kanety, Y. Zick, A molecular basis for insulin resistance. Elevated serine/threonine phosphorylation of IRS-1 and IRS-2 inhibits their binding to the juxtamembrane region of the insulin receptor and impairs their ability to undergo insulin-induced tyrosine phosphorylation, *J Biol Chem* 272 (1997) 29911-29918.

[11] Y. Zick, Ser/Thr phosphorylation of IRS proteins: a molecular basis for insulin resistance, *Sci STKE* 2005 (2005) pe4.

[12] M.Y. Donath, J. Storling, L.A. Berchtold, N. Billestrup, T. Mandrup-Poulsen, Cytokines and beta-cell biology: from concept to clinical translation, *Endocr Rev* 29 (2008) 334-350.

[13] J.F. Youngren, Regulation of insulin receptor function, *Cell Mol Life Sci* 64 (2007) 873-891.

[14] A.D. Cann, R.A. Kohanski, Cis-autophosphorylation of juxtamembrane tyrosines in the insulin receptor kinase domain, *Biochemistry* 36 (1997) 7681-7689.

[15] S.J. Isakoff, Y.P. Yu, Y.C. Su, P. Blaikie, V. Yajnik, E. Rose, K.M. Weidner, M. Sachs, B. Margolis, E.Y. Skolnik, Interaction between the phosphotyrosine binding domain of Shc and the insulin receptor is required for Shc phosphorylation by insulin in vivo, *J Biol Chem* 271 (1996) 3959-3962.

[16] S. Rocchi, S. Tartare-Deckert, J. Murdaca, M. Holgado-Madruga, A.J. Wong, E. Van Obberghen, Determination of Gab1 (Grb2-associated binder-1) interaction with insulin receptor-signaling molecules, *Mol Endocrinol* 12 (1998) 914-923.

[17] J. Liu, A. Kimura, C.A. Baumann, A.R. Saltiel, APS facilitates c-Cbl tyrosine phosphorylation and GLUT4 translocation in response to insulin in 3T3-L1 adipocytes, *Mol Cell Biol* 22 (2002) 3599-3609.

[18] A.R. Saltiel, C.R. Kahn, Insulin signalling and the regulation of glucose and lipid metabolism, *Nature* 414 (2001) 799-806.

[19] J. Hu, J. Liu, R. Ghirlando, A.R. Saltiel, S.R. Hubbard, Structural basis for recruitment of the adaptor protein APS to the activated insulin receptor, *Mol Cell* 12 (2003) 1379-1389.

[20] D.J. Withers, M. White, Perspective: The insulin signaling system--a common link in the pathogenesis of type 2 diabetes, *Endocrinology* 141 (2000) 1917-1921.
[21] R. Bohni, J. Riesgo-Escovar, S. Oldham, W. Brogiolo, H. Stocker, B.F. Andruss, K. Beckingham, E. Hafen, Autonomous control of cell and organ size by CHICO, a Drosophila homolog of vertebrate IRS1-4, *Cell* 97 (1999) 865-875.
[22] M.F. White, IRS proteins and the common path to diabetes, *Am J Physiol Endocrinol Metab* 283 (2002) E413-422.
[23] D. Cai, S. Dhe-Paganon, P.A. Melendez, J. Lee, S.E. Shoelson, Two new substrates in insulin signaling, IRS5/DOK4 and IRS6/DOK5, *J Biol Chem* 278 (2003) 25323-25330.
[24] A.D. Keegan, K. Nelms, M. White, L.M. Wang, J.H. Pierce, W.E. Paul, An IL-4 receptor region containing an insulin receptor motif is important for IL-4-mediated IRS-1 phosphorylation and cell growth, *Cell* 76 (1994) 811-820.
[25] L. Pirola, A.M. Johnston, E. Van Obberghen, Modulation of insulin action, *Diabetologia* 47 (2004) 170-184.
[26] M.F. White, The insulin signalling system and the IRS proteins, *Diabetologia* 40 Suppl 2 (1997) S2-17.
[27] S. Hanke, M. Mann, The phosphotyrosine interactome of the insulin receptor family and its substrates IRS-1 and IRS-2, *Mol Cell Proteomics* (2008).
[28] I. Pe'er, C.E. Felder, O. Man, I. Silman, J.L. Sussman, J.S. Beckmann, Proteomic signatures: amino acid and oligopeptide compositions differentiate among phyla, *Proteins* 54 (2004) 20-40.
[29] H. Kanety, R. Feinstein, M.Z. Papa, R. Hemi, A. Karasik, Tumor necrosis factor alpha-induced phosphorylation of insulin receptor substrate-1 (IRS-1). Possible mechanism for suppression of insulin-stimulated tyrosine phosphorylation of IRS-1, *J Biol Chem* 270 (1995) 23780-23784.
[30] L. Rui, M. Yuan, D. Frantz, S. Shoelson, M.F. White, SOCS-1 and SOCS-3 block insulin signaling by ubiquitin-mediated degradation of IRS1 and IRS2, *J Biol Chem* 277 (2002) 42394-42398.
[31] M.F. White, Regulating insulin signaling and beta-cell function through IRS proteins, *Can J Physiol Pharmacol* 84 (2006) 725-737.
[32] C.M. Taniguchi, B. Emanuelli, C.R. Kahn, Critical nodes in signalling pathways: insights into insulin action, *Nat Rev Mol Cell Biol* 7 (2006) 85-96.
[33] C.M. Taniguchi, J.O. Aleman, K. Ueki, J. Luo, T. Asano, H. Kaneto, G. Stephanopoulos, L.C. Cantley, C.R. Kahn, The p85alpha regulatory subunit of phosphoinositide 3-kinase potentiates c-Jun N-terminal kinase-mediated insulin resistance, *Mol Cell Biol* 27 (2007) 2830-2840.
[34] V. Aguirre, T. Uchida, L. Yenush, R. Davis, M.F. White, The c-Jun NH(2)-terminal kinase promotes insulin resistance during association with insulin receptor substrate-1 and phosphorylation of Ser(307), *J Biol Chem* 275 (2000) 9047-9054.
[35] P. Gual, Y. Le Marchand-Brustel, J.F. Tanti, Positive and negative regulation of insulin signaling through IRS-1 phosphorylation, *Biochimie* 87 (2005) 99-109.
[36] B.J. Goldstein, A. Bittner-Kowalczyk, M.F. White, M. Harbeck, Tyrosine dephosphorylation and deactivation of insulin receptor substrate-1 by protein-tyrosine phosphatase 1B. Possible facilitation by the formation of a ternary complex with the Grb2 adaptor protein, *J Biol Chem* 275 (2000) 4283-4289.
[37] M.F. White, The IRS-signalling system: a network of docking proteins that mediate insulin action, *Mol Cell Biochem* 182 (1998) 3-11.
[38] Y. Kaburagi, T. Yamauchi, R. Yamamoto-Honda, K. Ueki, K. Tobe, Y. Akanuma, Y. Yazaki, T. Kadowaki, The mechanism of insulin-induced signal transduction mediated by the insulin receptor substrate family, *Endocr J* 46 Suppl (1999) S25-34.

[39] T. Kadowaki, Insights into insulin resistance and type 2 diabetes from knockout mouse models, *J Clin Invest* 106 (2000) 459-465.
[40] M. Niessen, On the role of IRS2 in the regulation of functional beta-cell mass, *Arch Physiol Biochem* 112 (2006) 65-73.
[41] S. Mohanty, G.A. Spinas, K. Maedler, R.A. Zuellig, R. Lehmann, M.Y. Donath, T. Trub, M. Niessen, Overexpression of IRS2 in isolated pancreatic islets causes proliferation and protects human beta-cells from hyperglycemia-induced apoptosis, *Exp Cell Res* 303 (2005) 68-78.
[42] D.J. Withers, J.S. Gutierrez, H. Towery, D.J. Burks, J.M. Ren, S. Previs, Y. Zhang, D. Bernal, S. Pons, G.I. Shulman, S. Bonner-Weir, M.F. White, Disruption of IRS-2 causes type 2 diabetes in mice, *Nature* 391 (1998) 900-904.
[43] C.M. Taniguchi, K. Ueki, R. Kahn, Complementary roles of IRS-1 and IRS-2 in the hepatic regulation of metabolism, *J Clin Invest* 115 (2005) 718-727.
[44] C. Huang, A.C. Thirone, X. Huang, A. Klip, Differential contribution of insulin receptor substrates 1 versus 2 to insulin signaling and glucose uptake in l6 myotubes, *J Biol Chem* 280 (2005) 19426-19435.
[45] B.A. Joblin, Identification of new insulin receptor substrate binding proteins: filamin and GRP78, Thesis University Zurich, Zurich, 2004.
[46] A.J. Bruce Alberts, Julian Lewis, Martin Faff, Keith Roberts, Peter Walter, The cell, Garland Science, New York, 2002.
[47] M.G. Myers, Jr., M.F. White, Insulin signal transduction and the IRS proteins, *Annu Rev Pharmacol Toxicol* 36 (1996) 615-658.
[48] A.M. Valverde, C. Mur, S. Pons, A.M. Alvarez, M.F. White, C.R. Kahn, M. Benito, Association of insulin receptor substrate 1 (IRS-1) y895 with Grb-2 mediates the insulin signaling involved in IRS-1-deficient brown adipocyte mitogenesis, *Mol Cell Biol* 21 (2001) 2269-2280.
[49] W. Ogawa, T. Matozaki, M. Kasuga, Role of binding proteins to IRS-1 in insulin signalling, *Mol Cell Biochem* 182 (1998) 13-22.
[50] A. Virkamaki, K. Ueki, C.R. Kahn, Protein-protein interaction in insulin signaling and the molecular mechanisms of insulin resistance, *J Clin Invest* 103 (1999) 931-943.
[51] T. Noguchi, T. Matozaki, K. Horita, Y. Fujioka, M. Kasuga, Role of SH-PTP2, a protein-tyrosine phosphatase with Src homology 2 domains, in insulin-stimulated Ras activation, *Mol Cell Biol* 14 (1994) 6674-6682.
[52] M.G. Myers, Jr., R. Mendez, P. Shi, J.H. Pierce, R. Rhoads, M.F. White, The COOH-terminal tyrosine phosphorylation sites on IRS-1 bind SHP-2 and negatively regulate insulin signaling, *J Biol Chem* 273 (1998) 26908-26914.
[53] K. Zhang, R.J. Kaufman, Signaling the unfolded protein response from the endoplasmic reticulum, *J Biol Chem* 279 (2004) 25935-25938.
[54] E. Lai, T. Teodoro, A. Volchuk, Endoplasmic reticulum stress: signaling the unfolded protein response, *Physiology (Bethesda)* 22 (2007) 193-201.
[55] D.T. Rutkowski, R.J. Kaufman, A trip to the ER: coping with stress, *Trends Cell Biol* 14 (2004) 20-28.
[56] U. Ozcan, Q. Cao, E. Yilmaz, A.H. Lee, N.N. Iwakoshi, E. Ozdelen, G. Tuncman, C. Gorgun, L.H. Glimcher, G.S. Hotamisligil, Endoplasmic reticulum stress links obesity, insulin action, and type 2 diabetes, *Science* 306 (2004) 457-461.
[57] N.K. Sharma, S.K. Das, A.K. Mondal, O.G. Hackney, W.S. Chu, P.A. Kern, N. Rasouli, H.J. Spencer, A. Yao-Borengasser, S.C. Elbein, Endoplasmic reticulum stress markers are associated with obesity in nondiabetic subjects, *J Clin Endocrinol Metab* 93 (2008) 4532-4541.
[58] H.L. Kammoun, H. Chabanon, I. Hainault, S. Luquet, C. Magnan, T. Koike, P. Ferre, F. Foufelle, GRP78 expression inhibits insulin and ER stress-induced SREBP-1c activation and reduces hepatic steatosis in mice, *J Clin Invest* (2009).

[59] S.L. Madden, E.A. Galella, D. Riley, A.H. Bertelsen, G.A. Beaudry, Induction of cell growth regulatory genes by p53, *Cancer Res* 56 (1996) 5384-5390.
[60] K.L. Borden, P.S. Freemont, The RING finger domain: a recent example of a sequence-structure family, *Curr Opin Struct Biol* 6 (1996) 395-401.
[61] Current Protocols in Molecular Biology, John Wiley and Sons, Inc. 2007.
[62] F.E.F. Sambrook J., Maniatis T., Molecular cloning, a laboratory manual 1989.
[63] Webcutter, http://rna.lundberg.gu.se/cutter2/, cited 29.Dezember 2008.
[64] NCBI Blast, http://blast.ncbi.nlm.nih.gov/Blast.cgi, cited 29. Dezember 2008.
[65] Composition/molecular weight, http://pir.georgetown.edu/pirwww/search/comp_mw.shtml, cited 29. Dezember 2008.
[66] EXPASY, http://www.expasy.ch/, cited 29. Dezember 2008.
[67] A. Egli, Characterization of the interaction between insulin receptor substrates (IRS) and glucose-regulated protein 78 (GRP78), Diploma Thesis University Zurich, Zurich, 2005.
[68] Protein Information Resource (PIR), http://pir.georgetown.edu/pirwww/search/pattern.shtml, cited 4. February 2009.
[69] NetPhosK, http://www.cbs.dtu.dk/services/NetPhosK/, cited 5. February 2009.
[70] T.C. Elleman, M.J. Frenkel, P.A. Hoyne, N.M. McKern, L. Cosgrove, D.R. Hewish, K.M. Jachno, J.D. Bentley, S.E. Sankovich, C.W. Ward, Mutational analysis of the N-linked glycosylation sites of the human insulin receptor, *Biochem J* 347 Pt 3 (2000) 771-779.
[71] K. Vosseller, L. Wells, M.D. Lane, G.W. Hart, Elevated nucleocytoplasmic glycosylation by O-GlcNAc results in insulin resistance associated with defects in Akt activation in 3T3-L1 adipocytes, *Proc Natl Acad Sci U S A* 99 (2002) 5313-5318.
[72] F. Tremblay, S. Brule, S. Hee Um, Y. Li, K. Masuda, M. Roden, X.J. Sun, M. Krebs, R.D. Polakiewicz, G. Thomas, A. Marette, Identification of IRS-1 Ser-1101 as a target of S6K1 in nutrient- and obesity-induced insulin resistance, *Proc Natl Acad Sci U S A* 104 (2007) 14056-14061.
[73] Y. Li, T.J. Soos, X. Li, J. Wu, M. Degennaro, X. Sun, D.R. Littman, M.J. Birnbaum, R.D. Polakiewicz, Protein kinase C Theta inhibits insulin signaling by phosphorylating IRS1 at Ser(1101), *J Biol Chem* 279 (2004) 45304-45307.
[74] Z. Yi, P. Langlais, E.A. De Filippis, M. Luo, C.R. Flynn, S. Schroeder, S.T. Weintraub, R. Mapes, L.J. Mandarino, Global assessment of regulation of phosphorylation of insulin receptor substrate-1 by insulin in vivo in human muscle, *Diabetes* 56 (2007) 1508-1516.
[75] G. Inoue, B. Cheatham, R. Emkey, C.R. Kahn, Dynamics of insulin signaling in 3T3-L1 adipocytes. Differential compartmentalization and trafficking of insulin receptor substrate (IRS)-1 and IRS-2, *J Biol Chem* 273 (1998) 11548-11555.
[76] R.K. Reddy, C. Mao, P. Baumeister, R.C. Austin, R.J. Kaufman, A.S. Lee, Endoplasmic reticulum chaperone protein GRP78 protects cells from apoptosis induced by topoisomerase inhibitors: role of ATP binding site in suppression of caspase-7 activation, *J Biol Chem* 278 (2003) 20915-20924.
[77] P.D. Borge, J. Moibi, S.R. Greene, M. Trucco, R.A. Young, Z. Gao, B.A. Wolf, Insulin receptor signaling and sarco/endoplasmic reticulum calcium ATPase in beta-cells, *Diabetes* 51 Suppl 3 (2002) S427-433.

Part B:

Do free fatty acids regulate the expression of interleukin-1β and chemokine KC via Toll-like receptors in mouse islets?

B. Summary (English)

Type 2 diabetes is characterised by a combination of insulin resistance in the periphery and inadequate insulin secretion of pancreatic β-cells. At the beginning of the disease increasing functional β-cell mass compensates for insulin resistance and the resulting increased insulin demand. At later stages compensation by β-cells fails due to a loss of β-cell function and mass. Hyperglycemia, chronically elevated free fatty acids (FFA) and cytokines contribute to this maladaption and apoptosis of the β-cells.

The cytokine IL-1β is a central proinflammatory cytokine regulating β-cell function and β-cell mass [12] and it is involved in inflammatory processes associated with diabetes. The important role of IL-1β in type 2 diabetes was supported in a recent study with diabetic patients where blockage of IL-1 signalling with IL-1Ra resulted in improved blood sugar levels and insulin secretion. β-cells (human and rat), ductal cells, endothelial cells and resident macrophages were identified as the islet cellular source of IL-1β.

The mechansims regulating IL-1β and IL-1β-regulated chemokine expression (e.g. KC) in pancreatic islets is largely unknown. In other tissues, FFA may induce an inflammatory response. Therefore we hypothesized that FFA may contribute to the regulation of islet-derived IL-1β and KC. Furthermore, we tested whehter this is mediated via TLR and MyD88.

We found that FFA induced IL-1β and KC in mouse islets and that FFA-induced IL-1β and KC expression was MyD88-dependent. As TLR2 and TLR4 activation with specific ligands stimulated IL-1β and KC as well, we investigated whether FFA signalled via TLR2 or TLR4 using islets from the respective knockout mice. In contrast to MyD88, TLR2-deficiency only partially protected islets from FFA-induced IL-1β and KC expression. FFA-induced IL-1β and KC mRNA induction was not TLR4-dependent, whereas basal KC mRNA level was. The IL-1RI antagonist IL-1Ra completely abolished FFA-induced KC expression in mouse islets. This result strongly indicates that FFA-induced activation of IL-1RI in mouse islets was mediated indirectly by induction of functional receptor ligand, most likely IL-1β.

In summary we showed that in mouse islets FFA induce an inflammatory resonse characterised by IL-1β and KC expression. This signal is amplified by an IL-1β auto-stimulation loop via the IL-1RI and is MyD88- and partly TLR2-dependent.

B. Summary (Deutsch)

Charakteristisch für Typ 2 Diabetes ist eine Kombination von Insulinresistenz im peripheren Gewebe mit einer unzulänglichen Insulinproduktion der β-Zellen der Bauchspeicheldrüse. Im Anfangsstadion der Krankheit kann eine Erhöhung der funktionellen β-Zell-Masse den durch die Insulinresistenz verursachten erhöhten metabolischen Bedarf kompensieren. Im Verlauf der Krankheit nehmen die sekretorische Funktion sowie die Masse der β-Zellen ab. Dies wird unter anderem verursacht durch Hyperglykämie, chronisch erhöhte Konzentrationen freier Fettsäuren (free fatty acids, FFA) und Cytokine.

Interleukin-1β (IL-1β) ist ein proinflammatorisch wirkendes Zytokin, welches die Funktion und die Masse der β-Zellen reguliert. Zudem ist es in den Entzündungsprozess involviert, welcher auch beim Diabetes eine wichtige Rolle spielt. Die wichtige Funktion von IL-1β in Typ 2 Diabetes wurde in einer kürzlich publizierten Studie belegt: In Typ 2 Diabetikern führte die Blockierung des IL-1 Signalübertragungswegs mit IL-1Ra zur Verbesserung der Blutzuckerwerte und der Insulin Sekretion. Es konnte gezeigt werden, dass IL-1β in Langerhans-Inseln von β-Zellen, Zellen des Duktes, Endothelzellen sowie Insel-ansässigen Makrophagen produziert wird.

Der Mechanismus, welcher IL-1β- und IL-1β-regulierte Chemokin-Expression reguliert, ist grösstenteils unbekannt. In anderen Gewebetypen können FFA Entzündungsfaktoren induzieren. Daher stellten wir die Hypothese auf, dass FFA zur Regulation von IL-1β und KC Expression in Inseln beitragen. Zudem wollten wie herausfinden, ob dies via TLR und MyD88 geschieht.

Wir konnten zeigen, dass FFA IL-1β und KC in Mausinseln induzieren und dass diese FFA-induzierte IL-1β und KC Expression vollständig MyD88-abhängig war. Da auch die Aktivierung von TLR2 und TLR4 mit spezifischen Liganden IL-1β and KC stimulierte, untersuchten wir in Inseln der jeweiligen Knockout-Mäuse, ob die FFA via TLR2 oder TLR4 wirkten. Im Gegensatz zum Fehlen des MyD88 schützte das Fehlen des TLR2 nur partiell vor der durch die FFA bewirkten IL-1β und KC Expression. Die FFA-induzierte IL-1β und KC mRNA Expression war nicht vom TLR4 abhängig; das basale KC mRNA Level hingegen zeigte Abhängigkeit vom TLR4. Der IL-1RI Antagonist IL-1Ra verhinderte in Mausinseln die FFA-induzierte KC Expression vollständig. Dieses Resultat deutet darauf hin, dass die FFA-induzierte Aktivierung von IL-1RI in Mausinseln indirekt durch die

Induktion des funktionellen Rezeptorliganden bewirkt wird, höchstwahrscheinlich durch IL-1β.

Zusammenfassend haben wir gezeigt, dass FFA in Mausinseln eine Entzündungsantwort induzieren, welche durch IL-1β und KC Expression charakterisiert ist. Das Signal wird durch einen IL-1β Auto-Stimulations-Loop via IL-1RI amplifiziert und ist vollständig von MyD88 und teilweise von TLR2 abhängig.

B. Abbreviations

ANOVA	analysis of variance
ATP	adenosine triphosphate
BSA	bovine serum albumin
CD14/ CD36	cluster of differentiation 14/ cluster of differentiation 36
(c)DNA	(complementary) deoxyribonucleic acid
DD	death domain
dNTP	desoxyribonukleosidtriphosphate
ECM	extracellular matrix
FFA	free fatty acid
FLIP	FLICE-inhibitory protein
GLP	glucagon-like peptides
IFN-γ	interferon-γ
IL	interleukin
IL-1RI	interleukin-1 receptor type I
IL-1Ra	interleukin-1 receptor antagonist
IL-1RAcP	interleukin-1 receptor accessory protein
iNOS	inducible nitric oxide synthase
IRAK	IL-1 receptor-associated kinase
IRF3	interferon regulatory factor 3
KC	keratinocyte chemoattractant chemokine
LPS	lipopolysaccharide
LRR	leucine-rich repeat
Mal (=Tirap)	MyD88 adaptor like
MCP-1	macrophage chemoattractant protein-1
MIN6	mouse insulinoma cell line
(m)RNA	(messenger) ribonucleic acid
MyD88	myeloid differentiation factor 88
NF-κB	nuclear factor κB
PCR	polymerase chain reaction
PBS	phosphate buffered saline
RT-PCR	reverse transcription polymerase chain reaction
SEM	standard error
TIR	toll-IL-1-receptor

TLR	toll-like receptor
TRAM	TRIF-related adapter molecule
TRIF	TIR-related adaptor protein inducing interferon
TNF-α	tumour necrosis factor-α

B.1 Introduction

B.1.1 The endocrine pancreas

The pancreas harbours two functionally different parts, the exocrine and the endocrine tissue. The exocrine part is the source of digestive enzymes for processing of ingested food and thereby enabling absorption of nutrients. The hormones secreted by the endocrine pancreas are necessary to maintain blood glucose in tight range. In humans, the endocrine pancreas consists of 0.7 – 1 million islets of Langerhans, that account for 1 – 2 % of the total pancreas mass. Four major cell types are contained in islets: α, β, δ and PP cells. α-cells produce glucagon, β-cells produce insulin, proinsulin, amylin and γ-aminobutyric acid (GABA), δ-cells produce somatostation and PP cells produce pancreatic polypeptide [78]. A fifth cell type, the ghrelin producing ε-cells, were described a few years ago. A recent study was able to show that large numbers of ε-cells are present in human pancreas during fetal life [79]. However, this cell type was shown to decline postnatally [80].

The different cell types are not randomly distributed within islets and species differences were reported in several studies. In isolated mouse islets and in pancreas sections β-cells were detected in the centre, surrounded by a ring of α- and δ-cells. In isolated human islets α-, β and δ-cells were intermingled and dispersed throughout the islets [81]. Another species difference besides islet architecture is the islet cell composition: isolated human islets contain fewer β-cells (54 %) than mouse islets (75 %), while in human islets proportionally more α-cells (34 %) exist than in mouse islets (19 %) [81].

B.1.2 Cytokine IL-1β and its role in diabetes

B.1.2.1 Overview on IL-1β

Interleukin-1β (IL-1β) is a master regulator of inflammatory processes in many tissues. It was originally described to play a role in host defence and was induced by various infectious agents [82]. IL-1β is a very potent cytokine that is biologically active at low concentrations, therefore, tight regulation is required for processing, release and receptor binding. Unlike other cytokines IL-1β does not have a leader sequence and inactive proIL-1β is cleaved to IL-1β in the cytoplasm by caspase 1 (also termed IL-1β converting

enzyme, ICE) [83, 84]. Caspase 1 in turn is tightly regulated by the inflammasome, a multiprotein complex that is required for activation of caspase 1 [84].

Also in pancreatic islets IL-1β is a central cytokine because it is important for regulation of β-cell function, viability and replication [12]. It was observed that IL-1β mediates the destruction of β-cells in type 1 diabetes. Infiltrating macrophages produce IL-1β in islets, which inhibits β-cell function and decreases β-cell mass by inducing apoptosis. Therefore IL-1β is regarded as important effector in the development of type 1 diabetes [85]. The important role of IL-1β in type 2 diabetes was supported by a recent study with diabetic patients where blockage of IL-1 signalling with IL-1Ra resulted in improved blood sugar levels and insulin secretion [86]. IL-1β signalling is involved in inflammatory processes associated with diabetes, and induces chemokines and cytokines (for IL-1β-mediated glucotoxicity see B.1.2.2). In islets IL-1β production was demonstrated for β-cells [87, 88], ductal cells [89], islet endothelial cells [89] and for resident macrophages [90].

To date there is only limited knowledge on regulation of IL-1β in islets and IL-1β-regulated chemokine expression (as e.g. KC). So far, IL-1β itself and high glucose concentrations were identified as inducers of IL-1β mRNA expression in cultured human islets and purified human and rat β-cells [91], the first being a strong and the latter a weak inducer [92]. IL-1β auto-stimulation was blocked by IL-1 antagonism with IL-1Ra, just as release of IL-1β regulated factors IL-8 (homologue of mouse KC) and IL-6 [92].

Another ligand of the IL-1 receptor (IL-1R) is IL-1α. Upon binding to its receptor it induces the same signal transduction cascade as IL-1β (binding and downstream signalling of IL-1α and IL-1β is described below in part B.1.4.1). The exact mechanism for IL-1α release is not known. Like pro-IL-1β pro-IL-1α does not have a signal sequence. In murine macrophages it was shown that IL-1α precursor was bound to the plasma membrane, probably mediated via interaction of cell surface lectin with glycosylated residues on pro-IL-1α [93]. In addition to this membrane-bound form that can be secreted to elicit classical function as ligand for a specific receptor, the intracellular IL-1α precursor also acts in the nucleus as a transcription factor [94].

B.1.2.2 IL-1β-mediated glucotoxicity in β-cells

Glucose is the main regulator of insulin secretion and β-cell turnover. Short term exposure of islets to high glucose concentration induces β-cell proliferation [88, 95]. This adjustment mechanism allows the β-cells to cope with increased insulin demand e.g. during stress

conditions or at the onset of type 2 diabetes when insulin resistance of the periphery is present. However, chronically elevated glucose levels impaired islet function, reduced proliferation and increased apoptosis, leading to the concept of islet glucotoxicity [95, 96].

It has been proposed that IL-1β is a link between chronically elevated glucose concentrations and β-cell dysfunction [88]. Several below-mentioned facts underline this hypothesis. In cultured human islets and purified human and rat β-cells high glucose concentrations induced IL-1β mRNA and protein expression [88, 92]. Additionally, β-cells of type 2 diabetic patients revealed increased IL-1β mRNA expression [92]. In high-fat-fed diabetic mouse model blockage of IL-1 activity with either IL-1Ra [97] or with an IL-1β antibody [98] resulted in improved glycemia and insulin secretion. Furthermore, a recent clinical study demonstrated that the blockade of IL-1β in type 2 diabetic patients with the IL-1 receptor antagonist IL1-Ra resulted in improved blood glucose levels and insulin secretion as well [86].

Just as its regulator glucose, IL-1β shows dual role in β-cell proliferation/ apoptosis as well: Low and transient concentrations of IL-1β induce β-cell proliferation and enhance glucose-stimulated insulin secretion, without affecting insulin content. However, sustained and higher IL-1β concentrations impair insulin secretion and induce apoptosis [99].

Two receptors on β-cells might be involved in IL-1β-mediated apoptosis: the IL-1 receptor type 1 (IL-1RI) and the Fas receptor [12]. Binding of IL-1β to IL-1RI leads to recruitment of intracellular adapter protein MyD88. Downstream signalling involves two main pathways, one leading to activation of MAPKs (ERK and Jnk) and one finally leading to activation of transcription factor NF-κB (more details in part B.1.4.1). Another signalling pathway leading to apoptosis of β-cells involves Fas, a death receptor. Fas activation by the Fas ligand (FasL) results in Caspase 8 activation leading to transmission of apoptotic signals also via NF-κB. Fas signalling has a dual effect as it can be switched from apoptotic signalling towards proliferation in the presence of active FLICE-inhibitory protein (FLIP). FLIP is a caspase 8 inhibitor that is able to shift Fas-mediated death signals towards proliferation and to protect human β-cells from glucose-induced apoptosis [100]. The Fas-FLIP pathway is triggered by cytokines, since Fas is induced by many cytokines, particularly IL-1β. FasL is constitutively expressed on neighbouring β-cells [101] and so signalling depends on expression level of Fas. Furthermore chronic exposure of islets to IL-1β leads to induction of Fas receptor expression and it decreases FLIP and activates proteases caspase 3 and 8, shifting the pathway towards apoptosis [12, 101]. In

correlation to these findings less FLIP was present in the pancreas of diabetic patients [100].

An addtional mechanism underlying β-cell death involves inducible nitric oxide synthase (iNOS) as key player. A combination of IL-1β and IFNγ induced iNOS in rodent islets, resulting in excess nitric oxide (NO) formation [102]. It was proposed that NO-induced mitochondrial dysfunction and subsequently decreased ATP production was leading to necrosis and apoptosis in islets [102]. In rat insulinoma cell line (RIN-r) synergistic action of the two cytokines IL-1β and IFNγ was confirmed and cytokine-induced apoptosis via activation of caspases was shown [103].

B.1.3 Lipotoxicity on β-cells

In addition to glucotoxicity (see B.1.2.2) lipotoxicity contributes to impaired β-cell function in type 2 diabetes as well. Free (non-esterified) fatty acids (FFA or NEFA) are released into the bloodstream by lipolysis of stored fat in adipocytes. FFA are important substrates for β-cells and physiological plasma levels of FFA are known to be important for β-cell function, however they become toxic when chronically high levels are present. Insulin resistance in adipocytes at the onset of type 2 diabetes results in elevated lipolysis leading to increased FFA level in the bloodstream [104]. In type 2 diabetes and in obesity it was shown that FFA plasma levels are elevated [105].

In general, acute exposure of β-cells to FFA resulted in an increase of insulin release, whereas a chronic exposure led to decreased secretion [104]. Beside the duration of FFA exposure (chronic or acute) another important determinant for effects on β-cell function is the FFA degree of saturation. Exposure of isolated human islets to the saturated FFA palmitate increased apoptosis, reduced proliferation and impaired insulin secretion. In contrast, the monounsaturated FFA palmitoleic acid did not affect apoptosis, increased proliferation and improved function [106].

Beside above mentioned investigations on effects of FFA on β-cell function, there is only limited knowledge on potential FFA effects on inflammatory markers or cytokine induction in islets. In other cell types, studies on FFA-induced inflammatory factors were performed. In a myotube cell line, palmitate induced IL-6 [107]. In fat tissue and liver from high fat fed mice, inflammatory markers including TNF-α, IL-6 and MCP-1 were increased [108]. Several publications suggested that TLRs, particularly TLR2 [107, 109] and TLR4 [108], are involved in FFA-induced insulin resistance in periphery.

A hint that FFA can induce a proinflammatory response in pancreatic islets comes from two gene array studies: In MIN6 cell line [110] and in human islets [111] inflammatory markers as e.g. MCP-1 were elevated after incubation in the presence of FFA. Furthermore, a previous study from our laboratory showed that incubation of isolated human and mouse islets with a combination of palmitate and high glucose concentrations induced various chemo- and cytokines. Similarly, isolated islets from high-fat-fed mice secreted elevated pro-inflammatory factors compared to islets from chow fed mice [112].

B.1.4 IL-1R and TLRs

Toll-like receptors (TLRs) are evolutionarily conserved pattern recognition receptors. They recognise molecular structures (called pathogen-associated molecular patterns, PAMPs) that are found on pathogens and alert the innate immune system of the host body. TLR stimulation typically leads to activation of proinflammatory cytokines. TLRs are present in vertebrates as well as in invertebrates, and they are expressed in many different tissues. In human and mouse, 11 TLRs are known [113]. In the context of this project and of type 2 diabetes TLR2 and TLR4 are of special interest as both receptors recognise lipid-based structures. They may bind to FFA that are elevated in the blood of type 2 diabetic patients. Therefore TLR2 and TLR4 are described in more detail in chapter B.1.4.2, respectively B.1.4.3.

The IL-1 receptor type 1 (IL-1RI) and IL-1 receptor type 2 (IL-1RII) are structurally related to the TLRs and they all belong to the Toll/IL-1 receptor superfamily. The characteristic of this superfamily is their common cytosolic TIR (Toll-IL-1-receptor) domain responsible for signalling. The extracellular part of the TLRs and the IL-1R is structurally unrelated. While the IL-1RI and IL-1RII contain three Ig-like domains, the TLRs contain leucine-rich repeats (LRR) [114].

Upon ligand binding TLRs dimerize, mainly forming homodimers, but some TLRs are functional as heterodimers (e.g. TLR2, see below). Adapter proteins in the cytoplasm are recruited and the intracellular signalling pathways are initiated.

B.1.4.1 IL-1 receptors (IL-1R)

The IL-1 receptor type 1 (IL-1RI) is present in soluble and in membrane-bound form. For the membrane-bound form, two agonist ligands exist, IL-1α and IL-1β, that initiate inflammatory response. Resolution of the crystal structure of IL-1β bound to the IL-1RI showed that IL-1β connects at two places with the IL-1RI, at a large region in the groove

between the first and the second Ig-like domain and at a smaller side exclusively on the third Ig-like domain [115]. Besides the two agonistic ligands, the antagonist IL-1Ra is also able to bind to IL-1RI preventing further signalling through the receptor. The structure of IL-1Ra bound to the IL-1RI was also solved and showed that binding takes place in the same main area where also IL-1β binds but there is no binding to the third Ig-like domain of IL-1RI. Modelling revealed that the structure of the IL-1Ra/IL-1RI complex was less rigid and close than the one of the IL-1β/IL-1RI complex [116]. In addition, in the same study binding affinity for IL-1β (and IL-1α) and IL-1Ra was determined for a truncated IL-1RI consisting only of Ig-like domains 1 and 2. The overall conclusion was that IL-1 but not IL-1Ra needed domain 3 for high affinity binding, indicating that domain 3 strongly interacts with IL-1 agonists but not with the antagonist [116].

Binding of IL-1 with IL-1RI is not sufficient to initiate signalling and another component is needed. The IL-1R accessory protein (IL-1RAcP) is a coreceptor with structural similarity to IL-1RI. IL-1RAcP is recruited to the IL-1RI once IL-1α or IL-1β are bound [82]. It was suggested that IL-1RAcP binds to the interface that was newly created by interaction of IL-1 with IL-1RI [117]. When IL-1Ra is bound to the IL-1RI the model used in the same study did not calculate any interaction for that IL-1Ra/ IL-1RI complex with IL-1RAcP [117]. With complex formation of IL-1RAcP/ IL-1/ IL-1RI the two intracellular domains of IL-1RI and IL-1RAcP come in close proximity. Signalling is initiated by recruitment of MyD88 to the cytosolic part of the complex [82] (see part B.1.5.1).

Besides IL-1RI, the related IL-1 receptor type 2 (IL-1RII) has been described [113]: Although this receptor lacks a cytoplasmic TIR domain it belongs to the IL-1R/TLR family because of its high similarity of the extracellular domain to the IL-1RI. The receptor exists in a membrane-bound form and in a soluble form (after cleavage of the membrane-bound IL-1RII on the cell surface by a specific metalloproteinase). IL-1RII binds IL-1β and less efficiently IL-1α and IL-1Ra. It does not contain a TIR domain to initiate signalling and therefore, serves as a negative regulator of IL-1 signalling by preventing binding of agonists to IL-1RI. The coreceptor IL-1RAcP can also be recruited to the IL-1β/ IL-1RII complex but no signalling emanates from this complex. Thus IL-RII has two different ways to inhibit IL-1 signalling: it traps agonistic IL-1β (and less potently antagonist IL-1Ra) and also the coreceptor IL-1RAcP which then can not interact with the IL-1RI anymore.

B.1.4.2 TLR2 and its ligands

TLR2 and TLR4 expression was demonstrated in human islets by RT-PCR [118]. Moreover previous experiments in our group showed that TLR2 in islets was functional and predominantly expressed on β-cells (J. Ehses et al, manuscript submitted). TLR2 forms heterodimers with TLR1 or TLR6, each dimer having distinct ligand specificity. TLR2/ TLR1 recognises bacterial lipoproteins that contain conserved triacylated cysteines in their N-termini, TLR2/ TLR6 diacylated lipopeptides [119, 120].

Additional adapter molecules are necessary for TLR2-mediated signalling: CD14, a protein that is retained at the cell surface by a glycosyl-phosphatidyl-inositol (GPI) anchor, is needed for binding of TLR2 to MyD88 [121]. Co-receptor CD36 was shown to be essential for microbial diacylglyceride recognition by TLR2/TLR6 [122]. Intracellular TLR2 adapters Mal and MyD88 are recruited simultaneously to promote signalling (see B.1.5.1).

Recently, FFA were shown to stimulate TLR2 as well. In the human embryonic kidney cell line (293T) it was demonstrated that saturated FFA activated TLR2 [123]. Furthermore, in a myoblast cell line inhibition of TLR2 counteracted palmitate-induced insulin resistance and IL-6 production, suggesting that TLR2 mediates free fatty acid-induced insulin resistance in muscle [107]. A recent *in vivo* study suggested that TLR2 is a key modulator of the crosstalk between inflammatory and metabolic pathways, as inhibition of TLR2 expression improved insulin sensitivity and signalling in muscle and white adipose tissue of high-fat fed mice [109].

B.1.4.3 TLR4 and its ligands

TLR4 expression was observed in many tissues such as adipocytes, liver, skeletal muscle and macrophages. Furthermore it was recently shown that functional TLR4 is expressed in pancreatic islets as well [118], predominantly on non-β-cells (J. Ehses, unpublished). The most prominent ligand for TLR4 is lipopolysaccaride (LPS) of gram-negative bacterial cell walls. Saturated fatty acids of the lipid A moiety of LPS were shown to be essential for TLR4 stimulation by LPS [124]. For signalling TLR4 forms homodimers that bind to bacterial LPS. An additional LPS binding protein, CD14, is required for LPS signalling via the Trif-Tram pathway downstream of TLR4, whereas CD14 is dispensable for initiation of the MyD88-dependent pathway [121] (see B.1.5.1 and B.1.5.2). Additionally, protein MD2 enhances signal transduction via TLR4 by binding to the LRR domains of TLR4 [118]. Beside the lipid moieties of LPS, saturated free fatty acids themselves were shown to activate TLR4 in a macrophage cell line (RAW 264.7) [124].

A study by the group of J. Flier revealed that TLR4 could be the molecular link between innate immunity and FFA-induced insulin resistance [108]: Mice deficient for TLR4 were protected against high fat diet-induced insulin resistance in peripheral tissues. At the molecular level, TLR4 deficiency attenuated lipid-induced Ser307 phosphorylation of IRS1 and normalised its Tyr phosphorylation.

B.1.5 Signalling downstream of IL-1R/ TLR

B.1.5.1 Signalling via IL-1R/ TLR docking protein MyD88

MyD88 (myeloid differentiation factor 88) is the most broadly recruited downstream molecule of the IL1R/TLR superfamily. It consists of an N-terminal death domain (DD) separated from its C-terminal TIR domain by a short linker sequence [114]. MyD88 is an adapter protein binding to the IL-1RI and as well to most TLRs expect for TLR3. Association might be mediated via the TIR domain of TLRs and IL-1RI [121]. After binding to the receptor, MyD88 recruits IRAK1 and IRAK4 (IRAK: IL-1 receptor-associated kinase), probably via DD-DD interactions. The Ser/Thr kinase IRAK1 is in turn activated leading to subsequent activation of TRAF-6 (tumor necrosis factor receptor-associated factor 6) and then ECSIT (evolutionarily conserved signalling intermediate in Toll pathway). Finally MEKK-1 (mitogen actiovated kinase (MAPK) kinase) is activated which phosphorylates and thereby activates MAPKs Jnk1/2 and p38. Transcription factors are activated that can induce apoptotic signalling (e.g. via AP-1). Another signalling pathway branches out from TRAF6 binding. Recruitment of adaptor protein TAB (TAK1 binding protein) to TRAF6 leads to activation of TAK-1 (transforming growth factor-β activating kinase), which in turn activates IκK. Phosphorylation of IκB by IκK leads to dissociation of IκB from transcription factor NF-κB [80]. The released NF-κB translocates to the nucleus where it induces target gene expression as e.g. proinflammatory cytokines including IL-1, IL-6, KC and TNFα, certain growth factors and immunoregulatory molecules [125].

B.1.5.2 Other IL-1R/ TLR docking proteins

Beside these signalling molecules that are broadly required by all TLR and IL-1RI (see part B.1.5.1), several additional proteins are implicated in the TLR-induced pathways as well (e.g. Tollip, Pellinos, MEKK1 and MEKK3). Their exact roles in signal transduction is not clear yet, maybe they ensure signal specificity, as they might only be recruited by a certain TLR or in a certain cell type [121]. An overview on the different combinations of

intracellular adapters that are recruited for TLR and IL-1RI signalling is given in this paragraph and in Figure B.1.

Another important protein that might generate specificity in signalling is Mal (MyD88 adaptor like, also known as TIRAP). Mal is a TIR-domain containing adapter protein that is bound to the receptor together with MyD88. It was shown that it has a role in TLR4 and TLR2 signalling but not in IL-1 signalling [121].

Most of the TLR recruit MyD88 for signal transduction (signalling pathway described in part B.1.5.1), however TLR4 (and as well TLR3) also signals via a MyD88-independent pathway. A key component in this pathway is TRIF (TIR-related adaptor protein inducing interferon) which also docks to the receptor. Activation of this pathway via TLR3 and TLR4 leads to IFN-β expression via activation of transcription factor IRF3 [121].

TIR-domain containing protein Tram (Trif-related adapter molecule) only binds to TLR4 and it interacts with Trif, leading to IRF3-mediated IFN-β expression. In short, Tram and Mal function as binding adapters for TLR2 and TLR4 to mediate binding with Trif respectively MyD88. It is not clear yet why these adaptors are needed solely for TLR2 and TLR4 [121].

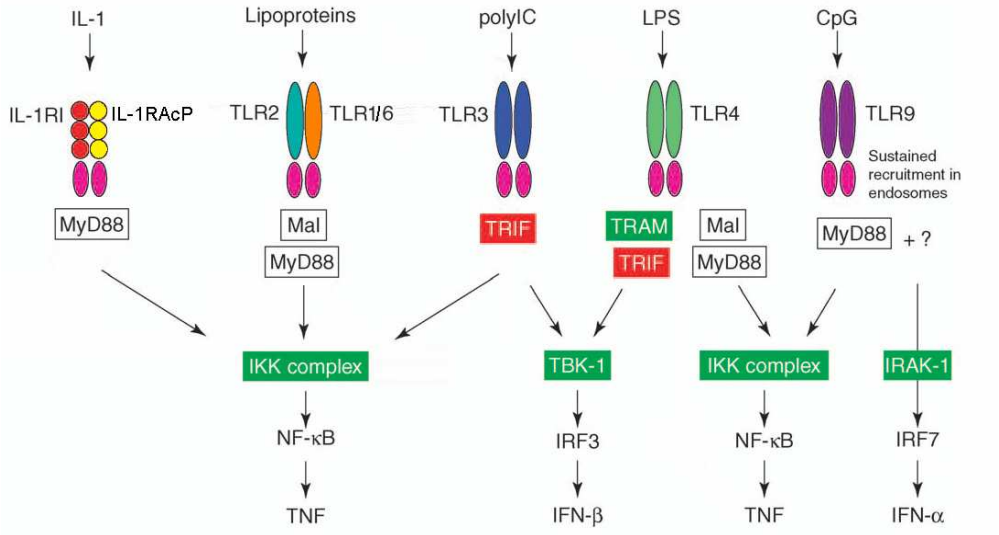

FIGURE B. 1: OVERVIEW IL-1RI/ TLR SIGNALLING
Different TLR and IL-1RI recruit diverse combinations of intracellular adapters. IL-1RI (with coreceptor IL-1RAcP) activates the NF-kB pathway via MyD88 and IKK complex. TLR2 (heterodimer with TLR1 or TLR6) requires Mal to enable MyD88 recruitment. TLR4 activates NF-kB via Mal and MyD88, and can also trigger IRF3 activation via MyD88-independent pathway via Tram and Trif. TLR3 recruits Trif, which leads to NF-kB and IRF3 activation. TLR9 also signals via MyD88, but causes a sustained recruitment of MyD88 to endosomes for IRF7 activation to occur via IRAK-1. Pink ellipse stands for Toll-IL-1-receptor (TIR) domain, red circle for Ig-like domain, differently coloured ellipses for leucine-rich repeats (LRR). Figure adapted from [121].

B.1.6 Hypothesis and aims

B.1.6.1 Our hypothesis

In pancreatic islets the mechanisms of regulation of IL-1β and KC expression and release are not well understood. In our group we have so far identified IL-1β and high glucose concentrations as inducers of IL-1β mRNA expression, the first being a strong and the latter a weak inducer [92]. In addition it was found that IL-1β-induced cytokine/ chemokine release (including IL-6, IL-8 and KC) was increased in normal mouse and human islets exposed to a diabetic milieu consisting of elevated concentrations of glucose and palmitate [112].

An important finding that finally lead to the hypothesis of the project was the fact that induction of inflammatory chemokine expression (IL-6 and KC) by IL-1β and high glucose concentration together with palmitate was totally blocked in islets of Myd88 knockout mice (J. Ehses, manuscript in preparation). As MyD88 couples to several TLRs and to IL-1RI we postulate that lipids alone or together with glucose, may induce IL-1β and KC in islets via activation of TLRs or IL-1RI. IL-1RI is known to be expressed in islets. TLR2 and TLR4 mRNA expression was also demonstrated in human islets, furthermore it was shown that TLR4 was functional [118]. TLR2 and TLR4 might be of special interest in the context of type 2 diabetes as both receptors recognise lipid-based structures and may bind to FFA. In addition, several studies propose that TLR2 and TLR4 are the molecular link between FFA and tissue inflammation inducing insulin resistance [108, 126].

B.1.6.2 Objective of the study

In order to investigate the regulation of IL-1β and KC in mouse islets, the following aims were defined and we wanted to test

- which FFA (oleate, palmitate or stearate) can stimulate IL-1β and IL-1β-regulated KC.
- if activation of TLR2 and TLR4 with specific ligands (Pam2CSK4 respectively LPS) can induce IL-1β and KC.
- if FFA induce IL-1β and KC via TLR2 or TLR4 using knockout mice for TLR2 or TLR4 (given that stimulation of TLR induces IL-1β and KC).
- whether IL-1RI activity is required for FFA-induced IL-1β and KC expression by using IL-1Ra to block the IL-1RI.

B.2 Materials and methods

B.2.1 Reagents

B.2.1.1 Reagents and antibodies for islets treatment

Recombinant mouse IL-1β was purchased from R&D (R&D systems, Minneapolis, USA). IL1Ra was obtained from Amgen (Seattle, USA). The TLR2 agonist Pam2CSK4 and the TLR4 agonist LPS (S. Minnesota LPS) were purchased from Invitrogen (San Diego, USA).

For TLR2 or TLR4 blocking in MIN6 cells and mouse islets the TLR2 (clone T2.5, cat. no. 16-9024) and TLR4 antibodies (clone MTS510, cat. no. 16-9924) and their respective isotype controls (cat. No. 16-4714 resp. 16-4321, eBioscience, San Diego, USA) were used.

B.2.1.2 Free fatty acids (FFA)

B.2.1.2.1 Conjugation to BSA

To solubilise the FFA coupling to a carrier protein, e.g. to BSA is required. Sodium salt of oleate, palmitate or stearate (Sigma-Aldrich, St. Louis, USA) was dissolved at 10 mM in CMRL medium containing 11 % BSA (FFA- and endotoxin-free, Sigma-Aldrich, St. Louis, USA) under N_2-atmosphere. The mixture was intensively vortexed and incubated over night at 50 °C in a shaking water bath. In the morning the solution was sonicated for 10 minutes and vortexed again. Then the pH was adjusted at 7.4 to 7.5. The FFA stock solutions were sterile filtrated, aliquoted and stored under N_2-atmosphere at -20 °C. For control experiments the same solution was prepared with BSA alone following the same procedure.

The effective FFA concentration in solution was determined using a commercially available kit (Wako Chemicals, Neuss, Germany) and it was not below 8 mM.

B.2.1.2.2 Endotoxin determination

FFA solutions were tested for endotoxin content using the commercially available Limulus Amebocyte Lysate QCL-1000 test (Cambrex, Charles City, USA).

B.2.2 RNA isolation and real time PCR

B.2.2.1 RNA isolation

Islets cultured on ECM dishes were washed 3 times with PBS, lysed and RNA was extracted according to the instructions of the manufacturer of the NucleoSpin kit (Macherey-Nagel GmBH, Oensingen, Switzerland) with the following modification. To increase the RNA yield the columns were incubated with elution buffer (60 µl) for 5 minutes prior to centrifugation and the eluate was then run a second time over the column.

B.2.2.2 Reverse transcription

RNA was reverse transcribed using SuperScriptTM II reverse transcriptase (Invitrogen, Basel, Switzerland) according to the manufacturer. The reaction was performed with 50 µl RNA eluate and 16 µl of a mixture containing 12 µl 5x first strand buffer, 3 µl DTT (stock 0.1 mM), 2 µl dNTP (10 mM), 0.4 µl primer random hexamers (50 ng/µl), 0.2 µl RNase inhibitor (10 U/ µl) and 0.5 µl reverse transcriptase (200 U/ µl). All the components except the random hexamers were bought from Invitrogen (Basel, Switzerland). Random hexamers were received from Microsynth (Balgach, Switzerland). The samples were incubated at 37 °C for 2 hours, and then the reaction was stopped by heating up to 72 °C for 15 minutes. After a quick centrifugation step the cDNA was stored at -20 °C.

B.2.2.3 cDNA quantitative preamplification

Transcripts that were at the lower limit of detection were preamplified using a quantitative preamplification kit from Applied Biosystems (Foster City, USA). The reaction was performed according to the manufacturers' instructions and involved a PCR preamplification reaction limited to 10 cycles. Per sample, a mix of 7.5 µl 2x TaqMan PreAmp Master Mix, 3.75 µl primer mix (100x diluted TaqMan primers in water) and 3.75 µl cDNA was used. After the PCR, the samples were diluted 1:4 with water. Preamplification was controlled by using stepwise dilutions of the same cDNA sample prior to preamplification. The shift of the C_t value (threshold cycle, defined as cycle number at which the signal was two standard deviations over background signal) in the TaqMan reaction upon preamplification between the different start-dilutions was compared and showed a constant shift.

B.2.2.4 Real time PCR (TaqMan)

For quantitative PCR, TaqMan technology (Applied Biosystems, Foster City, USA) was used. cDNA samples were diluted 1/12 in water. A 96-well reaction plate (MicroAmp fast optical 96-well reaction plate, Applied Biosystems) was loaded per well with 10 µl TaqMan 2x Universal PCR Master Mix, 1 µl of the specific primer and 9 µl of the diluted cDNA. All the applied TaqMan primers are listed in Table B.1. Each sample was measured in triplicates and corrected for different amounts of input cDNA between the samples using actin as housekeeping gene. C_t values of the cDNAs were measured with the real-time PCR system 7000 of Applied Biosystems. Changes of mRNA expression were determined with the delta-delta C_t method and the results were expressed as fold increase relative to untreated control condition.

gene	AssayID
actin β	Mm 00607939_s1
Il-1α	Mm 00439621_m1
Il-1β	Mm 00434228_m1
Il-1ra	Mm 00446185_m1
Kc (Cxcl1)	Mm 00433859_m1
Tlr1	Mm 00446095_m1
Tlr2	Mm 00442346_m1
Tlr4	Mm 00445274_m1
Tlr6	Mm 02529782_s1

TABLE B. 1: TAQMAN PRIMERS

B.2.2.5 Analysis of data from real time PCR

The data from the real time PCR experiments were analysed using Graph Pad Prism program (GraphPad, San Diego, USA). The result is shown as mean ± SEM with the number of repetition of a condition in the legend (n). ANOVA with Bonferroni's post hoc test and Student's t-test were used for significance testing (significant if $p<0.05$).

B.2.3 Detection of KC (CXCL1) protein in the supernatant

KC protein concentrations were measured in the supernatant of the islets cultures. 25 µl of the undiluted sample was measured per well using Milliplex™ Map kit for mouse cytokine (Millipore, Billerica, USA) according to the instructions of the manufacturer. Each sample was determined in duplicate. Results were expressed in pg/ml KC protein secreted from 70 cultured islets in 500 µl medium.

B.2.4 Mammalian cell line: mouse insulinoma cells (MIN6)

MIN6B1 β-cell line [127] was kindly provided by Dr. Philippe Halban (University of Geneva, Switzerland) with permission from Dr. Dr. Jun-ichi Miyazaki (University of Osaka, Japan) who produced the maternal MIN6 cell line [128]. The cells were cultured at 37 ℃ and 5 % CO_2 in DMEM (4500 mg glucose/ml medium) with L-glutamine supplemented with 15 % FBS, 100 U/ml penicillin, 100 µg/ml streptomycin, 1.2 % sodium pyruvate and 0.1 % β-mercaptoethanol.

B.2.5 Mouse islet cells

B.2.5.1 Mouse strains

Islets from male C57BL/6 mice (Harlan Laboratories, Horst, Netherlands) aging from 8 to 12 weeks were used for all experiments with wild type mouse islets.

TLR2 knockout mice backcrossed on C75BL/6J were initially bought from Jackson Laboratory (Bar Harbour, USA) and the strain was then maintained in our facility. For the experiments 8 to 12 weeks old male littermate knockout, heterozygote and wild type mice were chosen. Mice were genotyped with primers as specified by Jackson Laboratory (Bar Harbor, USA).

Male TLR4 knockout mice and C75BL/10J control mice were purchased from the Jackson Laboratory; they were 8 to 10 weeks old when islets were isolated.

MyD88 knockout mice backcrossed on C75BL/6J for 10 generations were kindly provided by Dr. S. Akira (Osaka University, Japan) and bread in our animal facility. Male knockout and heterozygote littermate mice from our facility and wild type C75BL/6J mice from the Institut für Labortierkunde (RCC, Füllinsdorf, Switzerland) were age-matched for the experiments. The mice were older than the ones usually used for islet isolation since they were leftover animals from another study, the average age was 6.5 month and the maximal age was 10 month. The mice were genotyped by PCR with the primer sets wtMyD88fwd 5'catggtggtggttgtttctg3' and wtMyD88rev 5'gggaaagtccttcttcatcgc3' for detection of the MyD88 wild type allele and MyD88neofwd 5'aaacgccggaacttttcg3' and MyD88neorev 5'gcttgccgaatatcatggtg3' for the neo-cassette.

B.2.5.2 Isolation and culture of mouse islets

Mouse pancreas was perfused with 2 ml collagenase solution (Worthington Biochemical Corporation, Lakewood, USA) and then the pancreas was resected. Collagenase solution was made with 50 ml Hank's Buffered Salt Solution (HBSS, Invitrogen, San Diago, USA), supplemented with 500 µl 1M HEPES (Invitrogen, San Diago, USA), 16.5 µl Dnase (10 µg/ml, Roche, Basel, Schweiz) and collagenase with 2 mg/ml final concentration. Further digestion in additional 2 ml collagenase solution for 30 minutes at 37 ℃ lead to the isolation of the islets. Addition of 30 ml ice cold quenching buffer (500 ml HBSS, 12 ml 1M HEPES, 2.5 g BSA) stopped digestion. After centrifugation, washing and filtration islets were separated from the exocrine tissue of the pancreas by density gradient centrifugation with 4 different density layers, each one 10 ml: density 1119 (Histopaque-1119, Sigma-Aldrich, St. Louis, USA), density 1100 (20 ml Histopaque-1119 + 4 ml HBSS), density 1080 (16 ml Histopaque-1119 + 8 ml HBSS), density 1060 (12 ml Histopaque-1119 + 12 ml HBSS). Handpicking of the islets after the gradient increased the purity.

Mouse islets were cultured in RPMI 1640 medium containing 11 mM glucose, 10 % FCS, 100 U/ml penicillin, 100 µg/ml streptomycin and 40 µg/ml Gentamycin. After isolation Islets were kept in suspension over night and then 70-80 islets/dish were plated on extracellular matrix (ECM) coated dishes (Novamed, Jerusalem, Israel). Care was taken to match islet sizes between dishes within one experiment. Islets were allowed to attach and spread for three days before the treatments were started. Unless otherwise noted islets were incubated in the presence of FFA or TLR ligands for 48 hours.

B.3 Results

B.3.1 FFA induce IL-1β and KC mRNA

B.3.1.1 Palmitate and stearate induce IL-1β and KC mRNA in mouse islets

Free fatty acids (FFA) were tested for their potential to stimulate IL-1β and KC in mouse islets. Oleate (C18:1), palmitate (C16:0) and stearate (C18:0) were chosen for the experiments as they are the most abundant FFA in the circulation of human and mouse. They were coupled to BSA and added to the culture medium of isolated mouse islets on ECM dishes. BSA alone was used as negative control in all the experiments with FFA treatment. RNA was extracted from cell lysates and reverse transcribed to cDNA. Real time PCR was performed with the cDNA samples to measure IL-1β and KC expression levels.

Since oleate did not affect IL-1β and KC mRNA levels compared to BSA-treated islets, preliminary time course experiments were only performed with palmitate and stearate. IL-1β and KC mRNA expression was analysed after 6 h, 24 h and 48 h of incubation. Palmitate induced maximal IL-1β and KC mRNA expression after 24 h. Stearate-induced IL-1β and KC mRNA expression was more constant over the whole time period, with a minor reduction after 1 day of incubation. Based on this experiment, 2 day incubations were chosen for the following experiments with FFA treatment in mouse islets (data not shown).

To find the most effective concentration of palmitate and stearate with respect to IL-1β and KC mRNA induction, mouse islets were cultured for 2 days with increasing FFA concentrations. Palmitate reached maximal stimulation with 0.2 mM and induced IL-1β mRNA 2.1 ±1.3 fold and KC mRNA expression 6.6 ±3.1 fold (Figure B.2A-B). Raising the concentration to 0.5 mM did not further induce IL-1β mRNA and KC mRNA level and was equal to that with 0.1 mM (both 2.3 fold). Like palmitate, stearate showed the strongest induction at 0.2 mM, stimulating IL-1β 3.3 ±0.5 fold and KC mRNA 13.2 ±0.7 fold. In contrast to palmitate at 0.5 mM, the IL-1β mRNA induction with the same concentration of stearate was still 2.8 ±0.5 fold elevated. Stearate at 0.5 mM induced KC mRNA 6.6 ±1.6 fold corresponding to a higher induction than with 0.1 mM (Figure B.2C-D). The optimal concentration for palmitate and stearate for two days incubation of mouse islets with respect to IL-1β and KC mRNA induction was 0.2 mM. Since this dose-response

experiment was not performed at the beginning of the study, part of the subsequent experiments were done with 0.1 mM palmitate and 0.5 mM stearate.

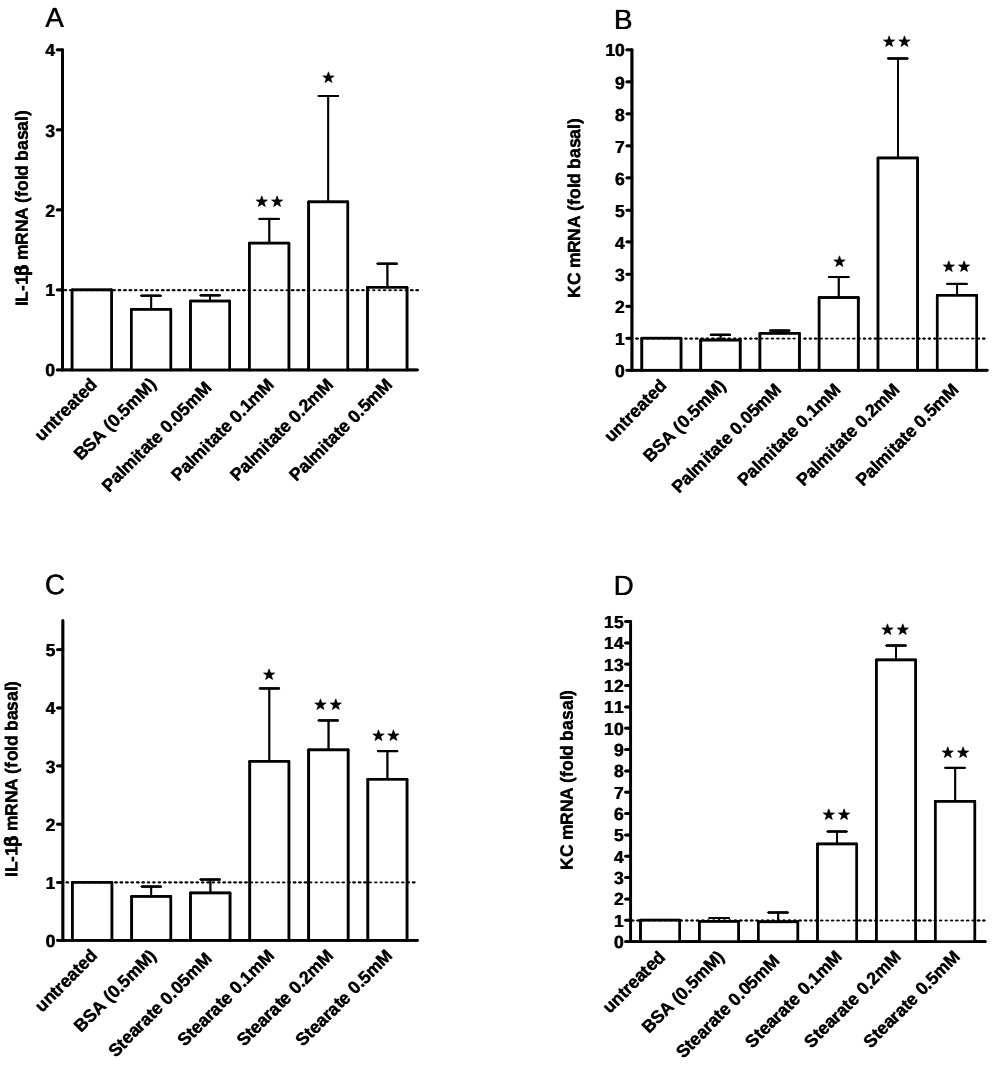

FIGURE B. 2: DOSE-RESPONSE OF FFA-INDUCED IL-1β AND KC mRNA IN ISLETS
Mouse islets were incubated for 2 days on ECM-coated dishes with BSA (n=12) or increasing concentrations of palmitate (n=2-8) or stearate (n=2-12). IL-1β and KC mRNA expression levels are expressed as fold of the untreated controls (mean ± SEM). A: Effect of different palmitate concentrations on IL-1β mRNA expression. B: Effect of different palmitate concentrations on KC mRNA expression. C: Effect of different stearate concentrations on IL-1β mRNA expression. D: Effect of different stearate concentrations on KC mRNA expression. Significance was determined for BSA vs FFA treated cultures for each individual concentration with Student's t test, * represents $p<0.05$ and ** $p<0.01$.

To assess if high glucose concentration can induce IL-1β and KC, islets were incubated at basal (11.1 mM) or high glucose (33.3 mM) concentrations. When islets were coincubated with high glucose and FFA IL-1β mRNA expression was reduced to basal level (data not shown). KC mRNA levels upon stearate treatment were similar at low or high glucose

concentrations. However, co-incubation of palmitate and high glucose amplified KC mRNA induction: In islets incubated in the presence of 0.5 mM palmitate and 33.3 mM glucose KC mRNA was increased 8.2 ±2.9 fold whereas palmitate alone only stimulated KC mRNA levels 2.3 ±0.4 fold and glucose alone 2.3 ±0.6 fold (Figure B.3).

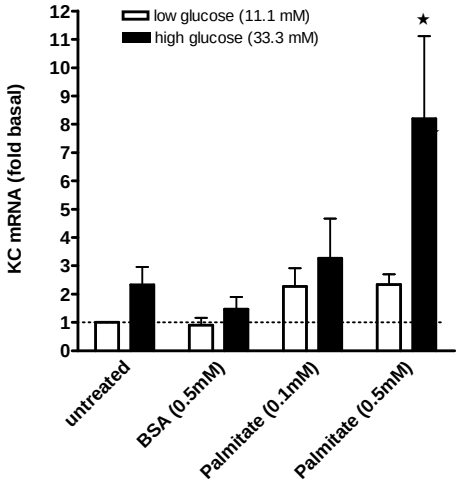

FIGURE B. 3: PALMITATE AND HIGH GLUCOSE AMPLIFIED KC mRNA INDUCTION IN ISLETS
Mouse islets were incubated for 2 days on ECM-coated dishes with 0.5 mM BSA, 0.1 mM palmitate or 0.5 mM palmitate in combination with low glucose (11.1 mM, open bars) or high glucose (33.3 mM, black bars). KC mRNA expression levels are expressed as fold of the untreated controls (means ± SEM, n= 2-7). Significance was determined for BSA under low glucose vs FFA treated cultures with Student's t test, * represents $p<0.05$.

B.3.1.2 Palmitate and stearate induce KC mRNA in MIN6

Murine MIN6 sublines A, B1 and C3 were tested in order to find a cell line suitable for mechanistic studies or for pilot-experiments. However, none of the tested sublines expressed IL-1β mRNA. Only the MIN6B1 subline (see part B.2.4) expressed KC mRNA that was inducible e.g. with IL-1β. All subsequent experiments were performed with this MIN6 cell line.

Like in mouse islets, oleate did not induce KC mRNA. A time course experiment revealed an increase in palmitate- and stearate-induced KC mRNA reaching a maximum after 24 h incubation. At 48 h the fold induction of KC mRNA was still higher compared to the untreated or BSA control but lower than after 24 h. Thus MIN6 cells were incubated for one day in the presence of FFA in all subsequent experiments.

In a dose-response experiment MIN6 cells were incubated for one day with various concentrations of palmitate or stearate (0.1 to 0.5 up to 1 mM). With increasing

concentration of FFA, KC mRNA induction increased as well (Figure B.4). For later treatment of MIN6 cells 0.5 mM palmitate or stearate was chosen. This concentration was in the same range as the optimal concentration for mouse islets treatment and a clear induction of KC mRNA could be demonstrated (3.5 ±1.2 fold for palmitate and 5.6 ±1.4 fold for stearate). Visual inspection of the cultures under the microscope showed less detached or dead cells in MIN6 cell cultures than in mouse islet cultures treated with the same concentration of a FFA, suggesting that mouse islets were more sensitive to toxic effects of FFA than MIN6 cells.

Addition of glucose up to 46.6 mM to the culture medium of MIN6 cells in the presence of the FFA did not change KC mRNA induction. However, one has to be aware that the culture media of MIN6 cells already contains 25 mM glucose while primary mouse islets are cultured at physiologic 11.1 mM glucose thus limiting for conclusions for the high glucose conditions in MIN6 cultures.

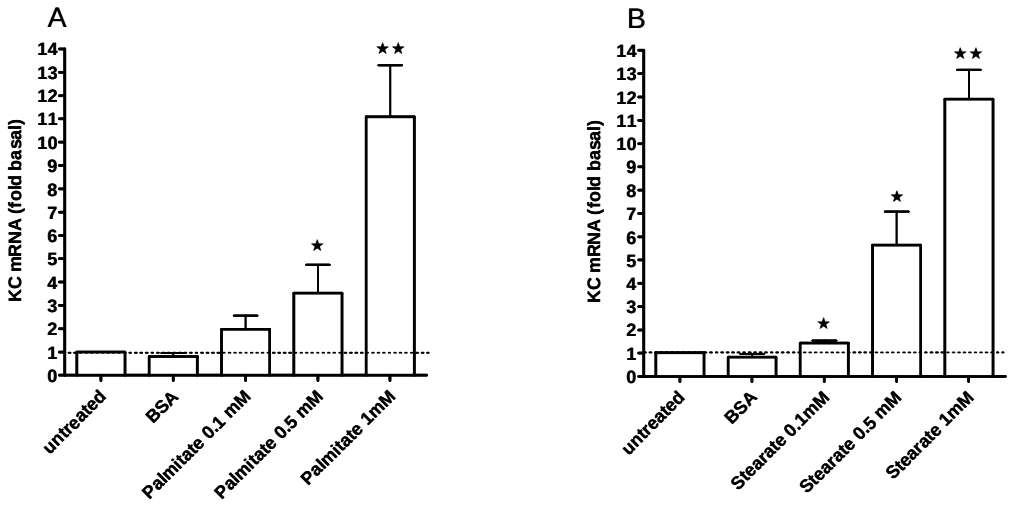

FIGURE B. 4: DOSE-RESPONSE OF FFA-INDUCED KC mRNA IN MIN6

MIN6 cells were incubated for 1 day with BSA or increasing concentrations of palmitate or stearate. KC mRNA expression levels are expressed as fold of the untreated controls (mean ± SEM, n=3). A: Effect of different palmitate concentrations on KC mRNA expression. B: Effect of different stearate concentrations on KC mRNA expression. Significance was determined for BSA vs FFA treated cultures for each individual concentration with Student's t test, * represents $p<0.05$ and ** $p<0.01$.

B.3.2 Specific TLR2 and TLR4 ligands induce IL-1β and KC mRNA

B.3.2.1 LPS and Pam2CSK4 induce IL-1β and KC-mRNA in mouse islets

As TLR2 and TLR4 are activated by lipid-based structures we hypothesised that FFA induce IL-1β and KC mRNA via TLR (see part B.1.6.1). First, we tested whether TLR2 and TLR4 are functional in mouse islets and whether their activation can induce IL-1β and KC mRNA. For this purpose islets were incubated for 2 days with the TLR2 ligand Pam2CSK4 or with the TLR4 ligand LPS. Both TLR ligands significantly induced IL-1β and KC mRNA expression. LPS increased IL-1β 8.1 ±1.6 fold and KC mRNA 5.2 ±0.8 fold. Pam2CSK4 was the strongest inducer for both IL-1β (47.7 ±7.5 fold) and KC mRNA (59.9 ±18.6 fold) (Figure B.5). As IL-1β is known for its auto-stimulatory action it was used as a positive control in this experiment. IL-1β mRNA was increased 3.9 ±0.7 fold and KC mRNA 22.2 ±4.6 fold upon IL-1β treatment of islets, as depicted in Figure B.5. Preliminary time course experiments showed that IL-1β auto-stimulation and IL-1β-induced KC mRNA was maximal at the first measured time point after 6 h of incubation (ca 20-fold for IL-1β resp. 300-fold for KC mRNA), then it decreased rapidly. IL-1β mRNA induction after 24 and 48 h was in the range of the induction with the FFA, whereas IL-1β-induced KC mRNA expression was higher than FFA-induced KC mRNA level at all time points.

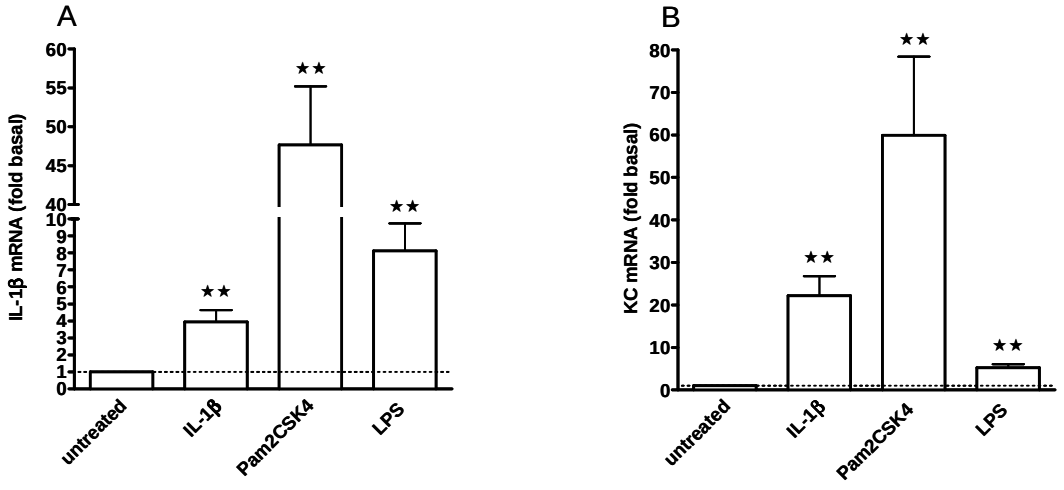

FIGURE B. 5: TLR LIGAND-INDUCED IL-1β AND KC mRNA IN ISLETS

Mouse islets were incabated for 2 days on ECM-coated dishes with 0.2 ng/ml IL-1β (n=9), 0.1 μg/ml Pam2CSK4 (n=4) or 1 μg/ml LPS (n=4). IL-1β and KC mRNA expression levels are expressed as fold of the untreated controls (mean ± SEM). A: IL-1β auto-stimulation and effect of Pam2CSK4 and LPS treatment on IL-1β mRNA expression. B: Effect of IL-1β, Pam2CSK4 and LPS treatment on KC mRNA expression. Significance was determined for untreated islets vs treated cultures with Student's t test, * represents $p<0.05$ and ** $p<0.01$.

These previously described experiments demonstrate that there is expression of functional TLR2 and TLR4 in islets. In support, we detected TLR2 and TLR4 mRNA in mouse islets (data not shown).

B.3.2.2 Pam2CSK4 induces KC mRNA in MIN6

Specific TLR2 and TLR4 ligands (Pam2CSK4 and LPS, respectively) and IL-1β were also tested in MIN6 cells upon incubation for 1 day. The strongest inducer in this cell line was IL-1β stimulating KC mRNA 46.7 ±7.5 fold. Pam2CSK4 induced KC mRNA 13.7 ±1.7 fold. LPS, the ligand for TLR4, had no effect (Figure B.6). Different incubation times (3h to 48h) and doses (up to 10 μg/ml) of LPS were tested, but no induction of KC mRNA was observed (data not shown). A preliminary time course experiment for Pam2CSK4 in MIN6 cells revealed that induction of KC mRNA after 3 and 6 hours was even higher than after 24 hours, the timepoint used during the previous experiment.

Increased glucose concentrations during the incubation with IL-1β, Pam2CSK4 or LPS did not further stimulate KC mRNA induction (data not shown).

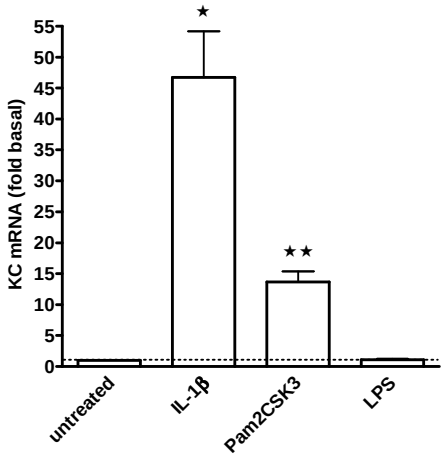

FIGURE B. 6: TLR LIGAND-INDUCED KC mRNA IN MIN6

MIN6 cells were incubated for 1 day in the presence of 0.2 ng/ml IL-1β, 0.1 μg/ml Pam2CSK4 (TLR2 ligand) or 1 μg/ml LPS (TLR4 ligand). KC mRNA expression levels are expressed as fold of the untreated controls (mean ± SEM, n=3-6). Significance was determined for untreated islets vs treated cultures with Student's t test, * represents $p<0.05$ and ** $p<0.01$.

B.3.2.3 Dose-dependence of LPS-induced IL-1β and KC mRNA in mouse islets

As LPS was very potent in inducing IL-1β and KC mRNA in mouse islets we wanted to exclude that the reaction of the cells to incubation with FFA solution was due to endotoxin contaminations in our samples. Therefore, the endotoxin content of different FFA and BSA preparations was determined (see part B.2.1.2.2). All samples contained less than 0.15 ng/ml LPS in the dilution that was used to treat islets on the ECM dishes.

To affirm that this concentration was ineffective in triggering IL-1β or KC induction, different doses of LPS were tested in mouse islets (Figure B.7). 10 ng/ml of LPS, a dose more than 50 times higher than the highest concentration measured in endotoxin-test, did not induce IL-1β nor KC mRNA. Induction was only obtained with a dose of 100 ng/ml and higher.

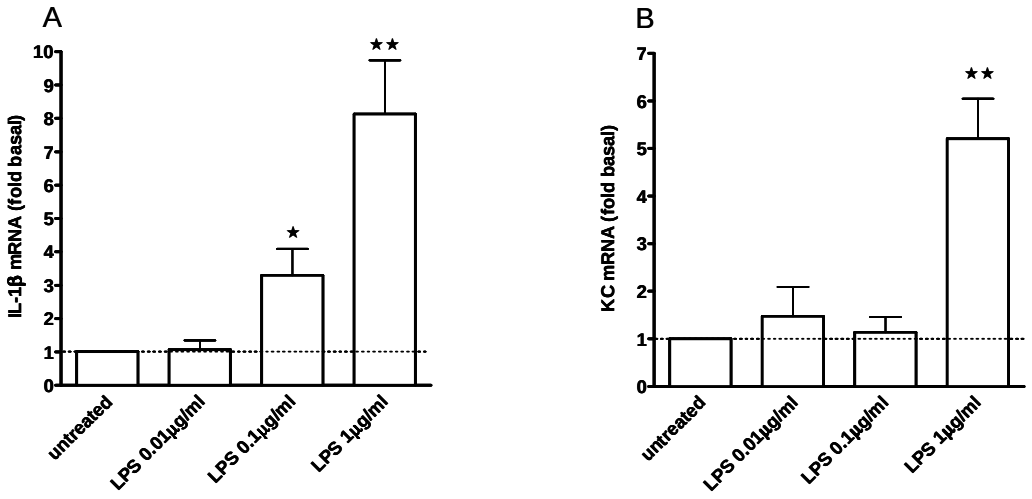

FIGURE B. 7: DOSE-RESPONSE OF LPS-INDUCED IL-1β AND KC mRNA IN ISLETS
Mouse islets were incubated for 2 days in the presence of increasing concentrations of LPS on ECM-coated dishes. IL-1β and KC mRNA expression levels are expressed as fold of the untreated controls (mean ± SEM, n=4). A: Effect of different LPS concentrations on IL-1β mRNA expression. B: Effect of different LPS concentrations on KC mRNA expression. Significance was determined for untreated islets vs LPS treated cultures for each individual concentration with Student's t test, * represents $p<0.05$ and ** $p<0.01$.

To exclude synergism between FFA and with low endotoxin concentrations (that alone did not have any effect), mouse islets were co-incubated with palmitate and 10 ng/ml LPS. The fold induction of IL-1β and KC mRNA by palmitate and LPS together never exceeded that of palmitate or LPS alone (data not shown).

B.3.3 FFA-induced IL-1β and KC mRNA and IL-1β auto-stimulation are MyD88-dependent

TLRs and IL-1 receptor use similar intracellular signalling components, e.g. MyD88 that couples to the IL-1 receptor and to many TLRs including TRL2 and TLR4. To test if FFA stimulate IL-1β and KC mRNA via IL-1R and TLRs, islets isolated from MyD88 knockout mice were incubated in the presence of FFA followed by assessment of IL-1β and KC mRNA.

Islets of male wild type, heterozygous and MyD88-deficient mice were incubated in the presence of palmitate, stearate or IL-1β (positive control) for 2 days. Stearate- and IL-1β-induced IL-1β and KC mRNA stimulation was significantly lower in knockout islets than in wild type islets and not different from untreated wild type islets (Figure B.8). Similarly, palmitate treatment showed a trend to a decrease in IL-1β and KC mRNA levels in knockout islets, although the data were not significant.

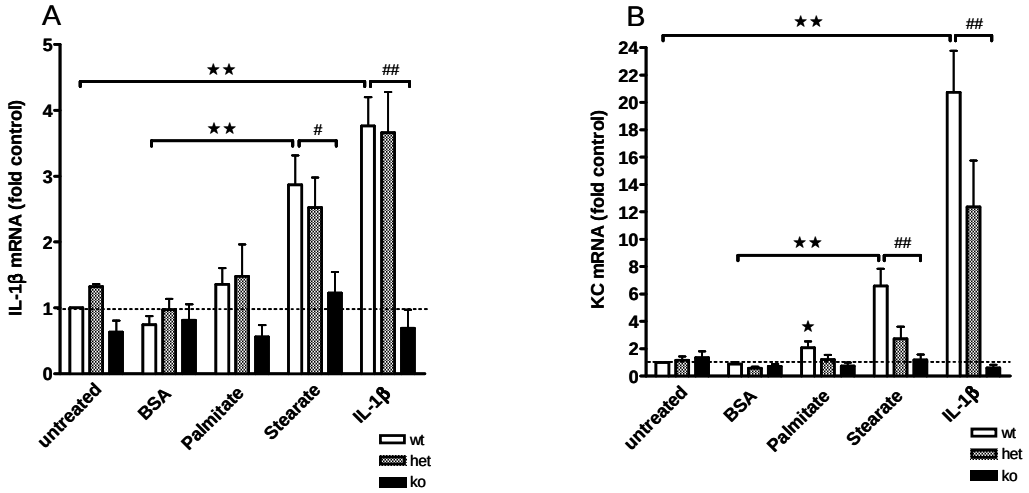

FIGURE B. 8: FFA- AND IL-1β-INDUCED IL-1β AND KC mRNA EXPRESSION WAS MYD88-DEPENDENT

Islets from MyD88 knockout mice, heterozygote and respective C75BL/6J wild type control were incubated for 2 days in the presence of 0.5 mM BSA, 0.1 mM palmitate, 0.5 mM stearate or 0.2 ng/ml IL-1β on ECM-coated dishes. IL-1β and KC mRNA expression levels are expressed as fold of the untreated wild type controls (mean ± SEM, n=3-16). For this experiment a total of 15 mice per genotype were sacrificed in 3 separate isolations. A: Effect of FFA and IL-1β treatment on IL-1β mRNA expression in MyD88 knockout mice. B: Effect of FFA and IL-1β treatment on KC mRNA expression in MyD88 knockout mice. Significance was determined by ANOVA with Bonferroni's post hoc test, * and # represents $p<0.05$, ** and ## $p<0.01$.

B.3.4 FFA-induced IL-1β and KC mRNA expression is partially TLR2-dependent

B.3.4.1 FFA-induced change in IL-1β and KC mRNA expression in TLR2 knockout mice?

As a next step, it was tested if TLR2 is required for FFA-induced stimulation of IL-1β and KC. Islets of a TLR2 knockout mouse strain were incubated in the presence of FFA, the results are shown in Figure B.9. Palmitate-induced IL-1β mRNA showed a trend to a reduction in TLR2 knockout mice compared to littermate wild type. When islets were incubated in the presence of stearate or IL-1β, level of IL-1β mRNA expression was not lower in knockout islets compared to wild type islets. For KC mRNA induction there was a trend towards a decrease in the palmitate-stimulated wild type islets vs knockout islets, and a strong trend (p=0.063) upon stearate treatment. However, in contrast to islets of MyD88 knockout mice FFA-induced IL-1β and KC mRNA expression was not completely blocked in TLR2 knockout mice.

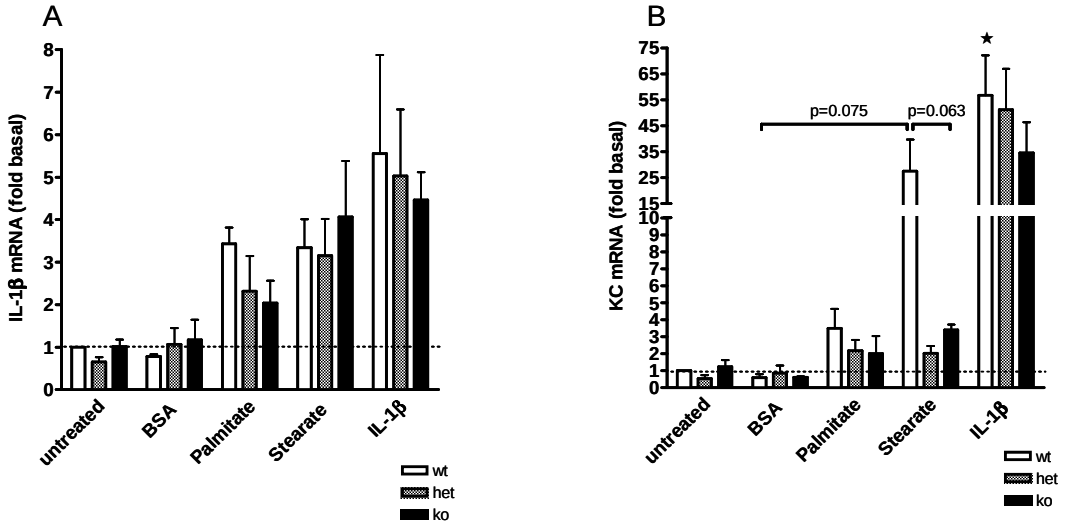

FIGURE B. 9: FFA- AND IL-1β-INDUCED IL-1β AND KC MRNA WERE PARTLY TLR2-DEPENDENT
Islets from TLR2 knockout mice, heterozygote and respective C75BL/6J wild type control were incubated for 2 days in the presence of 0.5 mM BSA, 0.1 mM palmitate, 0.5 mM stearate or 1 ng/ml IL-1β on ECM-coated dishes. IL-1β and KC mRNA expression levels are expressed as fold of the untreated wild type controls (mean ± SEM, n=3-8). For this experiment 21-28 mice per genotype were sacrificed in 4 separate isolations. A: Effect of FFA and IL-1β treatment on IL-1β mRNA expression in TLR2 knockout mice. B: Effect of FFA and IL-1β treatment on KC mRNA expression in TLR2 knockout mice. Significance was determined by ANOVA with Bonferroni's post hoc test, * represents $p<0.05$ in IL-1β treated wild type vs untreated wild type, p-values of stearate treated wild type vs BSA treated wild type and stearate treated wild type vs stearate treated TLR2 knockout are indicated.

B.3.4.2 FFA-induced change in KC mRNA expression in MIN6 cells incubated in the presence of TLR2 antibody?

To gain further evience for a role of TLR2 in mediating the effects of FFA on pro-inflammatory cytokine expression we performed experiments with a TLR2 blocking antibody. In a first experiment we used MIN6 cells and added a mouse TLR2 antibody together with palmitate or stearate (Figure B.10). Stearate- and palmitate-induced KC mRNA expression was unchanged when the TLR2 antibody was added to the cells. Incubation with the TLR2 ligand Pam2CSK4 confirmed that the antibody prevents a TLR2 response since Pam2CSK4-induced KC mRNA induction was completely blocked when cells were co-incubated with TLR2 antibody. Therefore, the induction of KC by FFA is independent of TLR2 in MIN6 cells.

Unfortunately, preliminary experiments in isolated mouse islets revealed that the TLR2 antibody was not effective in islets. Pam2CSK4-induced IL-1β and KC mRNA levels were only slightly decreased when the antibody was added as well and we decided not to further pursue these experiments in mouse islets.

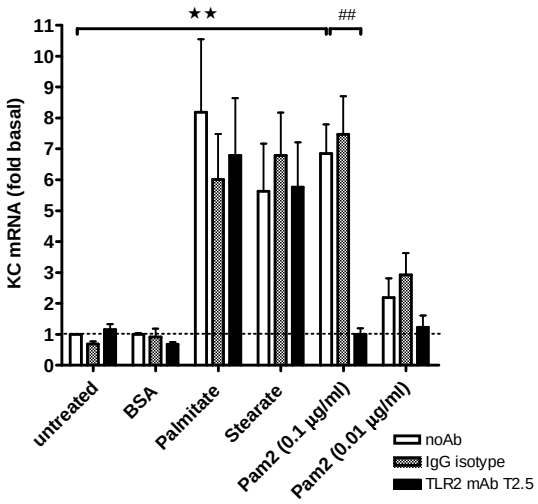

FIGURE B. 10: TLR2 ANTIBODY IN MIN6

MIN6 cells were preincubated for 1 h with 10 µg/ml TLR2 antibody or with 10 µg/ml IgG isotype control and then 0.5 mM BSA (n=2), 0.5 mM palmitate (n=4), 0.5 mM stearate (n=4), 0.1 µg/ml Pam2CSK4 (n=4) or 0.01 µg/ml Pam2CSK4 (n=2) were added during 1 day. Effect of the TLR2 blocking antibody during FFA or Pam2CSK4 treatment on KC mRNA expression levels are expressed as fold of the untreated controls (mean ± SEM). Significance was determined by ANOVA with Bonferroni's post hoc test, ** represents $p<0.01$ in Pam2CSK4 treated vs untreated cells, ## represent $p<0.01$ in Pam2CSK4 treated vs Pam2CSK4 and TLR2 antibody treated cells.

B.3.5 FFA-induced IL-1β and KC mRNA expression is not TLR4-dependent

Given the fact that FFA-induced IL-1β and KC mRNA expression was completely MyD88-dependent but only partially TLR2-dependent, we next investigated TLR4, which also docks to MyD88 and which is also activated by FFA. TLR4 knockout mouse islets and appropriate wild type control were incubated in the presence of FFA, LPS and IL-1β. The TLR4 ligand LPS neither stimulated IL-1β nor KC mRNA in the knockout mice confirming that TLR4 was not functional. Palmitate- and stearate-induced IL-1β mRNA expression was increased in both wild type and TLR4 knockout mouse islets, however, there was no difference between respective wild type and knockout islets (Figure B.11A). KC mRNA levels of palmitate treated islets were significantly decreased in the knockout islets compared to the wild type islets and the same trend was observed for stearate treated knockout islets. Similarly, IL-1β-induced KC mRNA level was drastically reduced in the TLR4 knockout mice (7.8 times) (Figure B.11B). Interestingly, the basal KC mRNA level in the knockout mice was about 70 % lower than in the wild type. Therefore, in Figure B.11C basal wild type and basal knockout KC mRNA level were both set to 1. When basal levels of wild type and knockout islets were equalised, the fold KC mRNA induction by the FFA was very similar in knockout and wild type islets, while LPS- and IL-1β-induced KC mRNA expression was still significantly reduced in knockout islets. Hence the different stimulation in wild type and knockout TLR4 islets was not due to a reduced responsiveness to FFA, but rather due to a lower KC expression level in the basal state.

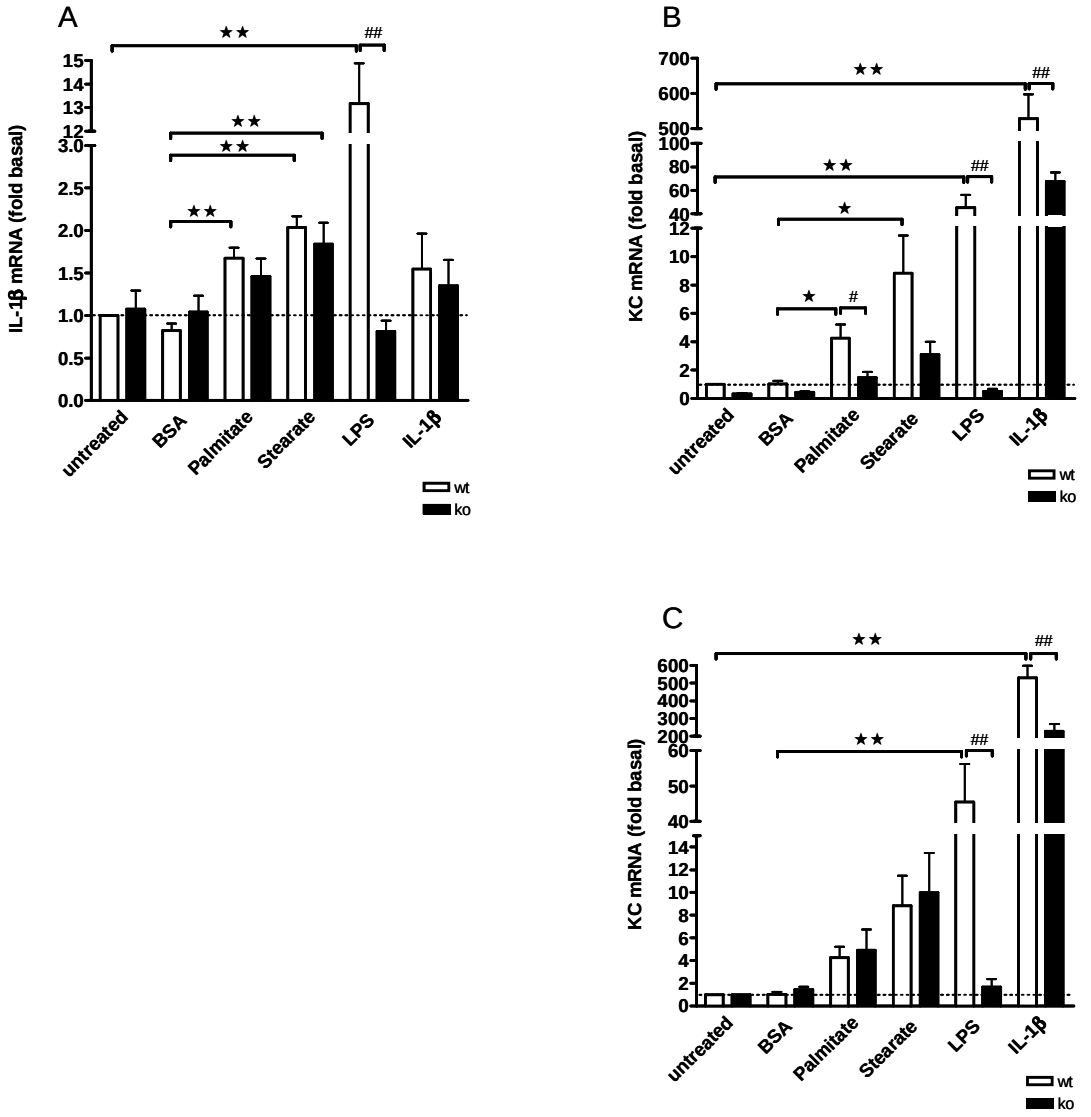

FIGURE B. 11: FFA- AND IL-1β-INDUCED IL-1β AND KC mRNA WERE NOT TLR4-DEPENDENT
Islets from TLR4 knockout mice and respective C75BL/10J wild type control were incubated for 2 days in the presence of 0.2 mM BSA, 0.2 mM palmitate, 0.2 mM stearate, 1 μg/ml LPS or 1 ng/ml IL-1β on ECM-coated dishes. In (A-B) IL-1β respectively KC mRNA expression levels are expressed as fold of the untreated wild type controls, in (C) KC mRNA expression of untreated wild type and knockout are both set to 1, then all wild type conditions are expressed relative to untreated wild type and all knockout conditions relative to untreated knockout (mean ± SEM, n=5-11). For this experiment 25 mice per genotype were sacrificed in 3 separate isolations. A: Effect of FFA, LPS and IL-1β treatment on IL-1β mRNA expression in TLR4 knockout mice. B-C: Effect of FFA, LPS and IL-1β treatment on KC mRNA expression in TLR4 knockout mice. Significance was determined by ANOVA with Bonferroni's post hoc test, * and # represents $p<0.05$, ** and ## represents $p<0.01$.

To complete the data from the TLR4 knockout mice it was planned to use a TLR4 blocking antibody. In part B.3.2.2., it was demonstrated that MIN6 did not induce KC mRNA expression upon LPS stimulation. Either the TLR4 was not functional in this cells or one of the signalling complex partners (CD14 or MD2) needed for LPS signalling were not expressed or not functional in MIN6. So the functionality of the TLR4 antibody could not be tested in MIN6. Nevertheless a preliminary experiment in MIN6 was realised where the TLR4 antibody did not have any effect on FFA-induced KC mRNA expression (Figure B.12). Therefore the TLR4 antibody was not applied in isolated mouse islets.

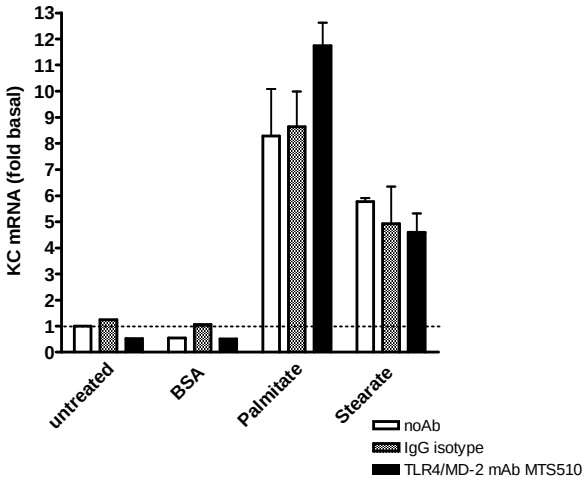

FIGURE B. 12: TLR4 ANTIBODY IN MIN6

MIN6 cells were preincubated for 1 h with 10 μg/ml TLR4 antibody or with 10 μg/ml IgG isotype control and then additionally incubated for 1 day in the presence of 0.5 mM BSA (n=1), 0.5 mM palmitate (n=2) or 0.5 mM stearate (n=2). Effect of the TLR4 blocking antibody during FFA treatment on KC mRNA expression levels are expressed as fold of the untreated controls (mean ± SEM).

B.3.6 FFA-induced IL-1β and KC mRNA expression requires IL-1R activity

To test whether FFA-induced IL-1β and KC mRNA expression requires IL-1R activity, recombinant IL-1Ra was added to the cells to antagonise with the IL-1 activity. At the mRNA level IL-1β-induced KC was significantly blocked with IL-1Ra. FFA-induced KC mRNA expression was decreased as well in presence of the IL-1Ra, even if the stimulation with the FFA alone was not significant (Figure B.13A). KC protein was determined in the supernatant of the cultured mouse islets. Stearate- and IL-1β-induced KC protein expression was blocked with simultaneous IL-1Ra treatment. KC protein level

after palmitate treatment was not significantly higher than in untreated or BSA treated islets, but significantly decreased when IL-1Ra was added (Figure B.13B).

Unfortunately IL-1β mRNA could not be detected in this experiment due to technical reasons. The concentration of released IL-1β protein in the medium by islets is low, as the protein is known to be biologically active at very low concentrations. Therefore detection of IL-1β protein by ELISA is typically not possible. However, since IL-1Ra was able to block KC protein expression under various treatment conditions we conclude that the IL-1R was engaged in signalling most likely via functional IL-1β or IL-1α protein produced by islets.

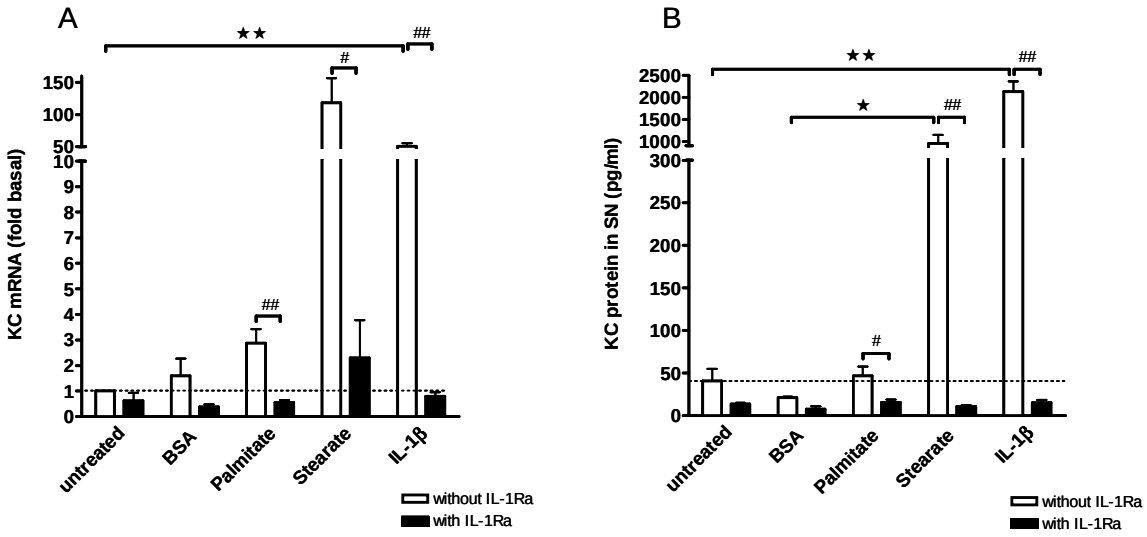

FIGURE B. 13: INCUBATION OF ISLETS WITH IL-1RA

Mouse islets on ECM-coated dishes were incubated for 2 days in the presence of 0.5 mM BSA (n=2-4), 0.1 mM palmitate (n=6), 0.5 mM stearate (n=5) or 1 ng/ml IL-1β (n=3) in the absence (open bars) or presence (black bars) of IL-1Ra (1 μg/ml, 15 minutes preincubation). IL-1β and KC mRNA expression levels are expressed as fold of the untreated controls (mean ± SEM). A: Effect of IL-1Ra on FFA- or IL-1β-induced IL-1β mRNA expression. B: Effect of IL-1Ra on FFA- or IL-1β-induced KC mRNA expression. Significance was determined by ANOVA with Bonferroni's post hoc test, * and # represents $p<0.05$, ** and ## represents $p<0.01$.

MIN6 cells were incubated with the IL-1Ra as well. There was no effect on palmitate-, stearate- or Pam2CSK4-induced KC mRNA expression level when the cells were cotreated with IL-1Ra (Figure B.14). IL-1β-stimulated KC mRNA induction was completely blocked, indicating that IL-1Ra was active and IL-1RI was functional in these cells. In contrast to mouse islets, MIN6 cells do not express IL-1RI ligand IL-1β, therefore no antagonism on FFA-induced KC level by IL-1Ra was expected.

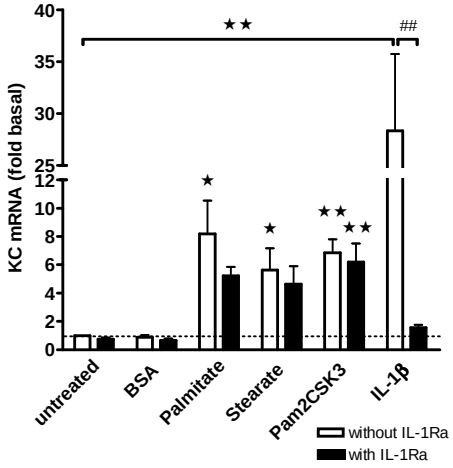

FIGURE B. 14: INCUBATION OF MIN6 WITH IL-1RA
MIN6 cells were incubated for 1 day in the presence of 0.5 mM BSA , 0.5 mM palmitate, 0.5 mM stearate, 0.1 μg/ml Pam2CSK4 or 0.2 ng/ml IL-1β in the absence (open bars) or presence (black bars) of IL-1Ra (1 μg/ml, 15 minutes preincubation). Effect of the IL-1Ra on FFA-, Pam2CSK4- or IL-1β-induced KC mRNA expression levels are expressed as fold of the untreated controls (mean ± SEM, n=2-6). Significance was determined by ANOVA with Bonferroni's post hoc test, * represents $p<0.05$ and ** $p<0.01$, ## represents $p<0.01$.

B.3.7 Do FFA induce IL-1α or IL-1Ra mRNA?

In mouse islets FFA-induced IL-1β and KC expression is IL-1R-dependent (see part B.3.6). Beside IL-1β there are two other ligands for the IL-1R, IL-1α and IL-1Ra. It was tested whether mRNA induction of IL-1α and IL-1Ra mRNA were FFA-dependent as well.

IL-1β stimulated IL-1α mRNA expression 5.7 ±0.8 fold, whereas the FFA palmitate and stearate did not have any significant effect on IL-1α mRNA expression (Figure B.15).

FFA also did not significantly induce IL-1Ra m RNA, even though stearate shows a trend towards an increased expression level. IL-1Ra expression was significantly stimulated upon IL-1β treatment (Figure B.16).

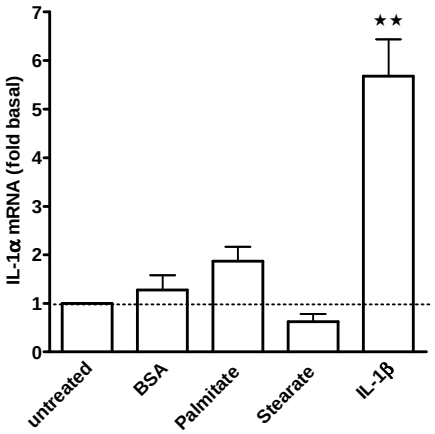

FIGURE B. 15: FFA AND IL-1β INDUCED IL-1α mRNA EXPRESSION IN ISLETS

Mouse islets were incubated for 2 in the presence of 0.5 mM BSA (n=7), 0.1 mM palmitate (n=12), 0.5 mM stearate (n=20) or 1 ng/ml IL-1β (n=4) on ECM-coated dishes. Effect of FFA and IL-1β treatment on IL-1α mRNA expression levels are expressed as fold of the untreated controls (means ± SEM). Significance was determined for BSA vs FFA treated cultures respectively untreated vs IL-1β treated cultures with Student's t test, ** represents p<0.01.

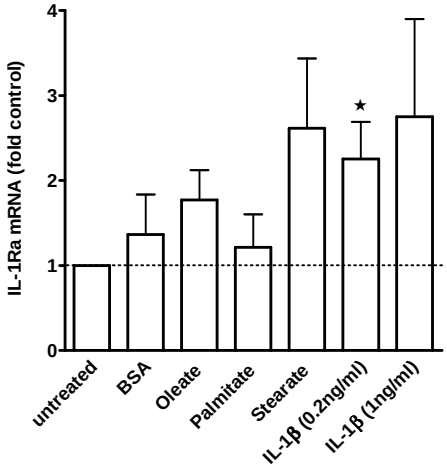

FIGURE B. 16: FFA AND IL-1β INDUCED IL-1RA mRNA EXPRESSION IN ISLETS

Mouse islets were incubated for 2 days in the presence of 0.5 mM BSA (n=8), 0.5 mM oleate (n=4), 0.1 mM palmitate (n=7), 0.5 mM stearate (n=9), 0.2 ng/ml IL-1β (n=3) or 1 ng/ml IL-1β (n=3) on ECM-coated dishes. Effect of FFA and IL-1β treatment on IL-1Ra mRNA expression levels are expressed as fold of the untreated controls (means ± SEM). Significance was determined for BSA vs FFA treated cultures respectively untreated vs IL-1β treated cultures with Student's t test, * represents p<0.05.

B.4 Discussion

B.4.1 IL-1β and KC induction depends on type of FFA

Lipotoxicity and glucotoxicity impair pancreatic β-cell function and turnover in type 2 diabetes. Supporting the concept of lipotoxicity, FFA plasma levels are elevated in type 2 diabetes and in obesity [105]. Another interesting finding was that increased IL-1β mRNA expression was detected in β-cells of type 2 diabetic patients [92]. So far, there is only limited knowledge on regulation of IL-1β in islets or IL-1β-regulated chemokine expression. We tested whether the three most abundant FFA in mammalian circulation were able to stimulate IL-1β expression and IL-1β-mediated KC expression. In mouse islets we found that the saturated FFA stearate (C18:0) and palmitate (C16:0) induced both IL-1β and KC expression, while stearate was the stronger inducer than palmitate. The mono-unsaturated FFA oleate did neither induce IL-1β nor KC. Unfortunately, FFA composition in C57BL/6 or C57BL/10 mouse circulation is not published. In blood plasma of nude BALB/c mice, oleate and palmitate were equally abundant and stearate levels were lower [129]. In blood plasma of rat, palmitate is the most abundant FFA, stearate concentrations are about half of it and oleate levels are a little lower [130]. The composition of different FFA in human blood is slightly different to the BALB/c mice and quite different to rat: Oleate is the most abundant FFA, the concentration of oleate: palmitate: stearate is around 1: 0.8: 0.34 [131]. Interestingly, in human islets the potency of FFA to induce IL-1β and KC differed from mouse islets. In human islets oleate was the strongest inducer of IL-1β, IL-8 (KC homologue) and IL-6 compared to palmitate and stearate (M. Böni-Schnetzler, manuscript in preparation). We also tested the different FFA in MIN6 cells for their ability to induce KC. Like in mouse islets, oleate did not induce KC mRNA, whereas stearate was the stronger inducer than palmitate. MIN6 cells do not produce IL-1β, therefore only KC was measured as read-out.

The observation that stearate was more potent than palmitate to induce inflammatory factors (IL-6 and TNF-α), was previously also shown in a mouse macrophage cell line [108] and in murine 3T3-L1 adipocytes [132]. However, the different potentials of the FFA to induce inflammatory factors does not reflect a species different but rather appears to be cell type specific, as it was shown that human aortic endothelial cells showed strongest IL-1β expression after treatment with stearate, a weaker to palmitate and no significant induction was observed with oleate (M. Böni-Schnetzler, manuscript in preparation).

B.4.2 MyD88 is required for FFA-induced IL-1β and KC induction

In islets isolated from MyD88 knockout mice IL-1β auto-stimulation and IL-1β-induced KC mRNA expression was completely blocked compared to wild type control islets. Since MyD88 is a direct docking protein of the IL-1RI this finding was expected. Treatment of the islets from MyD88 knockout mice with stearate also revealed complete blockage of IL-1β and KC mRNA expression, demonstrating that MyD88 is indispensable for FFA-mediated induction of IL-1β and KC in mouse islets.

Because MyD88 is a universal docking protein that couples not only to the IL-1RI but also to most TLRs (except TLR3), both, IL-1 signalling and TLR signalling, might be affected by MyD88 deficiency. Therefore, induction of IL-1β expression is expected to be mediated via a target upstream of MyD88, either IL-1RI or certain TLR.

In cell types other than islets or β-cells, free fatty acids were shown to stimulate TLR2 [123] and TLR4 signalling[124]. In addition, it was postulated that TLR2 [109] or TLR4 [108] are the link between elevated circulating FFA and the induction of inflammatory factors and insulin resistance in peripheral tissue. These findings prompted us to test whether FFA-induced IL-1β and KC expression is TLR2- or TLR4-dependent.

B.4.3 Function of TLRs in regulation of IL-1β and KC

We showed that TLR2 and TLR4 were expressed and functional in mouse islets. Specific TLR2 ligand Pam2CSK4 and TLR4 ligand LPS induced IL-1β and KC mRNA expression. Further, TLR1, 2, 4 and 6 mRNA were detected in islets by real-time PCR. β-cells preferentially expressed TLR2 while islet endothelial cells contained both TLR2 and TLR4 (J. Ehses, unpublished).

But is TLR signalling required for FFA-induced IL-1β and KC expression in mouse islets? To answer this question, islets from TLR2 and TLR4 knockout mice were incubated in the presence of FFA and the expression of IL-1β and KC was determined. In islets from TLR2 knockout mice only palmitate induced IL-1β mRNA showed a trend to a reduction in TLR2 knockout mice compared to littermate wild type, whereas stearate or IL-1β treated islets from knockout mice did not show any change in IL-1β mRNA level. For KC mRNA induction there was a trend towards a decrease in the palmitate- or stearate-stimulated wild type islets versus TLR2 knockout islets.

Islets from TLR4 knockout mice did not show any difference to wild type islets in FFA-induced IL-1β mRNA level. KC mRNA expression was significantly reduced in TLR4

knockout islets after FFA treatment, but interestingly, the basal KC mRNA level in the knockout mice was also about 70 % reduced compared to wild type. Hence the different KC mRNA induction level in wild type and TLR4 knockout islets was rather due to a lower basal KC mRNA than due to a reduced responsiveness to FFA. In short, unlike in islets of MyD88 knockout mice, FFA-induced IL-1β and KC mRNA expression was only partially reduced and not completely blocked in islets from TLR2 knockout mice. Thus FFA-induced cytokine expression does not solely function via TLR2.

To further investigate signalling via TLR2 and TLR4, inhibitory anti-TLR antibodies were applied. The TLR2 antibody was functional in MIN6 cells and completely blocked Pam2CSK4-induced KC mRNA expression. However, anti-TLR2 antibody treatment did not affect FFA-induced KC mRNA. The anti-TLR4 antibody was tested in a preliminary experiment in MIN6, however, these cells did not respond to LPS stimulation and therefore the inhibitory effect of the antibody could not be tested. The facts that TLR2 blockage did not influence FFA signalling and TLR4 was most probably absent or not functional in MIN6 cells indicate that FFA-induced KC stimulation is not mediated by TLR2 or TLR4 in MIN6 cells. This points to additional mechanisms for FFA-mediated induction of inflammatory factors. A study by Senn investigated palmitate-induced IL-6 production in a myotube cell line. Both, the inhibitory TLR2 antibody or siRNA to TLR2 decreased FFA-induced IL-6 by ~50 %, whereas siRNA to MyD88 could completely block palmitate-induced IL-6 production [107]. This is similar to our findings showing that MyD88 depletion blocked FFA- or IL-1β-induced IL-1β or KC, whereas TLR depletion in islets from knockout mice resulted at most in a partial inhibition.

However, in vivo results with TLR2 knock out mice strongly indicate that TLR2 is involved in the upregulation of IL-1β upon high fat feeding (J. A. Ehses, manuscript in preparation), Further, in other cell types free fatty acids were identified to stimulate TLR2 and TLR4 [123, 124]. But do FFA directly bind and activate TLR? FFA-induced TLR stimulation was confirmed so far only in functional assays. For TLR4 it was hypothesised that binding of FFA could take place in a large hydrophobic pocket that was shown to accommodate the acyl chains of the lipid moiety of LPS. However, direct binding of FFA to TLR4 was excluded by a biochemical approach using the LPS-trap in lysates of 3T3 adipocytes [126]. The authors speculate that TL R4-dependent FFA-induced signalling is mediated by an endogenous ligand [126]. To our knowledge, binding studies for FFA and TLR2 do not exist so far.

Alternatively, it is also possible TLR2 involvement in FFA-signalling is due to secondary effects, e.g. via upregulation of TLR2 expression after increased IL-1β expression.

Supporting this notion we observed that IL-1β or a combination of high glucose concentration and palmitate increased TLR2 mRNA expression level (J. Ehses, unpublished).

B.4.4 IL-1RI is required for amplification of IL-1β and KC mRNA

In mouse islets IL-1RI blockage with the IL-1Ra completely blocked IL-1β–, palmitate- and stearate-induced KC mRNA and protein expression. Secreted IL-1β protein was, however, not detectable in mouse islets supernatants due to a limited sensitivity of available detection assays and furthermore, IL-1β transcript levels were much lower compared to KC mRNA levels. In the past, detection of secreted IL-1β was also found to be difficult as very low levels are biologically active [133, 134]. However, blockage of KC induction by IL-1Ra in mouse islets provided evidence that stimulation proceeded via mature IL-1β protein which can not bind to IL-1RI anymore in the presence of an excess IL-1Ra. Another important conclusion from this finding is that IL-1RI activation is necessary and important for FFA-induced IL-1β-regulated KC expression.

Experiments in MIN6 cells support this conclusion. In contrast to mouse islets, IL-1Ra had no inhibitory effect on FFA-induced KC expression most likely because MIN6 cells do not express IL-1β. Addition of IL-1Ra to MIN6 cells blocked exogenous IL-1β-mediated KC mRNA induction, confirming that IL-1Ra and IL-1RI were functional in this cell line. We propose that FFA-induced IL-1RI activity in mouse islets is mediated indirectly by the induction of functional receptor ligand. Two agonistic IL-1RI ligands exist: IL-1α and IL-1β. Because IL-1α expression was not significantly stimulated by palmitate or stearate, we hypothesise that IL-1β is the major contributor to receptor activation in this context. Combined with the previous findings in MyD88, TLR2 and TLR4 knockout mice we suggest that FFA-induced IL-1β and KC induction is MyD88- and partially TLR2-dependent and that basal KC mRNA and not FFA-induced IL-1β and KC mRNA expression is TLR4-dependent. FFA treatment results in the induction of IL-1β, which in turn activates IL-1RI and amplifies the signal via auto-stimulation loop.

Gene array studies and real time PCR (Marianne Böni et al, mansucript in preparation) revealed that the IL-1RI expression was several fold higher in mouse islets and MIN6 cells compared to 22 other mouse tissues (co-receptor IL-1RAcP expression was similar in all tissue) supporting the notion that IL-1 signalling plays an important role in islets.

B.4.5 Conclusions

The main conclusions from this project regarding the regulation of IL-1β and KC in mouse islets are:

- FFA induce IL-1β and KC expression.
- TLR activation with specific ligands stimulates IL-1β and KC expression.
- FFA-induced IL-1β and KC expression is MyD88-dependent.
- FFA-induced IL-1β and KC expression is partly TLR2-dependent.
- FFA-induced IL-1β and KC mRNA expression is not TLR4-dependent (whereas basal KC mRNA expression is TLR4-dependent).
- An unidentified (TLR2/4-independent) signalling pathway for FFA-induced MyD88-dependent IL-1β and KC stimulation might exist as well.
- Signal amplification was achieved by IL-1β auto-stimulation via the IL-1RI. This amplification loop was blocked by the IL-1RI antagonist IL-1Ra and prevented further upregulation of KC and IL-1β expression.

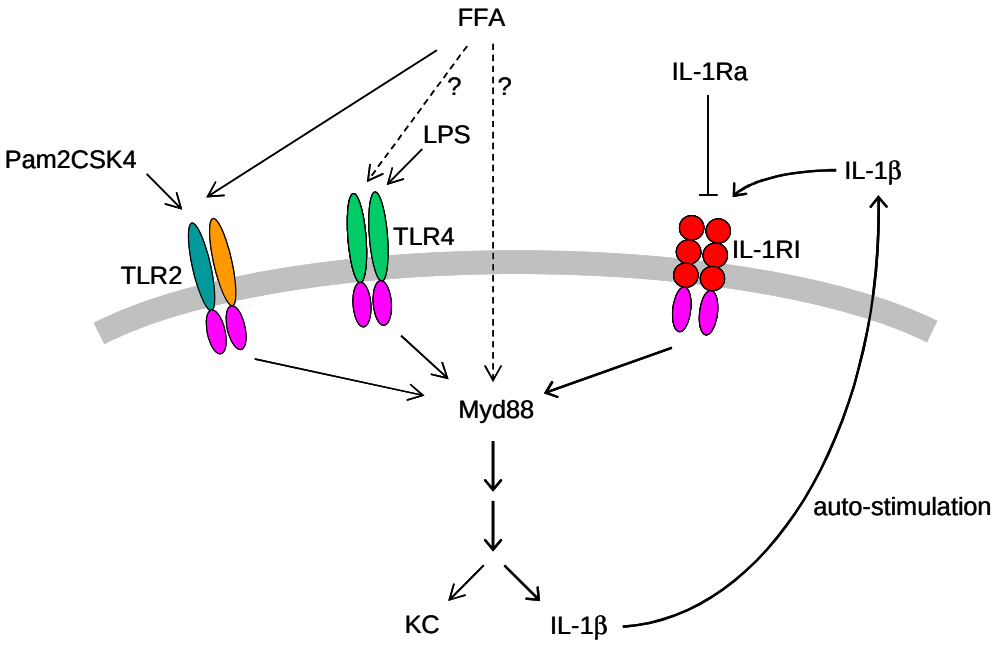

FIGURE B. 17: MODEL DESCRIBING FFA-INDUCED IL-1β AND KC EXPRESSION IN MOUSE ISLETS

FFA-induced IL-1β and KC expression was MyD88-dependent and at least partly TLR2-dependent. An additional signalling pathway with so far undefined components might exist as well. Intracellular pathway finally lead to induction of KC and IL-1β. Signal amplification was achieved by IL-1β auto-stimulation via the IL-1RI (associated with coreceptor IL-1RAcP upon ligand binding). This amplification loop was blocked by the IL-1RI antagonist IL-1Ra, that completely abolished KC and IL-1β expression.

B.4.6 Further directions

Further examinations of the pathways involved in FFA signalling will be necessary for a deeper understanding of the regulation of pro-inflammatory factors in islets. Because none of the tested pancreatic insulinoma cell lines expressed IL-1β, key experiments will have to be done in primary cells.

As mentioned above, IL-1β auto-stimulation has an important function as signal amplifier. Interestingly, IL-1β auto-stimulation was higher in islets from wild type mice with C57BL/6 background (all "normal" mice, wild type controls of TLR2 and MyD88 knockout) than from wild type mice with C57BL/10 background (wild type controls of TLR4 knockout mice). Whereas IL-1β auto-stimulation in islets from C57BL/10 mice was almost not detected, KC mRNA induction was about 10-times higher in islets from C57BL/10 than from C57BL/6 mice. To test the influence of the genetic background, more experiments have to be performed, as a first step e.g. simultaneous IL-1β treatment of islets from mice with different genetic backgrounds to compare IL-1β-induced IL-1β and KC mRNA levels.

Our experiments show that TLR2 is partially required for FFA-induced IL-1β and KC induction, because islets from TLR2 knockout mice showed a partial reduction of FFA-induced IL-1β and KC expression. Although TLR4 depletion does not influence responsiveness to FFA-induced IL-1β and KC mRNA, TLR4 is required to maintain basal KC mRNA expression. As islets from TLR2 knockout mice still express TLR4 and vice versa and both strains additionally express IL-1RI, it is difficult to judge the relative importance of TLRs, particularly in the face of the abundantly expressed IL-1RI, which amplifies the signal. Hence, it would be enlightening to test FFA-induced IL-1β and KC expression in islets from TLR2-TLR4 double-knockout mice (existing strain [135]) and in islets from IL-1RI knockout mice (commercially available [136]).

Another possibility would be to optimise the TLR2 and TLR4 antibody treatment in mouse islets. This assay did not work in whole islets, maybe the 3D architecture of islets prevented antibody binding to cells localised in the centres of the islets. A solution to this problem could be the treatment of islets single cells with the inhibitory TLR antibodies. This could confirm *in vivo* data from TLR2 knockout mice and could allow us to test combinations of TLR2 and TLR4 blocking antibody.

Beside these loss of function experiments, also gain of function assays might be considered. For this purpose IL-1RI or TLR2/4 and combinations could be overexpressed in islets using adenoviral transfection with the respective construct.

Besides TLRs many other mechanisms for FFA-induced IL-1β and KC expression should be considered. When high FFA levels are present, intermediates from FFA metabolism or e.g. the end-product from β-oxidation, acetyl-CoA, can accumulate in the cell and maybe effect other signalling branches. Another molecule that could be studied in this context is ceramide, as it is known to function as signalling molecule for apoptotic signals. De novo synthesis of ceramide is based on condensation of palmitate and Ser to form 3-keto-dihydrosphingosine and excess of palmitate might influence ceramide synthesis.

B.5 References

[78] G.D.G. Greenspan F. S., Basic & Clinical Endocrinology, 6 ed., Lange Medical Book 2001.

[79] K.M. Andralojc, A. Mercalli, K.W. Nowak, L. Albarello, R. Calcagno, L. Luzi, E. Bonifacio, C. Doglioni, L. Piemonti, Ghrelin-producing epsilon cells in the developing and adult human pancreas, *Diabetologia* 52 (2009) 486-493.

[80] B.G.I.e. Seino S. , Pancreatic Beta Cell in Health and Disease, Springer, Shinano, Japan, 2008.

[81] M. Brissova, M.J. Fowler, W.E. Nicholson, A. Chu, B. Hirshberg, D.M. Harlan, A.C. Powers, Assessment of human pancreatic islet architecture and composition by laser scanning confocal microscopy, *J Histochem Cytochem* 53 (2005) 1087-1097.

[82] L.A. O'Neill, The interleukin-1 receptor/Toll-like receptor superfamily: 10 years of progress, *Immunol Rev* 226 (2008) 10-18.

[83] C.A. Dinarello, A signal for the caspase-1 inflammasome free of TLR, *Immunity* 26 (2007) 383-385.

[84] F. Martinon, J. Tschopp, Inflammatory caspases and inflammasomes: master switches of inflammation, *Cell Death Differ* 14 (2007) 10-22.

[85] T. Mandrup-Poulsen, The role of interleukin-1 in the pathogenesis of IDDM, *Diabetologia* 39 (1996) 1005-1029.

[86] C.M. Larsen, M. Faulenbach, A. Vaag, A. Volund, J.A. Ehses, B. Seifert, T. Mandrup-Poulsen, M.Y. Donath, Interleukin-1-receptor antagonist in type 2 diabetes mellitus, *N Engl J Med* 356 (2007) 1517-1526.

[87] M.R. Heitmeier, M. Arnush, A.L. Scarim, J.A. Corbett, Pancreatic beta-cell damage mediated by beta-cell production of interleukin-1. A novel mechanism for virus-induced diabetes, *J Biol Chem* 276 (2001) 11151-11158.

[88] K. Maedler, P. Sergeev, F. Ris, J. Oberholzer, H.I. Joller-Jemelka, G.A. Spinas, N. Kaiser, P.A. Halban, M.Y. Donath, Glucose-induced beta cell production of IL-1beta contributes to glucotoxicity in human pancreatic islets, *J Clin Invest* 110 (2002) 851-860.

[89] T. Matsuda, K. Omori, T. Vuong, M. Pascual, L. Valiente, K. Ferreri, I. Todorov, Y. Kuroda, C.V. Smith, F. Kandeel, Y. Mullen, Inhibition of p38 pathway suppresses human islet production of pro-inflammatory cytokines and improves islet graft function, *Am J Transplant* 5 (2005) 484-493.

[90] M. Arnush, A.L. Scarim, M.R. Heitmeier, C.B. Kelly, J.A. Corbett, Potential role of resident islet macrophage activation in the initiation of autoimmune diabetes, *J Immunol* 160 (1998) 2684-2691.

[91] P. Ribaux, J.A. Ehses, N. Lin-Marq, F. Carrozzino, M. Boni-Schnetzler, E. Hammar, J.C. Irminger, M.Y. Donath, P.A. Halban, Induction of CXCL1 by extracellular matrix and autocrine enhancement by interleukin-1 in rat pancreatic beta-cells, *Endocrinology* 148 (2007) 5582-5590.

[92] M. Boni-Schnetzler, J. Thorne, G. Parnaud, L. Marselli, J.A. Ehses, J. Kerr-Conte, F. Pattou, P.A. Halban, G.C. Weir, M.Y. Donath, Increased interleukin (IL)-1beta messenger ribonucleic acid expression in beta -cells of individuals with type 2 diabetes and regulation of IL-1beta in human islets by glucose and autostimulation, *J Clin Endocrinol Metab* 93 (2008) 4065-4074.

[93] D.T. Brody, S.K. Durum, Membrane IL-1: IL-1 alpha precursor binds to the plasma membrane via a lectin-like interaction, *J Immunol* 143 (1989) 1183-1187.

[94] C.A. Dinarello, Historical insights into cytokines, *Eur J Immunol* 37 Suppl 1 (2007) S34-45.

[95] M.Y. Donath, D.J. Gross, E. Cerasi, N. Kaiser, Hyperglycemia-induced beta-cell apoptosis in pancreatic islets of Psammomys obesus during development of diabetes, *Diabetes* 48 (1999) 738-744.

[96] J.L. Leahy, S. Bonner-Weir, G.C. Weir, Beta-cell dysfunction induced by chronic hyperglycemia. Current ideas on mechanism of impaired glucose-induced insulin secretion, *Diabetes Care* 15 (1992) 442-455.

[97] N.S. Sauter, F.T. Schulthess, R. Galasso, L.W. Castellani, K. Maedler, The antiinflammatory cytokine interleukin-1 receptor antagonist protects from high-fat diet-induced hyperglycemia, *Endocrinology* 149 (2008) 2208-2218.

[98] O. Osborn, S.E. Brownell, M. Sanchez-Alavez, D. Salomon, H. Gram, T. Bartfai, Treatment with an Interleukin 1 beta antibody improves glycemic control in diet-induced obesity, *Cytokine* 44 (2008) 141-148.

[99] K. Maedler, D.M. Schumann, N. Sauter, H. Ellingsgaard, D. Bosco, R. Baertschiger, Y. Iwakura, J. Oberholzer, C.B. Wollheim, B.R. Gauthier, M.Y. Donath, Low concentration of interleukin-1beta induces FLICE-inhibitory protein-mediated beta-cell proliferation in human pancreatic islets, *Diabetes* 55 (2006) 2713-2722.

[100] K. Maedler, A. Fontana, F. Ris, P. Sergeev, C. Toso, J. Oberholzer, R. Lehmann, F. Bachmann, A. Tasinato, G.A. Spinas, P.A. Halban, M.Y. Donath, FLIP switches Fas-mediated glucose signaling in human pancreatic beta cells from apoptosis to cell replication, *Proc Natl Acad Sci U S A* 99 (2002) 8236-8241.

[101] K. Maedler, G.A. Spinas, R. Lehmann, P. Sergeev, M. Weber, A. Fontana, N. Kaiser, M.Y. Donath, Glucose induces beta-cell apoptosis via upregulation of the Fas receptor in human islets, *Diabetes* 50 (2001) 1683-1690.

[102] D.L. Eizirik, M.I. Darville, beta-cell apoptosis and defense mechanisms: lessons from type 1 diabetes, *Diabetes* 50 Suppl 1 (2001) S64-69.

[103] C. Holohan, E. Szegezdi, T. Ritter, T. O'Brien, A. Samali, Cytokine-induced beta-cell apoptosis is NO-dependent, mitochondria-mediated and inhibited by BCL-XL, *J Cell Mol Med* 12 (2008) 591-606.

[104] E.P. Haber, H.M. Ximenes, J. Procopio, C.R. Carvalho, R. Curi, A.R. Carpinelli, Pleiotropic effects of fatty acids on pancreatic beta-cells, *J Cell Physiol* 194 (2003) 1-12.

[105] G.M. Reaven, C. Hollenbeck, C.Y. Jeng, M.S. Wu, Y.D. Chen, Measurement of plasma glucose, free fatty acid, lactate, and insulin for 24 h in patients with NIDDM, *Diabetes* 37 (1988) 1020-1024.

[106] K. Maedler, G.A. Spinas, D. Dyntar, W. Moritz, N. Kaiser, M.Y. Donath, Distinct effects of saturated and monounsaturated fatty acids on beta-cell turnover and function, *Diabetes* 50 (2001) 69-76.

[107] J.J. Senn, Toll-like receptor-2 is essential for the development of palmitate-induced insulin resistance in myotubes, *J Biol Chem* 281 (2006) 26865-26875.

[108] H. Shi, M.V. Kokoeva, K. Inouye, I. Tzameli, H. Yin, J.S. Flier, TLR4 links innate immunity and fatty acid-induced insulin resistance, *J Clin Invest* 116 (2006) 3015-3025.

[109] A.M. Caricilli, P.H. Nascimento, J.R. Pauli, D.M. Tsukumo, L.A. Velloso, J.B. Carvalheira, M.J. Saad, Inhibition of toll-like receptor 2 expression improves insulin sensitivity and signaling in muscle and white adipose tissue of mice fed a high-fat diet, *J Endocrinol* 199 (2008) 399-406.

[110] A.K. Busch, D. Cordery, G.S. Denyer, T.J. Biden, Expression profiling of palmitate- and oleate-regulated genes provides novel insights into the effects of chronic lipid exposure on pancreatic beta-cell function, *Diabetes* 51 (2002) 977-987.

[111] G. Bikopoulos, A. da Silva Pimenta, S.C. Lee, J.R. Lakey, S.D. Der, C.B. Chan, R.B. Ceddia, B.W. M, M. Rozakis-Adcock, Ex vivo transcriptional profiling of human pancreatic islets following chronic exposure to monounsaturated fatty acids, *J Endocrinol* 196 (2008) 455-464.
[112] J.A. Ehses, A. Perren, E. Eppler, P. Ribaux, J.A. Pospisilik, R. Maor-Cahn, X. Gueripel, H. Ellingsgaard, M.K. Schneider, G. Biollaz, A. Fontana, M. Reinecke, F. Homo-Delarche, M.Y. Donath, Increased number of islet-associated macrophages in type 2 diabetes, *Diabetes* 56 (2007) 2356-2370.
[113] D. Boraschi, A. Tagliabue, The interleukin-1 receptor family, *Vitam Horm* 74 (2006) 229-254.
[114] K. Takeda, S. Akira, TLR signaling pathways, *Semin Immunol* 16 (2004) 3-9.
[115] G.P. Vigers, L.J. Anderson, P. Caffes, B.J. Brandhuber, Crystal structure of the type-I interleukin-1 receptor complexed with interleukin-1beta, *Nature* 386 (1997) 190-194.
[116] H. Schreuder, C. Tardif, S. Trump-Kallmeyer, A. Soffientini, E. Sarubbi, A. Akeson, T. Bowlin, S. Yanofsky, R.W. Barrett, A new cytokine-receptor binding mode revealed by the crystal structure of the IL-1 receptor with an antagonist, *Nature* 386 (1997) 194-200.
[117] R. Casadio, E. Frigimelica, P. Bossu, D. Neumann, M.U. Martin, A. Tagliabue, D. Boraschi, Model of interaction of the IL-1 receptor accessory protein IL-1RAcP with the IL-1beta/IL-1R(I) complex, *FEBS Lett* 499 (2001) 65-68.
[118] M. Vives-Pi, N. Somoza, J. Fernandez-Alvarez, F. Vargas, P. Caro, A. Alba, R. Gomis, M.O. Labeta, R. Pujol-Borrell, Evidence of expression of endotoxin receptors CD14, toll-like receptors TLR4 and TLR2 and associated molecule MD-2 and of sensitivity to endotoxin (LPS) in islet beta cells, *Clin Exp Immunol* 133 (2003) 208-218.
[119] M.S. Jin, J.O. Lee, Structures of TLR-ligand complexes, *Curr Opin Immunol* 20 (2008) 414-419.
[120] K. Takeda, S. Akira, Toll-like receptors in innate immunity, *Int Immunol* 17 (2005) 1-14.
[121] L.A. O'Neill, How Toll-like receptors signal: what we know and what we don't know, *Curr Opin Immunol* 18 (2006) 3-9.
[122] K. Hoebe, P. Georgel, S. Rutschmann, X. Du, S. Mudd, K. Crozat, S. Sovath, L. Shamel, T. Hartung, U. Zahringer, B. Beutler, CD36 is a sensor of diacylglycerides, *Nature* 433 (2005) 523-527.
[123] J.Y. Lee, L. Zhao, H.S. Youn, A.R. Weatherill, R. Tapping, L. Feng, W.H. Lee, K.A. Fitzgerald, D.H. Hwang, Saturated fatty acid activates but polyunsaturated fatty acid inhibits Toll-like receptor 2 dimerized with Toll-like receptor 6 or 1, *J Biol Chem* 279 (2004) 16971-16979.
[124] J.Y. Lee, K.H. Sohn, S.H. Rhee, D. Hwang, Saturated fatty acids, but not unsaturated fatty acids, induce the expression of cyclooxygenase-2 mediated through Toll-like receptor 4, *J Biol Chem* 276 (2001) 16683-16689.
[125] M.J. May, S. Ghosh, Signal transduction through NF-kappa B, *Immunol Today* 19 (1998) 80-88.
[126] A. Schaeffler, P. Gross, R. Buettner, C. Bollheimer, C. Buechler, M. Neumeier, A. Kopp, J. Schoelmerich, W. Falk, Fatty acid-induced induction of Toll-like receptor-4/nuclear factor-kappaB pathway in adipocytes links nutritional signalling with innate immunity, *Immunology* 126 (2009) 233-245.
[127] V. Lilla, G. Webb, K. Rickenbach, A. Maturana, D.F. Steiner, P.A. Halban, J.C. Irminger, Differential gene expression in well-regulated and dysregulated pancreatic beta-cell (MIN6) sublines, *Endocrinology* 144 (2003) 1368-1379.

[128] J. Miyazaki, K. Araki, E. Yamato, H. Ikegami, T. Asano, Y. Shibasaki, Y. Oka, K. Yamamura, Establishment of a pancreatic beta cell line that retains glucose-inducible insulin secretion: special reference to expression of glucose transporter isoforms, *Endocrinology* 127 (1990) 126-132.

[129] C. Lin, E.W. Blank, R.L. Ceriani, N. Baker, Evidence of extensive phospholipid fatty acid methylation during the assumed selective methylation of plasma free fatty acids by diazomethane, *Lipids* 26 (1991) 548-552.

[130] S. Bassilian, S. Ahmed, S.K. Lim, L.G. Boros, C.S. Mao, W.N. Lee, Loss of regulation of lipogenesis in the Zucker diabetic rat. II. Changes in stearate and oleate synthesis, *Am J Physiol Endocrinol Metab* 282 (2002) E507-513.

[131] L. Hagenfeldt, J. Wahren, B. Pernow, L. Raf, Uptake of individual free fatty acids by skeletal muscle and liver in man, *J Clin Invest* 51 (1972) 2324-2330.

[132] M.J. Song, K.H. Kim, J.M. Yoon, J.B. Kim, Activation of Toll-like receptor 4 is associated with insulin resistance in adipocytes, *Biochem Biophys Res Commun* 346 (2006) 739-745.

[133] J.A. Ehses, M. Boni-Schnetzler, M. Faulenbach, M.Y. Donath, Macrophages, cytokines and beta-cell death in Type 2 diabetes, *Biochem Soc Trans* 36 (2008) 340-342.

[134] M. Boni-Schnetzler, J.A. Ehses, M. Faulenbach, M.Y. Donath, Insulitis in type 2 diabetes, *Diabetes Obes Metab* 10 Suppl 4 (2008) 201-204.

[135] M.T. Nguyen, S. Favelyukis, A.K. Nguyen, D. Reichart, P.A. Scott, A. Jenn, R. Liu-Bryan, C.K. Glass, J.G. Neels, J.M. Olefsky, A subpopulation of macrophages infiltrates hypertrophic adipose tissue and is activated by free fatty acids via Toll-like receptors 2 and 4 and JNK-dependent pathways, *J Biol Chem* 282 (2007) 35279-35292.

[136] The Jackson Laboratory, http://www.jax.org/, cited 2. March 2009.

Acknowledgement

I would like to thank Markus Niessen for giving me the chance to start my PhD work in his group, for his support and knowledge. To Prof. Dr. G.A. Spinas, Head of Department Endocrinology and Diabetologia, for giving me the possibility to work in the research group of Markus Niessen. A special thank goes to Marc Donath, who gave me the possibility to change to his group and with it the big opportunity to complete my thesis. I am deeply grateful for his help and support. And I want to thank Marianne Böni for her expert supervision and support during the second part of my PhD.

I would like to thank Alex Hajnal for representing me at the University of Zurich as my official supervisor, for his inputs and his support.

Many thanks go to all my colleges at the C-floor for the friendly atmosphere and the pleasing working environment and for their various contributions and helps. Many thanks especially to my co-workers Linhua Xu and Francesca Buzzi for their friendship and support and to Diri Schmid for technical assistance and support.
Finally I would like to express my gratitude to all who supported me in any kind during the whole PhD period, especially to my mother, my sister and my grand mother for their mental support and encouragement.

Curriculum vitae

Personal Information

Last name	BOLLER
First names	Simone Brigitte
Date of birth	March 7th, 1978
Nationality	Swiss
Place of citizenship	Zurich, ZH

Education

08.1993 – 01.1998	Kantonsschule Oerlikon, Zürich, Swiss maturity type C (Mathematics and Sciences)
10.1998 – 10.2003	Biology Studies with Specialization in Chemistry at ETH Zurich, 10.2003 Diploma in Natural Sciences Diploma subjects: Biological Chemistry, Molecular Biology and Biophysics, Organic Chemistry, Inorganic Chemistry, Toxicology Diploma Thesis: Title: Isolation, Identification and Activity Screening of Potential Tyr Kinase Inhibitors produced by γ-ray Synthesis
11.2004 – summer 2009	PhD study, University Hospital Zurich, Endocrinology and Diabetes Project A: A new role for insulin receptor substrate (IRS) proteins in signal transduction? Supervisor: Dr. Markus Niessen 11.2004 - 12.2007 Project B: Do free fatty acids regulate the expression of interleukin-1β and chemokine KC via Toll-like receptors in mouse islets? Supervisor: Dr. M. Böni/ Prof. Dr. Marc Donath 12.2007 – summer 2009